JUSTUS-LIEBIG-
UNIVERSITÄT
GIESSEN

Unraveling the role of heterotrophic feeding in coral tolerance to ocean warming and microplastic pollution

DISSERTATION

zur Erlangung des akademischen Grades

Doktor der Naturwissenschaften

– Dr. rer. nat. –

angefertigt am Institut für

Allgemeine und Spezielle Zoologie

am Fachbereich 08 - Biologie und Chemie

der Justus-Liebig-Universität Gießen

vorgelegt von

María Antonieta Panamá López Hernández

Gießen, September 2025

Prüfungskommission | Examination board

Betreuerin | Supervisor, 1. Gutachterin | 1. Reviewer

Prof. Dr. Maren Ziegler[1]

2. Gutachter | 2. Reviewer

Prof. Dr. Davide Seveso[2]

1. Prüfer | 1. Examiner

Prof. Dr. Thomas Wilke[1]

2. Prüferin | 2. Examiner

Prof. Dr. Anika Wagner[3]

[1] Fachbereich 08 – Biologie und Chemie | Faculty 08 – Biology and Chemistry
Department of Animal Ecology & Systematics

[2] Università degli Studi di Milano-Bicocca | University of Milano-Bicocca
Department of earth and environmental sciences - DISAT

[3] Fachbereich 09 – Agrarwissenschaften, Ökotrophologie und Umweltmanagement | Faculty 09 – Agricultural Sciences, Nutritional Sciences and Environmental Management
Department of Nutritional Science

Eingereicht am | Submitted on: 09.2025

Deutscher Titel | German title: Die Rolle der heterotrophen Ernährung für die Toleranz von Korallen gegenüber der Erwärmung der Ozeane und der Verschmutzung durch Mikroplastik entschlüsseln

Zitiervorschlag | Please cite as

María Antonieta López (2025), Unraveling the role of heterotrophic feeding in coral tolerance to ocean warming and microplastic pollution, Dissertation zur Erlangung des akademischen Grades „Doktor der Naturwissenschaften" des naturwissenschaftlichen Fachbereichs 08 - Biologie und Chemie der Justus-Liebig-Universität Gießen, Deutschland

The most revolutionary thing one can do is always to proclaim loudly what is happening.
– Rosa Luxemburg

DE: Das Revolutionärste, was man tun kann, ist immer, laut zu verkünden, was geschieht.

ES: Lo más revolucionario que se puede hacer es proclamar siempre en voz alta lo que está ocurriendo.

Selbstständigkeitserklärung | Declaration of Authorship

Erklärung gemäß der Promotionsordnung des Fachbereichs 08 vom 21.01.2016 § 17 (2):
Ich erkläre: Ich habe die vorgelegte Dissertation selbstständig und ohne unerlaubte fremde Hilfe und nur mit den Hilfen angefertigt, die ich in der Dissertation angegeben habe. Alle Textstellen, die wörtlich oder sinngemäß aus veröffentlichten Schriften entnommen sind, und alle Angaben, die auf mündlichen Auskünften beruhen, sind als solche kenntlich gemacht. Ich stimme einer evtl. Überprüfung meiner Dissertation durch eine Antiplagiat-Software zu. Bei den von mir durchgeführten und in der Dissertation erwähnten Untersuchungen habe ich die Grundsätze guter wissenschaftlicher Praxis, wie sie in der „Satzung der Justus-Liebig-Universität Gießen zur Sicherung guter wissenschaftlicher Praxis“ niedergelegt sind, eingehalten. Die Grafiken in Abb. 6 und Abb. 9 wurden neu gezeichnet und aus einem KI-generierten Bild von MidJourney und Canva adaptiert.

Declaration acc. to the doctoral regulations of Faculty 08 dated 21.01.2016 § 17 (2):
I declare that I have completed this dissertation single-handedly without the unauthorized help of a second party and only with the assistance acknowledged therein. I have appropriately acknowledged and cited all text passages that are derived verbatim from, or are based on, the content of published work of others, and all information relating to verbal communications. I consent to the use of an anti-plagiarism software to check my thesis. I have abided by the principles of good scientific conduct laid down in the charter of the Justus Liebig University Giessen “Satzung der Justus-Liebig-Universität Gießen zur Sicherung guter wissenschaftlicher Praxis” in carrying out the investigations described in the dissertation. The artwork of Fig. 6 and Fig. 9 were redrawn and adapted from an AI-generated image from MidJourney and Canva.

September 2025

Datum | date	Unterschrift | signature

Abstract

Coral reefs harbor the highest biodiversity of all marine ecosystems and support the livelihoods of nearly 500 million people worldwide. Yet, they are increasingly threatened by global warming. Marine heatwaves disrupt the symbiosis between corals and *Symbiodiniaceae* algae, leading to coral bleaching. As these algae provide up to 90% of coral energy requirements, their loss results in energy deficits that compromise coral health, reducing growth and reproduction, increasing disease susceptibility, and often leading to mortality. Heterotrophic feeding, as a secondary pathway of energy acquisition in reef-building corals, can sustain up to 100% of their metabolic demands under stress, thereby enhancing survival and resilience to bleaching caused by ocean warming. Consequently, trophic plasticity, i.e., the ability to modulate trophic strategies in response to environmental change, has emerged as a key trait distinguishing potential "winners" under climate change. However, trophic plasticity varies among species and may be compromised by emerging stressors such as microplastic pollution, which can interfere with coral feeding. Despite the importance of heterotrophy in coral resilience, there are still knowledge gaps regarding the role of food type and food availability on coral physiology, and how these interact with pollutants such as microplastic, particularly in an ocean warming context. These uncertainties are further compounded by a lack of field-based data. This thesis addresses these knowledge gaps through two controlled laboratory experiments and the first in situ application of compound-specific isotope analysis of amino acids during a natural bleaching event. Five coral species (*Galaxea fascicularis, Porites lobata, Stylophora pistillata, Ctenactis echinata,* and *Pocillopora verrucosa*) were assessed for key physiological traits (photophysiology, growth, energy reserves, $\delta^{15}N$ and $\delta^{13}C$), providing a comparative framework of heterotrophic strategies. Results indicated that complex diets enhanced the benefits of heterotrophy across coral species. Although these benefits varied among species when symbiotic, all bleached corals exhibited positive responses to more complex food sources. Physiological rates were consistently higher in symbiotic fragments compared to their bleached counterparts, with the magnitude of these differences increasing alongside the baseline productivity of the species, from *G. fascicularis* to *P. lobata* and *S. pistillata*. Food treatments did not affect respiration or photosynthetic rates, suggesting that growth gains were driven primarily by enhanced heterotrophic nutrient supply. *In situ* bleaching was associated with $\delta^{15}N$ enrichment in the trophic amino acids alanine (ALA), glutamic acid (GLU), isoleucine (ISO), proline (PRO), and valine (VAL), suggesting alterations in nitrogen acquisition and processing under stress. The trophic position (TP) of the symbiotic host and symbionts of *C. echinata* was 1.3, consistent with a mixotrophic diet. In contrast, *P. verrucosa* exhibited TP values of 1.2 for the host and 1.0 for the symbionts, indicating a stronger reliance on autotrophy. Under bleaching, *C. echinata* maintained a TP of 1.4, reflecting a stable mixotrophic strategy, whereas *P. verrucosa* shifted to a TP of 1.5, suggesting an increased reliance

on heterotrophy. These findings suggest higher heterotrophic plasticity in *P. verrucosa* compared to *C. echinata*. Microplastics (MPs) exposure significantly decreased the energy reserves of *P. verrucosa*, although it increased photosynthesis and respiration. High food availability partially mitigated the loss of tissue energy content observed while maintaining photosynthesis and respiration rates comparable to control conditions. *S. pistillata* was not affected by MP exposure alone, but when combined with high feeding, photosynthesis decreased below that of the Control. When exposed to short-term heat stress, all corals bleached severely, however, both species bleached less in the MP treatment suggesting that MPs may also disrupt the relationship between energy balance and thermal resilience. Overall, this thesis provides evidence supporting the central role of heterotrophic feeding in modulating coral tolerance to the combined pressures of ocean warming and microplastic pollution, while emphasizing the need to integrate trophic plasticity and interspecific variability into future conservation and management strategies.

Zusammenfassung

Korallenriffe beherbergen die größte Artenvielfalt aller Meeresökosysteme und sichern den Lebensunterhalt von fast 500 Millionen Menschen weltweit. Dennoch sind sie zunehmend durch die globale Erwärmung bedroht. Marine Hitzewellen stören die Symbiose zwischen Korallen und Symbiodiniaceae-Algen, was zur Korallenbleiche führt. Da diese Algen bis zu 90 % des Energiebedarfs der Korallen decken, führt ihr Verlust zu einem Energiedefizit, das die Gesundheit der Korallen beeinträchtigt, ihr Wachstum und ihre Fortpflanzung verringert, ihre Anfälligkeit für Krankheiten erhöht und oft zum Tod führt. Die heterotrophe Ernährung als sekundärer Weg der Energiegewinnung bei riffbildenden Korallen kann unter Stressbedingungen bis zu 100 % ihres Stoffwechselbedarfs decken und damit ihre Überlebensfähigkeit und Widerstandsfähigkeit gegenüber der durch die Erwärmung der Ozeane verursachten Bleiche verbessern. Folglich hat sich die trophische Plastizität, d. h. die Fähigkeit, trophische Strategien als Reaktion auf Umweltveränderungen anzupassen, als ein Schlüsselmerkmal herausgestellt, das potenzielle „Gewinner" im Klimawandel auszeichnet. Die trophische Plastizität variiert jedoch zwischen den Arten und kann durch neue Stressfaktoren wie Mikroplastikverschmutzung beeinträchtigt werden, die die Nahrungsaufnahme der Korallen stören kann. Trotz der Bedeutung der Heterotrophie für die Widerstandsfähigkeit von Korallen gibt es noch Wissenslücken hinsichtlich der Rolle der Nahrungsart und der Nahrungsverfügbarkeit für die Physiologie von Korallen und wie diese mit Schadstoffen wie Mikroplastik interagieren, insbesondere im Zusammenhang mit der Erwärmung der Ozeane. Diese Unsicherheiten werden durch einen Mangel an Felddaten noch verstärkt. Diese Arbeit befasst sich mit diesen Wissenslücken anhand von zwei kontrollierten Laborexperimenten und der ersten In-situ-Anwendung der verbindungsspezifischen Isotopenanalyse von Aminosäuren während eines natürlichen Bleichereignisses. Fünf Korallenarten (*Galaxea fascicularis, Porites lobata, Stylophora pistillata, Ctenactis echinata* und *Pocillopora verrucosa*) wurden auf wichtige physiologische Merkmale (Photophysiologie, Wachstum, Energiereserven, $\delta^{15}N$ und $\delta^{1}3C$) untersucht, um einen Vergleichsrahmen für heterotrophe Strategien zu schaffen. Die Ergebnisse zeigten, dass eine komplexe Ernährung die Vorteile der Heterotrophie bei allen Korallenarten verstärkte. Obwohl diese Vorteile bei symbiotischen Individuen je nach Art variierten, zeigten alle gebleichten Korallen positive Reaktionen auf komplexe Nahrungsarten. Die physiologischen Raten waren bei symbiotischen Fragmenten durchweg höher als bei ihren gebleichten Gegenstücken, wobei das Ausmaß dieser Unterschiede mit der Basisproduktivität der Arten von *G. fascicularis* über *P. lobata* bis hin zu *S. pistillata* zunahm. Die Fütterung hatte keinen Einfluss auf die Respirations- oder Photosyntheseraten, was darauf hindeutet, dass die Wachstumsgewinne in erster Linie auf eine verbesserte heterotrophe Nährstoffversorgung zurückzuführen waren. Die In-situ-Bleiche war mit einer Anreicherung von $\delta^{15}N$ in den trophischen Aminosäuren Alanin (ALA), Glutaminsäure (GLU), Isoleucin (ISO), Prolin (PRO) und Valin (VAL) verbunden, was auf Veränderungen in der Stickstoffaufnahme und -verarbeitung

unter Stress hindeutet. Die trophische Position (TP) des symbiotischen Wirts und der Symbionten von *C. echinata* betrug 1,3, was mit einer mixotrophen Ernährung übereinstimmt. Im Gegensatz dazu wies *P. verrucosa* TP-Werte von 1,2 für den Wirt und 1,0 für die Symbionten auf, was auf eine stärkere Abhängigkeit von Autotrophie hindeutet. Unter Bleichebedingungen behielt *C. echinata* eine TP von 1,4 bei, was eine stabile mixotrophe Strategie widerspiegelt, während *P. verrucosa* zu einer TP von 1,5 wechselte, was auf eine erhöhte Abhängigkeit von Heterotrophie hindeutet. Diese Ergebnisse deuten auf eine höhere heterotrophe Plastizität bei *P. verrucosa* im Vergleich zu *C. echinata* hin. Die Exposition gegenüber Mikroplastik (MP) verringerte die Energiereserven von *P. verrucosa* erheblich, obwohl sie die Photosynthese und Atmung erhöhte. Eine hohe Nahrungsverfügbarkeit milderte teilweise den beobachteten Verlust der nergiereserven im Gewebe ab, während die Photosynthese- und Respirationsraten im Vergleich zu den Kontrollbedingungen aufrechterhalten blieben. *S. pistillata* wurde durch die MP-Exposition allein nicht beeinträchtigt, aber in Kombination mit hoher Fütterung sank die Photosynthese unter das Niveau der Kontrolle. Bei kurzfristigem Hitzestress kam es bei allen Korallen zu einer starken Bleiche, jedoch war die Bleiche bei beiden Arten in der MP-Behandlung geringer, was darauf hindeutet, dass MPs auch die Beziehung zwischen Energiebilanz und thermischer Resilienz stören können. Insgesamt liefert diese Arbeit Belege für die zentrale Rolle der heterotrophen Ernährung bei der Modulation der Toleranz von Korallen gegenüber den kombinierten Belastungen durch die Erwärmung der Ozeane und die Verschmutzung durch Mikroplastik und betont gleichzeitig die Notwendigkeit, trophische Plastizität und interspezifische Variabilität in zukünftigen Schutz- und Managementstrategien zu berücksichtigen.

Table of contents

1 Introduction

1.1 Scleractinean corals as mixotrophic organisms

Scleractinian corals, Cnidarians from the class Hexacorallia, are classified as mixotrophic organisms, meaning that they are able to acquire nutrients through both autotrophic and heterotrophic pathways due to their symbiotic relationship with photosynthetic microorganisms (Selosse et al., 2017). The dual autotrophic–heterotrophic nature of corals was recognised early at the beginning of the 20th century (Yonge, 1931) and this association is essential for their survival in nutrient-poor waters. The autotrophic pathway, which constitutes the primary energy source for corals, is mediated by their association with photosynthetic dinoflagellates of the family Symbiodiniaceae (LaJeunesse et al., 2018). Under optimal light and temperature conditions, these symbionts fix carbon via photosynthesis and transfer a significant proportion of the resulting photosynthates, mainly sugars, but also lipids and amino acids to the coral host (Muscatine, 1980; Tremblay et al., 2012). This translocated carbon can exceed 90 % of the total fixed carbon and substantially supports the host's metabolic demands and calcification processes (Muscatine & Cernichiari, 1969). In return, the coral host provides the symbionts with nutrients derived from its own metabolism (Wang & Douglas, 1999) or from feeding on planktonic prey and detritus (Tremblay et al., 2015).

Heterotrophic feeding, the secondary energy acquisition pathway for corals, is facilitated by their ability to extend and move polyps and tentacles, enabling them to swirl water, capture plankton, and subsequently digest it (Price & Patterson, 2023) (Fig. 1). Ingested plankton accounts for between 0 and 66 % of the fixed carbon incorporated into coral skeletons (Grottoli & Wellington, 1999; Muscatine et al., 1989). In addition to supplying carbon, heterotrophic feeding is likely essential for most scleractinian corals, as it provides nitrogen, phosphorus, and other vital nutrients that cannot be obtained through photosynthesis and must instead be acquired by capturing zooplankton, particulate matter, or dissolved organic compounds (Grottoli & Wellington, 1999; Houlbrèque & Ferrier-Pagès, 2009). Corals exhibit remarkable trophic versatility, enabling them to efficiently capture zooplankton and other food particles through a variety of mechanisms, including nematocyst discharge, tentacle grasping and mucus entrapment (Lewis & Price, 1975; Sebens et al., 1998; Yonge, 1931). It has been demonstrated that corals can ingest a wide range of particle sizes, from dissolved and particulate organic matter (DOM and POM) to picoplankton, nanoplankton and meso to macrozooplankton (Anthony & Fabricius, 2000; Ferrier-Pagès et al., 2011; Houlbrèque et al., 2003; Lewis & Price, 1975; Sebens et al., 1998). Feeding induces significant changes in various physiological parameters in corals, with both the host and its algal symbionts responding rapidly to fluctuations in food availability (Houlbrèque & Ferrier-Pagès, 2009). Heterotrophic input promotes tissue and skeletal growth and

increases protein and lipid concentrations (Al-Moghrabi et al., 1995; Anthony & Fabricius, 2000; Ferrier-Pagès et al., 2011; Houlbrèque et al., 2003; Treignier et al., 2008). Additionally, it enhances the photosynthetic rates of the symbiotic algae through an increase in photosynthetic units i.e., number of microalgae (Prézelin, 1987), a higher quality of transferred photosynthates and an increase in amino acid concentrations (Swanson & Hoegh-Guldberg, 1998).

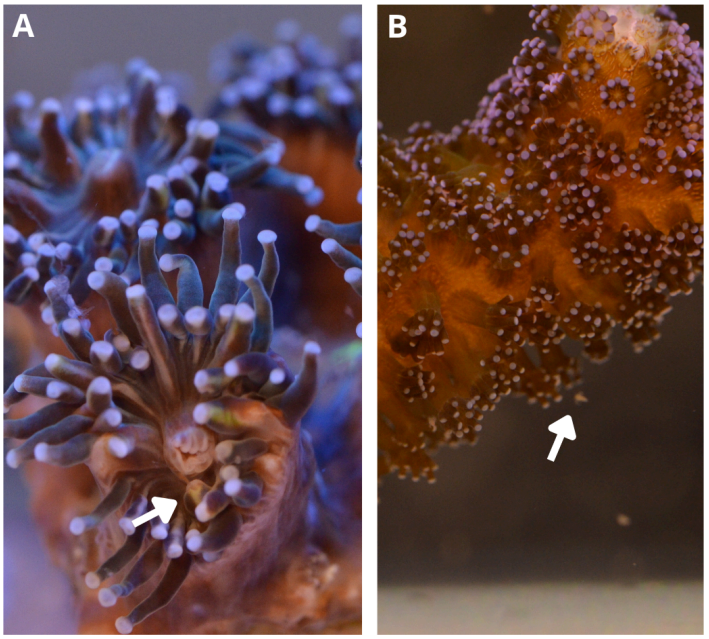

Fig. 1. Close-up of coral polyps during heterotrophic feeding. A) Symbiotic *Galaxea fascicularis* ingesting Artemia salina nauplii. B) Symbiotic *Stylophora pistillata* ingesting Artemia salina nauplii. These images were taken in the Marine Holobiomics Laboratory by María Antonieta López and Sina Ehlert.

In coral symbiosis, both partners benefit from their mixotrophic nature, as each organism can use nutrients acquired through autotrophic and heterotrophic pathways. The mutual exchange of metabolites between the coral host and its symbionts is fundamental to the structure and functioning of coral reef ecosystems (Martinez et al., 2022), and it plays a key role in determining coral resilience under stress (Denis et al., 2024). In order to accurately evaluate the capacity of corals to survive, there is an urgent need for detailed investigations into the potential of heterotrophic feeding to enhance coral physiology under stress conditions.

1.2 Heterotrophic food type as a driver of physiological changes on corals

The type of food consumed during heterotrophic feeding by corals may influence essential physiological processes (Tab. 1). The most commonly used food for feeding corals in aquaria is *Artemia salina* nauplii (called Artemia hereafter), which provides essential sources of nitrogen, phosphorus, and amino acids (Houlbrèque et al., 2004; Zaidi et al., 2023). Their use has been associated with improved coral growth rates (Conlan et al., 2018; Huang et al., 2020; Osinga et

al., 2011), enhanced photophysiology performance (Ferrier-Pagès et al., 2010; Tolosa et al., 2011) and increased energy storage (Bellworthy et al., 2019; Tolosa et al., 2011). Other food types have also demonstrated beneficial physiological effects. For example, a complex diet containing amino acids, picoplankton, nanoplankton, microplankton, mesoplankton, and yeast successfully induced spawning in *Acropora* species (Craggs et al., 2017). A mixture of Artemia and a fermented anchovy extract, improved growth and survival rates of *Acropora digitifera* corals compared to starved controls (Zaidi et al., 2023). Feeding with rotifers, increased the amount of heterotrophic carbon incorporated in *Montipora capitata* and *Porites compressa* (Hughes & Grottoli, 2013).

However, meeting the nutritional requirements of corals and optimizing their physiological performance remains a significant challenge in the aquaculture industry and in closed ex-situ systems (Arvedlund et al., 2003; Houlbrèque & Ferrier-Pagès, 2009; Leal et al., 2014; Toh et al., 2014). This is primarily due to the limited availability of data on coral feeding behaviour and nutritional requirements, making it difficult to successfully maintain corals under ex situ conditions (Arvedlund et al., 2003). Therefore, obtaining data on *in situ* heterotrophic feeding, particularly in corals under stress conditions is essential, as such information could provide valuable insights to improve the effectiveness of dietary supplementation strategies in restoration and conservation programs.

Tab. 1. Physiological response in corals fed with supplementary food. The cited studies refer to the results of laboratory experiments.

Species	Food type	Physiological response	Reference
Montipora capitata	Zooplankton	Increased energy reserves	Grottoli et al., 2006
Turbinaria reniformis	Zooplankton	Enhanced growth rate Increased lipids storage Increased protein content Increased chlorophyll content	Treignier et al., 2008
Stylophora pistillata *Galaxea fascicularis*	Zooplankton	Increased symbionts density Increased protein and lipids content Prevents depletion of energy reserves during heat stress	Borell et al., 2008
Stylophora pistillata *Turbinaria reniformis* *Galaxea fascicularis*	Artemia	Prevents damage to the photosynthetic machinery of the photosymbionts during heat stress	Ferrier‐Pagès et al., 2010
Turbinaria reniformis	Artemia	Increased symbionts density Increased protein and lipids content	Tolosa et al., 2011
Acropora intermedia	Rotifers	Recovery chlorophyll values to a comparable pre-bleaching level.	Connolly et al., 2012
Montipora capitata *Porites compresa*	Rotifers	Increased amount of heterotrophic carbon incorporated	Hughes & Grottoli, 2013

Favia fragum	Artemia	Increased accretion of $CaCO_3$	Drenkard et al., 2013
Acropora sp.	Amino acids Plankton Yeast Microalgae	Induced spawning	Craggs et al., 2017
Pocillopora acuta	Artemia	Enhanced growth	Conlan et al., 2018
Stylophora pistillata	Artemia	Increased protein content	Bellworthy et al., 2019
Goniopora columna	Mixture of high protein ingredients	Enhanced growth Increased protein content Up-regulated protease activity	Ding et al., 2021
Pocillopora acuta	Plankton	Enhanced growth Improve survival rates after heat	Huffmyer et al., 2020
Stylophora pistillata	Artemia	Underpinned the nutrition ($^{\delta 15}N$) of symbionts	Martínez et al., 2022
Acropora digitifera	Artemia Anchovy extract	Enhanced growth Improve survival rates	Zaidi et al., 2023
Galaxea fascicularis	Artemia	Enhanced photophysiology	Yu et al., 2023

1.3 Coral trophic plasticity under stress, a little-studied topic in natural environments

Differences in the ability to switch between autotrophic and heterotrophic feeding in response to environmental changes, i.e., trophic plasticity, can explain why some coral species are more resilient to a rapidly changing environment (Anthony & Fabricius, 2000; Grottoli et al., 2006; Swain et al., 2016). Despite its potential ecological importance, the degree to which corals depend on heterotrophy *in situ* remains poorly understood (Fox et al., 2019; Martinez et al., 2020). Predation and assimilation rates can fluctuate markedly under stress including bleaching, exhibiting either increases or decreases (Ferrier-Pagès et al., 2010). However, the actual reliance on heterotrophy by bleached corals in their natural environments is still largely unknown.

Compound-specific stable isotope analysis of amino acids (CSIA-AAs) has proven to be a powerful tool for investigating food sources in both deep and shallow marine animals, as well as for revealing variations in heterotrophic contributions among organisms (Fox et al., 2019; Gori et al., 2018; Martinez et al., 2022). The fundamental principle of CSIA-AAs is that essential amino acids are directly incorporated from the diet into an animal tissue, with limited and/or negligible fractionation, while non-essential amino acids undergo biochemical transformation during assimilation (Denis et al., 2024). Since essential amino acids can only be synthesized by autotrophs or bacteria, they are transferred to consumers with minimal to no carbon fractionation, their $\delta^{13}C$ values are distinct for each group and environment, serving as a unique 'fingerprint' that identifies the biosynthetic origin of the carbon (Chikaraishi et al., 2009, 2014; McMahon et al.,

2013, 2016) (Fig. 2A). Additionally, the stable nitrogen isotope ratios ($\delta^{15}N$ values) of amino acids in a consumer provide insights into both trophic position (TP) and the isotopic baseline. Certain amino acids, known as source AAs (e.g., phenylalanine, Phe), retain $\delta^{15}N$ values similar to those of the primary producers that synthesized them, making them useful indicators of nitrogen sources in the marine environment. In contrast, trophic AAs (e.g., glutamic acid, Glu) become progressively enriched in ^{15}N relative to source AAs with each trophic transfer (Popp et al., 2007). This distinction allows for a precise estimation of the trophic position of an organism by calculating the difference between $\delta^{13}C_{GLU}$ and $\delta^{15}N_{PHE}$. Corals with a TP of 1 are assumed to rely solely on autotrophy, while those with a TP greater than 1.5 are considered more heterotrophic (Ferrier-Pagès et al., 2021; Martinez et al., 2022) (Fig. 2B). The application of CSIA-AAs in bleached corals is still in its early stages. To date, no studies have applied CSIA-AAs to a bleaching event in the field. With mass coral bleaching increasing in frequency and severity, understanding the nutritional mechanisms that underlie species-specific heterotrophic plasticity is essential.

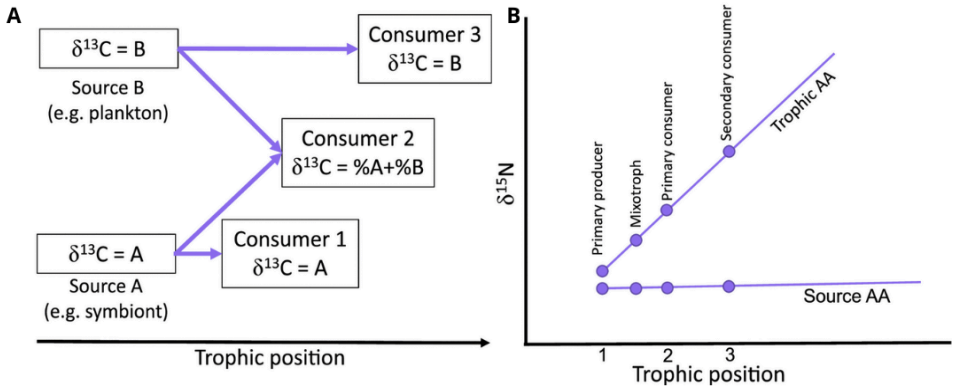

Fig. 2. Schematic explanation of changes in carbon and nitrogen isotope values of amino acids (AAs) along the food chain. A) Each food source has a carbon isotopic signature of essential AAs. A consumer feeding exclusively on one source has the same essential AAs carbon signature. A consumer who feeds on two (or more) food sources has their combined AAs signature, depending on the proportion of the diet. B) When the trophic position increases, the nitrogen isotope value of the source AAs remains unchanged. In contrast, the nitrogen isotope value of the trophic AAs increases (becomes more positive) with each change in trophic position. Image modified from: Martinez et al., (2022).

1.4 Coral reef ecosystems under the pressure of global warming and microplastic pollution

Despite the fact that coral reefs harbor the highest biodiversity of all marine ecosystems and provide essential economic support to an estimated 500 million people worldwide (De Groot et al., 2012; Fisher et al., 2015; Wilkinson, 2008), they are among the most severely affected

ecosystems, and currently face some of the most severe and urgent threats (Hughes et al., 2018; Mellin et al., 2024). Global warming occurs at an unprecedented rate and has a profound impact on all marine environments, including coral reefs (Ripple et al., 2024). Prolonged and intense temperature increases, known as marine heatwaves, disrupt the symbiotic relationship between coral hosts and the Symbiodiniaceae, leading to coral bleaching (Brown, 1997; Iglesias-Prieto et al., 1992). Because these symbionts supply up to 90% of the coral's energy needs (Muscatine & Cernichiari, 1969), their loss severely compromises coral health, increasing susceptibility to disease (Burge et al., 2014; Miller et al., 2023), reducing reproductive output (Baker et al., 2008), slowing skeletal growth (Cantin & Lough, 2014), and raising mortality risk (Brainard et al., 2013; Hughes et al., 2018). Over the past decade, global warming and marine heatwaves have affected an increasingly large percentage of the ocean surface (NOAA Physical Sciences Laboratory, Fig. 3). With continued warming, marine heat waves are predicted to become more severe, widespread and last longer (Frölicher et al., 2018). As a result, approximately 80 % of global coral cover has experienced bleaching events (Eakin et al., 2022; Hughes et al., 2018), driving disturbance dynamics of tropical reefs, presenting the major threat to the long-term resilience of these ecosystems.

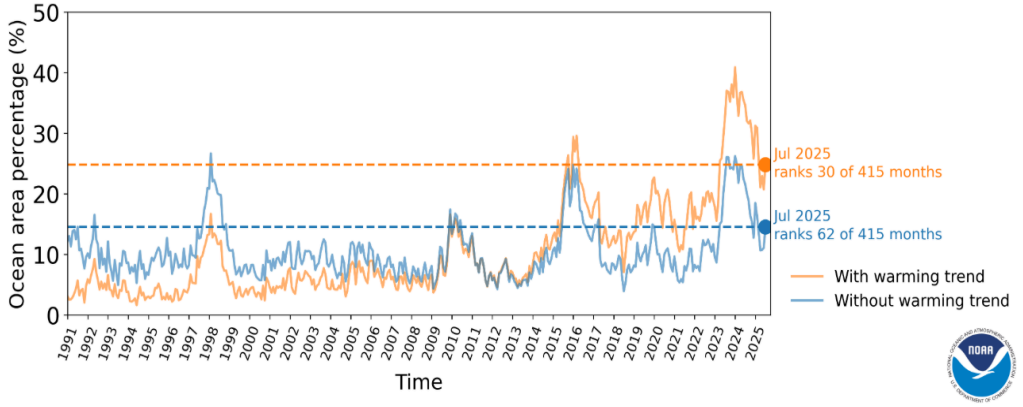

Fig. 3. Marine heatwave area percentage - Historical record. The yellow line represents observed conditions, and the blue line estimates the percentage of ocean area affected by marine heatwaves in the absence of anthropogenic warming. April 2025 ranked as the 37th highest month out of 412 in terms of the percentage of the global ocean affected by marine heatwaves. Image from: *Data/image provided by the NOAA/OAR/PSL, Boulder, Colorado, USA, from their Web site at https://psl.noaa.gov/*

Besides global warming, coral reef ecosystems face a variety of stressors. Plastic pollution has become widespread in marine environments and poses a significant threat to marine life (Jungblut et al., 2020). Microplastics (MPs), defined as particles smaller than 5 mm (Andrady, 2011), in particular have emerged as a novel stressor, adding pressure on already vulnerable coral reef systems (Reichert et al., 2021). The most common plastic polymers found in coral reefs include

polypropylene (PP), polyethylene terephthalate (PET), polyamide (PA), polyvinyl chloride (PVC), polyethylene (PE), and polystyrene (PS), which originate mainly from waste emissions from coastal cities and intensive fishing (Huang et al., 2021). They can occur in various forms, such as fibres, pellets, fragments, films and granules (Huang et al., 20

21). Concentrations in reef ecosystems are highly variable and range from 0.0001 particles L to more than 10,000 particles L (Badylak et al., 2021; Jensen et al., 2019). Depending on the concentration and exposure time, MPs can trigger a range of physiological responses in corals that increase with MPs concentration (Reichert, Tirpitz, Oponczewski, et al., 2024a). These effects are mostly attributed to the handling and ingestion of MPs (Reichert et al., 2024). The effects of high pollution scenarios on corals include increased mucus production, tissue necrosis, reduced growth, bleaching, and altered photosynthetic performance (Axworthy & Padilla-Gamiño, 2019; Lanctôt et al., 2020; Reichert et al., 2018).

Combined, global warming and MPs pollution represent a significant stressor for corals, leading to complex responses that can exacerbate or modulate the severity of their detrimental effects (Reichert et al., 2021). While ocean warming acts as a global stressor, MPs act as local stressors, the effects of which can intensify those of global pressures. Although MPs alone may represent a minor stressor compared to ocean warming (Isa et al., 2024; Reichert et al., 2021, 2024a), their interaction can elicit a marked physiological response (Bove et al., 2023). These responses are energetically costly (Sheridan et al., 2014), highlighting the importance of the interaction between corals and their energy sources, particularly the shift towards heterotrophy when autotrophic input is compromised during bleaching. However, it remains poorly understood whether corals may mitigate the combined effects of thermal stress and MPs pollution through heterotrophic feeding. As global warming and MPs pollution continue to intensify, it is becoming urgent to identify the physiological mechanisms that promote coral resilience in complex, multi-stressor environments.

1.5 Heterotrophic feeding during bleaching and microplastic pollution

Heterotrophic feeding becomes critical in meeting the entire energy demand in bleached corals, thereby enhancing their chances of survival and resilience (Houlbrèque & Ferrier-Pagès, 2009; Hughes & Grottoli, 2013). Bleached corals exhibit reduced levels of key macromolecules (i.e., carbohydrates, lipids, and proteins), resulting in the depletion of overall tissue energy reserves (Grottoli et al., 2006; Rodrigues & Grottoli, 2007). However, corals with higher heterotrophic food intake sustain their energy stores over time, supporting their capacity for recovery (Grottoli et al., 2006; Hughes & Grottoli, 2013). In addition, the transfer of essential metals (i.e., copper [Cu], zinc [Zn], boron [B], magnesium [Mg], and calcium [Ca]) and nitrogen [N]) acquired

through heterotrophic feeding and subsequently delivered to the symbionts, may further mitigate bleaching and is critical for supporting symbiont growth and symbiosis maintenance (Ferrier-Pagès et al., 2018; Martinez et al., 2022). In summary, heterotrophy plays a key role in coral resilience by mitigating bleaching (Conti-Jerpe et al., 2020), promoting recovery (Hughes & Grottoli, 2013), and reducing mortality (Tremblay et al., 2016). However, anthropogenic disturbances such as eutrophication, wastewater discharge, overfishing (Harris, 2020) and MPs pollution (Axworthy & Padilla-Gamiño, 2019) can compromise this resilience by disrupting heterotrophy of corals and nutrient cycling in reef ecosystems.

MPs pollution may interfere with heterotrophic feeding in corals (Rotjan et al., 2019). Corals have been observed to ingest and egest MPs, as they are initially unable to distinguish them from food particles (Reichert et al., 2024) (Fig. 4). Once a particle is ingested, feeding on other particles is likely reduced, caused by false satiation, and resulting in lower feeding rates (Corinaldesi et al., 2021; Savinelli et al., 2020). The presence of natural food can stimulate coral feeding responses, and it has been shown to both enhance and inhibit MPs ingestion (Reichert et al., 2024). Moreover, the rapid formation of natural biofilms on MPs occurring within minutes to hours of contact with water, particularly in marine environments (Ramsperger et al., 2020), which also influences coral feeding (Reichert et al., 2024).

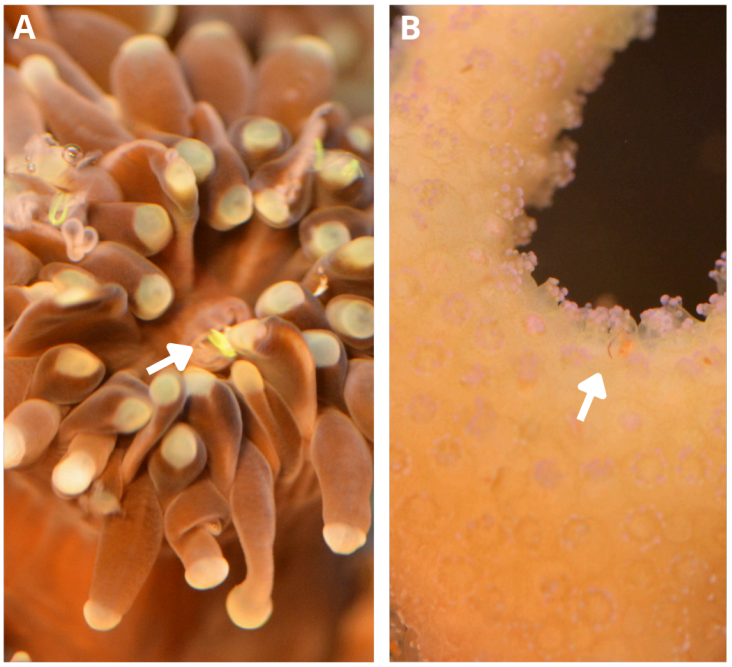

Fig. 4. MPs ingestion in corals. A) Symbiotic *Galaxea fascicularis* ingesting a yellow fiber of polyamide (PA). B) Bleached *Stylophora pistillata* with a red fiber of polyethylene terephthalate (PET) which has been ingested by the same polyp, along with an Artemia salina nauplii. These images were taken in the Marine Holobiomics Laboratory by María Antonieta López and Sina Ehlert.

In bleached corals, the ability to meet nutritional demands through heterotrophic feeding becomes crucial for survival (Houlbrèque et al., 2003; Hughes & Grottoli, 2013). Although this ability varies among species, corals with high heterotrophic plasticity, i.e., the ability to modulate trophic strategies in response to environmental change, are likely to be among the climate change "winners" (Conti-Jerpe et al., 2020). Unfortunately, coral species that exhibit higher heterotrophic capacity also tend to interact (reaction, ingestion, or egestion) more frequently with MPs (Reichert et al., 2024). The presence of MPs in the water column may significantly impair coral food intake, particularly under stressful conditions such as bleaching (Axworthy & Padilla-Gamiño, 2019). This interference could limit the capacity of corals to benefit from heterotrophic feeding, a critical mechanism for maintaining their energy balance and enhancing resilience during bleaching, periods of autotrophic compromise.

Despite its potential significance, the interactive effects of MPs, heat and heterotrophic feeding remains poorly explored. Among all peer-reviewed articles published between 2006 and 2025 on heterotrophic feeding in bleached corals, only two investigated its interaction with MPs exposure, one of which is part of the results of this thesis (Fig. 5, Tab. S1). Advancing our understanding of how MPs exposure and feeding are connected with coral bleaching susceptibility could offer valuable insights for the development of policies and conservation strategies aimed at strengthening coral reef resilience.

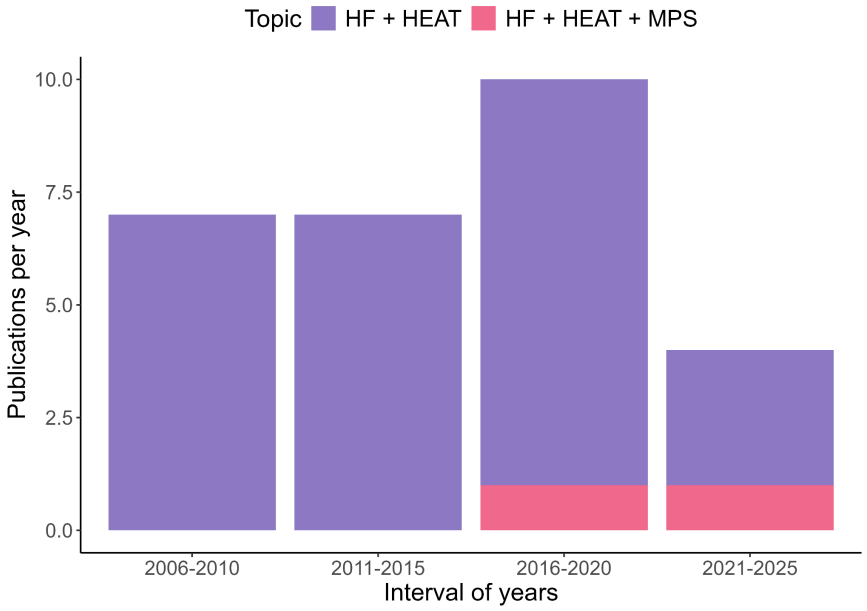

Fig. 5. Summary of the literature reviewed (2006 – July 2025). Heterotrophic feeding (HF) in bleaching corals. Of the 28 studies published, only two addressed the combined effects of HF, heat stress, and microplastics (MPS)

1.6 Scope and aims

Based on the knowledge gaps outlined above, this doctoral thesis aims to elucidate the role of heterotrophic feeding in coral tolerance to heat stress and MPs pollution. A central objective shared by coral reef researchers is to enhance coral resilience in the face of increasingly frequent mass-bleaching events. Heterotrophic feeding has emerged as a key survival strategy in this context. While it is well established that corals can supplement their metabolic demands through heterotrophy, the extent to which different food types can compensate for productivity loss during bleaching remains unclear. Accordingly, the first aim of this thesis was:

(I) To assess the effectiveness of different food types in compensating for productivity loss in bleached corals.

Despite the recognized importance of heterotrophy, the extent to which corals rely on it in their natural environment remains poorly understood. Thus, the second aim was:

(II) To assess the degree of heterotrophic dependence in corals during an *in situ* bleaching event.

In addition to thermal stress, MPs pollution is an emerging stressor that may further compromise reef health. MPs are suspected to interfere with coral feeding, yet little is known about how food availability influences coral tolerance to MPs, or how the interaction between these factors affects bleaching susceptibility. Therefore, the third aim was:

(III) To evaluate the effect of food availability on coral tolerance to MPs pollution, and to determine how the interaction between feeding and MPs exposure is linked to bleaching susceptibility.

By addressing these dimensions of heterotrophic plasticity through a combination of laboratory experiments and field-based data, this thesis provides essential knowledge to improve predictions of future shifts in reef community composition. Moreover, it offers a framework to guide conservation, restoration, and management strategies, ensuring they are better aligned with promoting coral resilience under current and future stress scenarios.

2 Materials and methods

2.1 Evaluating the effect of different feeding trials on coral physiology

The following sections (2.1.1–2.1.6) are based on a preprint publication López et al., (2025). For the purposes of this dissertation, the text has been revised and adapted; however, some similarities with the original version may remain.

2.1.1 Experimental design

This first study involved an experiment designed to investigate the influence of heterotrophic nutrition on the physiology of three scleractinian coral species: *Galaxea fascicularis* (Linnaeus 1767), *Porites lobata* (Dana 1846), and *Stylophora pistillata* (Esper, 1792), in symbiotic and bleached conditions. Over an 18-week period, the corals were fed a combination of dissolved and particulate food types, including thawed red plankton, freshly-hatched *Artemia salina* nauplii, three microalgae species, honey, yeast and amino acids (Fig. 6).

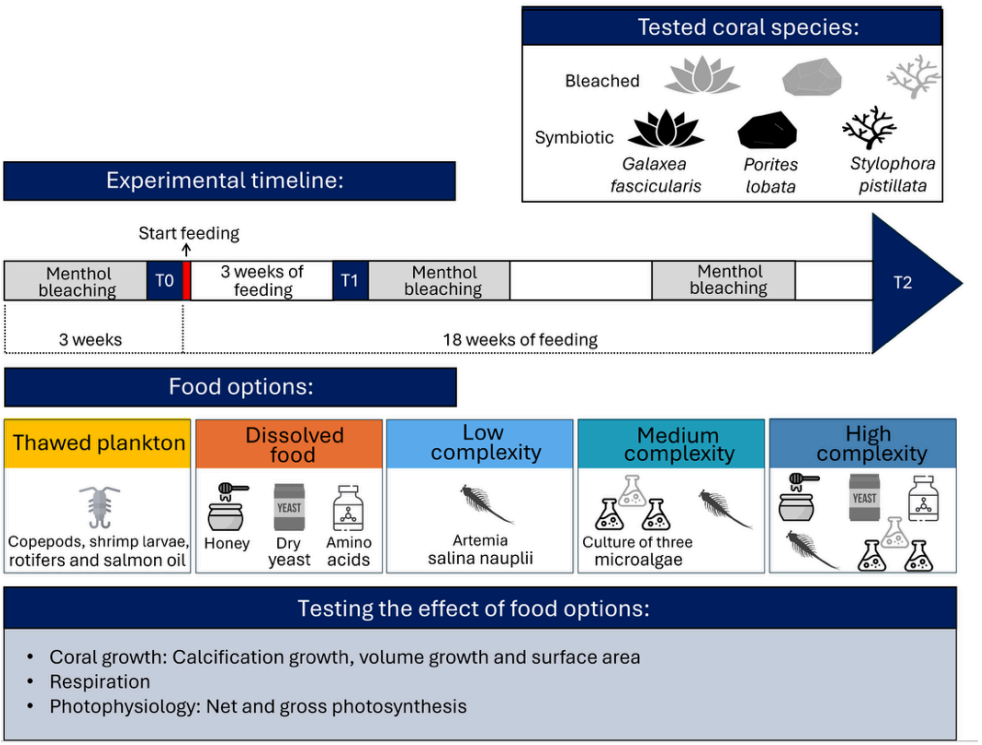

Fig. 6. Conceptual experimental overview. Symbiotic and bleached *Galaxea fascicularis, Porites lobata,* and *Stylophora pistillata*, exposed to five food treatments combining dissolved and particulate food types: thawed plankton; *Artemia salina* nauplii; three microalgae species; honey; yeast, and amino acids. Coral growth and respiration were measured at the beginning (T0) and at the end of the 18 weeks (T2), photosynthesis and respiration rates of symbiotic corals were measured at T0, after three weeks of feeding (T1), and at T2. Figure taken from: López et al., (2025).

A total of 15 × 40-L tanks were used for each of the five treatments, with each treatment being triplicated. These tanks formed part of a 3,000-L water recirculation system and each experimental tank had separate water inlet and outlet points, allowing for a water exchange rate of 20 L h^{-1}. Each tank was equipped with a wavemaker pump (EasyStream Pro ES-28, Aqualight GmbH, Bramsche/Lappenstuhl, Germany), a titanium heater to maintain a temperature of between 26 and 27 °C (Schego Heater 300 W, Schemel & Goetz GmbH, Germany) and four LED light strips providing photosynthetically active radiation (PAR) of between 140 and 190 µmol photons m^{-2} s^{-1} and a light-dark cycle of 10:14 hours. The coral fragments were suspended on three plastic rods in each tank (Fig. 7).

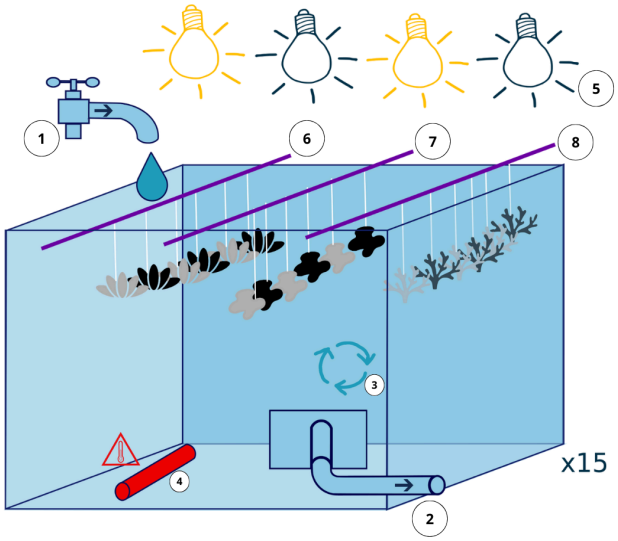

Fig 7. Schematic representation of the structure of a maintenance tank: 1: Water inflow. 2: Water drain. 3: Pump. 4: Heater. 5: 4 LED lights. 6: *Stylophora pistillata* hung on the side of the tank where the water inlet and pump were located. 7: *Porites lobata* hung in the middle. 8: *Galaxea fascicullaris* hung on the opposite side of the water inlet and pump. Each tank was replicated three times per feeding option. Figure taken from: López et al., (2025).

2.1.2 Coral species and replication

Three coral colonies of the species *Galaxea fascicularis*, *Porites lobata* and *Stylophora pistillata* were sourced for the experiment from the *Ocean2100* coral aquarium facility at Justus Liebig University in Giessen, Germany (Tab. 2). The colonies were fragmented into fragments of 3–8 cm length using a hammer and chisel. They were then allowed to heal for eight weeks before the experiment began. A total of 270 fragments were used: 30 fragments per colony and 90 fragments per species, half of which were bleached. These were evenly distributed among the tanks and treatments, resulting in 18 fragments per tank.

Tab. 2. Information about the studied coral species, origin, year of collection, and CITES permit numbers. Table taken from: López et al., (2025).

Species	Origin	Collection	CITES
Galaxea fascicularis	Red Sea	2019	19-SA-000096-PD
Porites lobata	Red Sea	2015	15-SA-000884-PD
Stylophora pistillata	Fiji	2016	15NL229192/11

2.1.3 Menthol bleaching

Following eight weeks of acclimation, the coral fragments were randomly divided into two groups, with each group containing half of the coral fragments per genotype (15 fragments per genotype, 45 fragments per group per species). To chemically bleach the corals, we followed the protocols modified by Wang et al., (2012) and Bauer et al., (2025). Briefly, the bleaching consists of three days of treatment with 0.38 mM menthol in filtered (65 µm) seawater, followed by one day of rest and another day of menthol treatment. Menthol incubations lasted 8 h during the light period (Puntin et al., 2023). The menthol bleaching process was repeated for two days when the corals started to regain their colour. *S. pistillata* was re-bleached once after nine weeks; *G. fascicularis* was re-bleached twice, once after nine weeks and again after thirteen weeks; and *P. lobata* was re-bleached five times, once after six weeks and again at three-weekly intervals up to week sixteen.

2.1.4 Feeding

Five different food options, combining dissolved and particulate food types, were used to feed the coral fragments (Tab. 3). These types of food were chosen based on their nutritional value, i.e., as sources of carbon and nitrogen, and their beneficial effects on coral physiology, such as increased growth and up-regulation of photosynthesis (see section 1.2).

Tab. 3. Information on the components and concentrations of the food treatments supplied to three stony coral species every day for three hours over an 18-week period. Table taken from: López et al., (2025).

Food components [Concentration]	Thawed plankton	Dissolved food	Low complexity	Medium complexity	High complexity
Amino acids [0.025 µl ml^{-1}]		✓			✓
Dry yeast [3,200 cells ml^{-1}]		✓			✓
Honey [20 µg ml^{-1}]		✓			✓
Microalgae: *Tisochrysis lutea*,				✓	✓

Chaetoceros calcitrans, *Tetraselmis chui* [5,000 cells ml^{-1} per species]				
Artemia salina nauplii [0.4 µg wet weight ml^{-1}]		✓	✓	✓
Thawed plankton [0.4 µg wet weight ml^{-1}]	✓			

Each feeding tank was equipped with a pump for water circulation and a heater to maintain the temperature between 26 and 27 °C. Feeding lasted three hours around dusk, i.e., it started 1.5 hours before the lights were turned off and took place at a light intensity about 10 µmol photons m^{-2} s^{-1} corresponding to a twilight phase. For each group of the food types, the following concentrations were used: 0.025 µl ml^{-1} of amino acid mixture (Pohl's Xtra special, Korallenzucht.de Vertriebs GmbH, Germany) was used. 0.03 g of dry baker's yeast (REWE supermarket, Germany) was used resulting in 3,200 cells ml^{-1}. For each feeding tank, the dry yeast was weighed on a precision balance (Kern KB 360-3N, KERN & Sohn GmbH, Germany, precision: 0.001 g). and dissolved with water from the aquarium system. Organic honey (REWE supermarket, Germany) was supplied at 20 µg ml^{-1}. The honey was weighed and mixed with water from the facility before addition to the tanks. Three species of microalgae were used: *Tetraselmis chui* (Chlorophyte, 10 to 25 µm diameter, Montoya Montoya et al., 2024), *Chaetoceros calcitrans* (Diatom, 5 to 10 µm, De La Peña et al., 2018), and *Tisochrysis lutea* (Haptophyte, 3 to 7.5 µm, Heimann & Huerlimann, 2015) at a concentration of 5000 cells ml^{-1} (5 x 10^6 cells L^{-1}) each. *T. lutea* was grown in 0.1 % sterile-filtered (0.22 µm) Walne's medium (aquacare-shop, Germany), while *T. chui* and *C. calcitrans* were grown in sterile-filtered Guillard's F/2 medium with 0.1 % silicate added to the medium for *C. calcitrans.* Microalgal cultures were maintained at 20-21 °C, 47 µmol photon m^{-2} s^{-1} µmol, and a light cycle of 12 hours. The cell count was determined daily from the cultures using a Thoma hemocytometer. The volumes of the microalgae cultures were then centrifuged twice at 3,000 g for 10 min and resuspended in 50 ml seawater to wash out the medium. 0.8 g of wet mass of freshly hatched *Artemia salina* nauplii (prepared 24 hours before the feeding, 400-500 µm length) was used, which corresponds to approximately 22,000 nauplii L^{-1}. 0.8 g of thawed red plankton (1000-2000 µm length) (Calanoide Copepoden, Zooschatz, Germany), resulting in approximately 1,000 organisms L^{-1}. Frozen food was thawed, thoroughly rinsed in a sieve, and mixed with seawater from the aquarium system before addition to a feeding tank. The red plankton consists mainly of marine copepods, micronized shrimp larvae, seawater rotifers and salmon oil. Each feeding tank was filled with 20 L of seawater, which was taken from the experimental aquarium system and roughly filtered (65 µm filter).

2.1.5 Physiological measurements

2.1.5.1 Coral growth

Changes in calcification, volume growth and surface area growth were used as an indicator of coral growth and as a measure of the response of the holobiont to food options. Calcification was measured using the buoyant-weighing method (Davies, 1989). In brief, an 8-L aquarium was filled with seawater from the experimental system. The corals were weighed using a precision balance with an underfloor weighing hook (Kern KB 360-3N, KERN & Sohn GmbH, Germany, precision: 0.001 g). The temperature of the water was kept constant at 26 ± 0.5 °C with a submersible heater and salinity at 35. Volume growth and surface area of each fragment were measured using 3D scanning. For this, a handheld 3D scanner (Artec Spider 3D, Artec 3D, Luxembourg) was used together with the scanning software Artec Studio 16 (Artec 3D, Luxembourg) following Reichert et al., (2016). Coral fragments were placed on an automatic turntable in an 80 x 80 x 80 cm macrophotography studio and scanned from two angles in two full rotations within 40–50 s. The scans of the corals resulted in image point clouds, from which polygonal structures were constructed. Models built for each fragment were exported as .obj files. Surface area and volume were calculated in MeshLab Visual Computing Lab-ISTI-CNR (v.1.3.4 B, 2014) using the ‘compute geometric measures’ tool. Growth rates were calculated as the difference between the measurements taken before the start of the feeding regimes and after 18 weeks of feeding at the end of the experiment. Calcification rate and volume growth were standardized to surface area.

2.1.5.2 Photosynthesis and respiration rates

The net photosynthesis, respiration and gross photosynthesis of symbiotic corals, as well as the respiration of bleached corals, were measured as a change in oxygen concentrations during incubations in both light and dark conditions. The corals were placed in airtight, 1-L incubation jars filled with seawater from the experimental system. Oxygen concentration was measured at the beginning and end of the 60-min incubation period using an optical oxygen sensor connected to a handheld multi-parameter probe (Multi 3620 IDS SET G, Xylem Analytics, Germany). Each incubation run included two control jars without corals as controls. Net photosynthesis and respiration were corrected for by adjusting for the change in oxygen in the controls, and were normalised according to incubation volume, incubation time and coral surface area. Gross photosynthesis was calculated as the sum of net photosynthesis and respiration.

2.1.6 Statistical analyses

Analyses were conducted in R (R version 4.2.2, R Core Team, 2022) using the graphical user interface 'RStudio' (Version 2022.12.0+353, RStudio Inc., USA). To obtain the values for coral growth, the buoyant weight values were converted to actual weight using the Seacarb package (Gattuso et al., 2021). Linear mixed-effects models with treatment (five levels: thawed plankton, dissolved food, low complexity, medium complexity, high complexity) as a fixed factor and coral colony as a random factor were used to test the effects of different food types on the physiology of symbiotic and bleached corals. Individual models were constructed for each response variable and species. The models were fitted using the lme4 package (Bates et al., 2015) and residual distributions were tested for normality and heteroscedasticity. Models were analyzed using a post hoc test from the 'multcomp' package (Hothorn et al. 2020) with Tukey comparison with 'holm' adjustment for multiple testing. The differences in symbiotic and bleached corals were tested using Hedges' g effect sizes within each feeding regime on raw data for each variable. This was done to calculate the magnitude of these differences between the different food types. Finally, all results were visualized using 'ggplot2' (Wickham, 2016).

2.2 Assessment of heterotrophic feeding of bleached coral *in situ*

2.2.1 Study area

The Red Sea is a narrow shelf basin that hosts some of the most productive coral reef ecosystems worldwide (DiBattista et al., 2016; Fine et al., 2019). Surrounded by hot arid deserts, it receives negligible precipitation and terrestrial runoff, while experiencing high evaporation rates and elevated salinity (Bower & Farrar, 2015; Edwards, 1987; Sofianos & Johns, 2003). These unique environmental conditions make the Red Sea ecosystem particularly vulnerable to climate change (Raitsos et al., 2011). Recent analyses indicate that maximum sea surface temperatures in the region are increasing at a rate of 0.17 ± 0.07 °C per decade, exceeding the global ocean warming rate of 0.11 °C per decade (Chaidez et al., 2017). Although Red Sea corals are among the most thermotolerant globally (Pineda et al., 2013; Voolstra et al., 2020), they remain susceptible to ocean warming, with bleaching events causing substantial declines in coral cover (DeCarlo, 2020; Furby et al., 2013; Hammerman et al., 2021; Monroe et al., 2018). Regarding the levels of $\delta^{13}C$ and $\delta^{15}N$ on coral reefs in the Red Sea, these are largely influenced by the latitudinal environmental gradient and local urban runoff (Kürten et al., 2014). Low organic matter $\delta^{15}N$ values in the north (zooplankton $\delta^{15}N$: 1.3‰) reflect the importance of N_2 fixation, while the higher $\delta^{15}N$ of organic matter in the south (zooplankton $\delta^{15}N$: 5.8‰) reflects N inputs from the Indian Ocean (Kürten et al., 2014).

2.2.2 Sampling area and sample collection

We sampled corals from three areas that represent the northern (Yanbu, 24.20 °N, 37.65 °E), central (Thuwal, 22.34 °N, 39.07 °E), and southern (Al Lith, 19.86 °N, 40.05 °E) regions within the central Red Sea (Fig. 8) in 2015 during the coral bleaching event in the central Red Sea (Monroe et al., 2018; Osman et al., 2018), enabling a characterization of the trophic strategies of symbiotic and bleached corals in the field. In each region, three coral fragments of *Ctenactis echinata* and *Pocillopora verrucosa* colonies were collected from three reefs at 10 m depth (9 colonies per region per symbiotic state, total n = 120). The symbiotic state of the corals depended on the site. At Yanbu, only symbiotic corals could be collected as bleaching was negligible (Osman et al., 2018). At Thuwhal, reefs suffered intermediate bleaching (Osman et al., 2018) so that symbiotic and bleached corals could be collected. Bleaching at Al Lith was severe (Osman et al., 2018) and only bleached corals could be collected there. Each fragment was placed in a zip-plock bag filled with seawater and transported to the laboratory. Upon arrival, the fragments were frozen in liquid nitrogen and stored at -80 °C for further analysis.

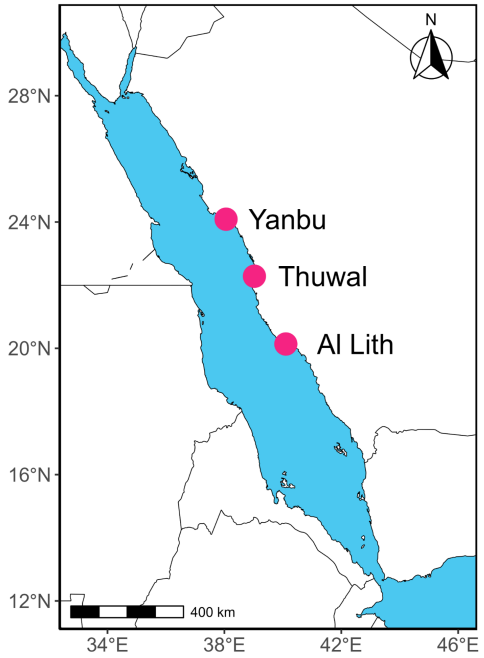

Fig 8. Sites surveyed for coral of *Ctenactis echinata* and *Pocillopora verrucosa* symbiotic and bleached in three regions (Yanbu, Thuwal, Al Lith) along the Saudi Arabian coast within the central Red Sea in start month-end month, year. Circles indicate survey sites within each of the regions. Coral reefs (not shown on map) can be found along its entire coastline.

2.2.3 Compound-specific stable isotope analysis of amino acids (CSIA-AAs) analyses

Compound-specific stable isotope analysis of amino acids (CSIA-AAs) analyses were conducted at the UC Davis Stable Isotope Facility using a Thermo Trace GC 1310 gas chromatograph coupled to a Thermo Scientific Delta V Advantage IRMS via a GC IsoLink II combustion

interface. Briefly, Amino acids were liberated by acid hydrolysis and subsequently derivatized to N-acetyl methyl esters (NACME) for gas chromatographic separation and isotope-ratio mass spectrometry (Corr et al., 2007). All samples were analyzed in duplicate, with additional replicates included when necessary. Quality control was ensured by routine measurement of calibrated amino acid mixtures traceable to international reference standards (Vienna Pee Dee Belemnite isotope (V-PDB) for $\delta^{13}C$ and Air for $\delta^{15}N$). Isotopic values were normalized to these standards following established calibration procedures, and accuracy and precision were verified using reference materials and replicate analyses (Docherty et al., 2001; Yarnes & Herszage, 2017).

2.2.4 Statistical analyses

The statistical analysis of CSIA-AA was conducted in R (R version 4.2.2, R Core Team, 2022) using the graphical user interface 'RStudio' (Version 2022.12.0+353, RStudio Inc., USA). To test the differences between host fractions and condition regarding to the variation observed in CSIA-AA, we used linear mixed-effects models with source amino acids (five levels: Asparagine, Glycine, Lysine, Methionine and Phenylananine) and trophic amino acids (five levels: Alanine, Glutamic acid, Isoleucine, Proline and Valine) as fixed factors and station (three levels: Yanbu, Thuwal and Al lith) as random factor. Individual models were constructed for each species. The models were fitted using the lme4 package (Bates et al., 2015) and residual distributions were tested for normality and heteroscedasticity. If necessary, data were log-transformed to ensure that test assumptions were met. Models were analyzed using a post hoc test from the 'multcomp' package (Hothorn et al. 2020) with Tukey comparison with 'Holm' adjustment for multiple testing. Finally, all results were visualized using 'ggplot' in R with the packages 'ggplot2' (Wickham, 2016).

2.3 Evaluating interactive effect of heterotrophic feeding, microplastics and heat

The following sections (2.3.1–2.3.7) are based on the publication López et al., (2025). For the purposes of this dissertation, the text has been revised and adapted; however, some similarities with the original version may remain.

2.3.1 Experimental design

The second experiment was designed to investigate how different feeding regimes can affect the impact of MPs on the scleractinian coral species *Pocillopora verrucosa* (Ellis & Solander, 1786) and *Stylophora pistillata* (Esper, 1792). Three experimental groups, each replicated in three independent tanks, received different combinations of food and MPs exposure: a control group that received no MPs and was fed twice weekly, an MP group that received MPs and was fed twice weekly, and an MP+HF group that received MPs and was fed daily. To evaluate the

combined impact of MPs and feeding regimes on coral holobionts and photosymbionts, we measured coral growth, photosynthetic efficiency, photosynthesis, respiration rates and tissue composition at the start of the experiment and again after six weeks. Following a six-week period, the corals were exposed to a brief heat stress test. This was used to assess their susceptibility to bleaching, with this assessment being based on the brightness of the tissue (Fig. 9).

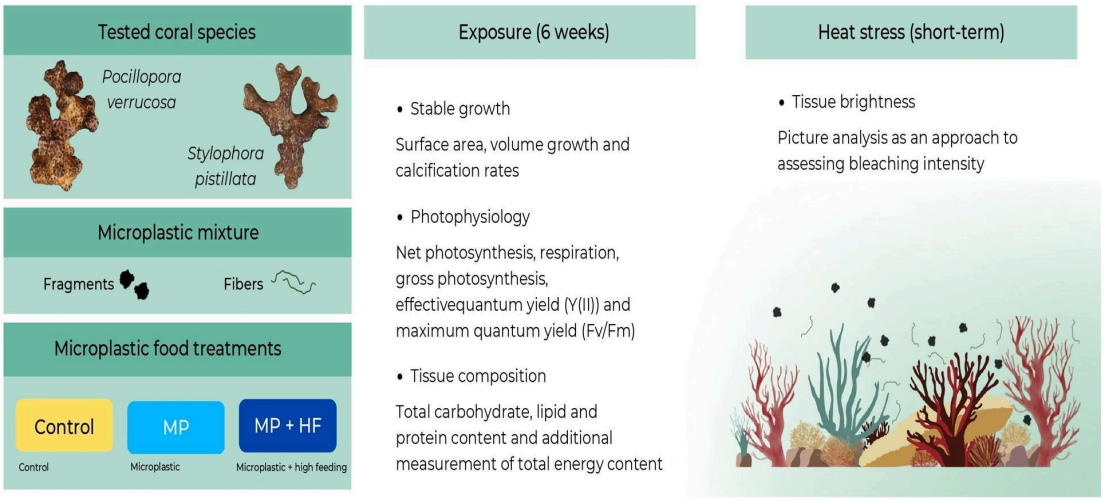

Fig. 9. Conceptual experimental overview. *P. verrucosa* and *S. pistillata* were exposed to MPs and two different feeding regimens for six weeks followed by a short-term heat stress phase. Control, MP = microplastic, MP+HF = microplastic and high feeding. Coral growth, photophysiology, and the tissue composition were measured at the beginning and at the end of the six weeks. Tissue brightness was measured after a short-term heat stress. Figure taken from: López et al., (2025).

2.3.2 Experimental setup

Nine 40-L tanks were used for the experiment, with three replicates for each of the three treatments. All the tanks were part of a 3,000-L water recirculation system and each experimental tank had separate inlets and outlets for water exchange at a rate of 20 L h^{-1}. To prevent MPs and other particles from entering or leaving each tank, each tank was equipped with two outflow filters and one inflow filter, each with a mesh size of 65 µm. A 'turnover' pump (Submarine Water Pump, Resun S-700, Resun, China) and a wavemaker pump (easyStream Pro ES-28, Aqualight GmbH, Germany) were also fitted to each tank to create a water current. The water temperature was feedback-controlled using a GHL Temp Sensor Digital (ProfiLux 3, GHL Advanced Technology GmbH, Germany) and was held at a constant temperature of 26.5 ± 0.5 °C using Schego 300 W submersible titanium heaters (Schemel & Goetz GmbH, Germany). Light was provided by four LED strips per tank (AQUARAY, Germany) at an intensity of 200 µmol photons m^{-2} s^{-1}. The phosphate concentration (PO_4^{3-}) was kept below 0.02 mg L^{-1} and measured weekly using a Spectroquant Phosphate Test (Merck KGaA, Germany). Nitrate (NO_3^-) and nitrite (NO_2^-)

concentrations were below the detectable range and were checked weekly using a Nitrate Test (Merckoquant, Merck KGaA, Germany). The calcium concentration was kept at an average of 400 mg L-1 and measured once a week using titration with EDTA. The magnesium concentration was maintained at an average of 1,300 mg L-1 and measured every four weeks using the Mg Profi Test (Salifert, the Netherlands). Furthermore, snails (Turbo sp. and Euplica sp.) were introduced to each experimental tank at the start of the experiment with the aim of reducing algal growth. To get rid of any accumulated algae or MP particles, all outflow filters were cleaned with hot water at least once a day. To remove strongly adhering organic material, the filters were placed in a solution of 14% NaClO (diluted with DI water at a ratio of 1:30) overnight.

2.3.3 Coral species and replication

The species studied were *Pocillopora verrucosa* and *Stylophora pistillata*. These are two of the most common scleractinian coral species found in coral reefs worldwide, and they are known to react to exposure to marine pollution (Reichert, Tirpitz, Plaza, et al., 2024). Four coral colonies of each species were sourced from the *Ocean2100* facility at Justus Liebig University Giessen in Germany. The colonies had been cultured there for several years prior to the experiment (Tab. 4). The colonies were fragmented (3–5 cm of length) using a small angle grinder (Dremel Multitool 3000-15, Robert Bosch Tool Corporation, Germany) and allowed to heal for 10 weeks before the start of the experiment. Nine fragments per colony, 36 fragments per species, and 72 fragments in total were used. The fragments were distributed evenly in the experimental tanks, resulting in eight fragments, with one fragment per colony, per species, per tank. The coral fragments were maintained under a 10:14 light:dark photoperiod at an intensity of 200 µmol photons m^{-2} s^{-1} and a temperature of 26 ± 0.5 °C for two months prior to the start of the experiment to allow for acclimation. During this time, all fragments received 0.6 g of copepods (Calanoide Copepoden, Zooschatz, Germany) per tank.

Tab. 4. Information about the studied coral colonies: Species, colony, origin, time of collection, time of entering the Ocean2100 facilities, and CITES registration numbers.

Species	Colony	Origin	CITES
P.verrucosa	A	Indonesia	14846/IV/SATS-LN/2007
	B	Indonesia	14NL214371/11
	C	Indonesia	14846/IV/SATS-LN/2007
	D	Saudi Arabia	19-SA-000091-PD
S. pistillata	A		
	B		
	C	Fiji	15NL229192/11
	D	Saudi Arabia	19-SA-000092-PD

2.3.4 Microplastics treatment

A mixture of six different MP types is used to simulate MPs pollution (Tirpitz et al., 2025), which have been documented to occur commonly in reef areas (Huang et al., 2021) were used: polystyrene (PS), polyvinyl chloride (PVC), polyethylene (PE), polyamide (PA), polyester - polyethylene terephthalate (PET), and polypropylene (PP) in a total concentration of 400 particles per liter (ppl) (Fig. S1-S3). PS, PVC, and PE were provided as fragments, PA, PET, and PP were provided as fibers. A sieve with a mesh size of 100 to 355 µm was used to separate the fragments. To achieve an even distribution of MP types with a final total MPs concentration of 400 ppl, the weight of each type of MPs was determined (Tab. 5). The concentration of MPs in areas of extremely polluted coral reefs can reach up to 200 ppl (Patterson et al., 2020), estimates for pollution scenarios for the year 2100 indicate an increase of MP concentrations by a factor of 3 (Koelmans et al. 2017) to 50 (Everaert et al. 2018). The six types of MPs were weighed and then combined into a single mixture. This mixture was introduced into a glass jar containing 50 ml of seawater from the aquarium system. The jar was left for one week before the mixture was added to the experimental tanks, to allow for the growth of a natural biofilm. Biofilms begin to develop on MPs within minutes to hours of contact with water, particularly in marine environments (Ramsperger et al., 2020). During the experiment, the concentration of MPs was measured weekly to guarantee a concentration of 400 ppl. For this, three 50 mL samples of seawater from each tank were taken with a glass pipette from the water column around the corals and filtered onto a 8 µm (Whatman filter papers Grade 540, General Electric Healthcare Life Sciences, United States). The number of fragments and fibres on each filter was counted under a stereo microscope, and this number was used to extrapolate the concentration per litre. MPs concentrations decreased over the course of the experiment in the tanks, as the MPs stuck to the sides of the aquarium and the filters, and were removed during cleaning. To compensate for this loss, the concentration was maintained at 400 ppl by adding more MPs at the two- and four-week points in the experiment.

Tab. 5. Information on the type, weight, and concentration of the used MPs to achieve a final concentration of 400 ppl.

Shape	Microplastic type	Weight (mg)	Concentration (ppl ± SD)
Fragment			
	Polystyrene (PS)	72	61 ± 3
	Polyvinyl chloride (PVC)	342	39 ± 2
	Polyethylene (PE)	240	86 ± 4
Fiber	Polyamide (PA)	171	27 ± 2
	Polyethylene terephthalate (PET)	40	216 ± 8
	Polypropylene (PP)	102	36 ± 2

2.3.5 Feeding treatment

The corals were fed 0.6 g of copepods per tank, resulting in a concentration of approximately 800 copepods per litre (Calanoide Copepoden, Zooschatz, Germany). This is the standard feed that the corals regularly receive at the facility and has been shown to be ingested by *P. verrucosa* and *S. pistillata* (Reichert et al., 2024). The copepods were defrosted, rinsed in a sieve and mixed with aquarium water before being evenly distributed across all tanks. The control group and the MP treatment group received food twice a week, while the MP+HF treatment group received food daily. As a nutritional supplement, 1 ml of an amino acid mixture (Pohl's Xtra Special, Korallenzucht.de Vertriebs GmbH, Germany) was added to each tank at the same time as the copepods, twice a week.

2.3.6 Physiological measurements

2.3.6.1 Coral growth

Coral growth was measured using the buoyant-weighing method (Davies, 1989) following the same protocol outlined in section 2.1.5.1.

2.3.6.2 Photosynthetic efficiency, photosynthesis and respiration rates

The effects of MPs and thermal stress on the photosymbionts were assessed by measuring photosynthetic efficiency, photosynthesis and respiration rates. Effective quantum yield (Y(II)) and maximum quantum yield (Fv/Fm) of photosystem II were measured using a pulse-amplitude modulation fluorometer (PAM-2500, Heinz Walz GmbH, Germany). Y(II) was determined during the light period at 14:00 (six hours after lights-on), with an average of three replicate measurements taken at different positions on the upward-facing side of each coral fragment. Fv/Fm was determined in darkness, after approximately 45 minutes of dark acclimation, at the end of the light period (18:45–19:00 hours), 45 minutes after the lights were turned off. The fragments were measured individually in an 8 L tank that was completely darkened and filled with seawater from the experimental system to prevent light exposure during the dark measurements.

Net photosynthesis, respiration and gross photosynthesis were derived from changes in oxygen concentrations during light and dark incubations. To achieve this, the corals were placed in airtight, 1000 ml incubation jars filled with seawater from the experimental system.

The oxygen concentration was measured at the beginning and end of the 60-minute incubation period using an optical oxygen sensor connected to a handheld multi-parameter probe (Multi 3620 IDS SET G, Xylem Analytics, Germany). Two control jars without corals were included in each incubation run so that biological activity in the seawater could be corrected for. Net photosynthesis and respiration were corrected for by measuring the change in oxygen in the

control jars, and were normalised according to incubation volume, coral surface area and incubation duration. Gross photosynthesis was then calculated as the sum of net photosynthesis and respiration.

2.3.6.3 Tissue composition

The total content of carbohydrates, lipids and proteins of the holobiont was measured to assess its tissue composition. Coral fragments were collected at the end of the six-week MP exposure period, flash frozen immediately in liquid nitrogen, and stored at -80 °C. The tissue was then removed from the skeleton by spraying it off with an airbrush containing 20 ml of filtered seawater from the system. The tissue samples were freeze-dried and stored at room temperature until analysis.The total content of carbohydrates, lipids, and proteins was determined following the protocol of (Tignat-Perrier et al., 2022). The total carbohydrate content was extracted from 15 mg of freeze-dried tissue by sonication (20 pulses) in 200 ml of cold 1x PBS at 4°C. The total content of carbohydrates was measured using the Total Carbohydrate assay kit (Sigma-Aldrich, USA). Kit standards were diluted in cold 1X PBS. The net absorbance values at 490 nm were read using a spectrofluorometer (Xenius, SAFAS, Monaco) and were compared with a standard curve made of known concentrations of d-glucose. To extract lipids, 10 mg of freeze-dried tissue was added to 1.5 mL of chloroform/methanol (2:1) in Pyrex tubes and incubated at room temperature for 20 min on an orbital shaker. The tubes were centrifuged at 1,000 g for 5 min to remove debris, and 1 mL of extract was subsequently evaporated in a dry bath at 90 °C. The total content of lipids was measured using a protocol based on the sulfo-phospho-vanillin reaction method (Barnes & Blackstock, 1973). The net absorbance values at 520 nm were read using a spectrofluorometer (Xenius, SAFAS, Monaco) and were compared with a standard curve made of known concentrations of cholesterol. The total content of proteins were extracted from 5 mg of freeze-dried tissue in 200 mL of 1 M sodium hydroxide and heated at 90 °C for 30 min. Total content of proteins was measured using the Pierce BCA Protein assay kit (Thermo Fisher Scientific, USA). The total content of carbohydrates, lipids, and proteins were expressed in µg per cm^2 surface area.

The total tissue energy content was calculated by adding together the amounts of carbohydrates, lipids and proteins, and taking into account the difference in energy content between these groups. For each of the compound groups energy assessments (specific combustion enthalpies: -23.9, -39.5, and -17.5 J mg^{-1}, respectively) have been made by (Gnaiger & Bitterlich, 1984). The final value was determined by summing the specific enthalpy of combustion (kJ g^{-1}) for carbohydrate, lipid, and protein biomass (Schoepf et al., 2015). The data on tissue composition was only available for P. verrucosa because of technical constraints.

2.3.6.4 Assessment of bleaching susceptibility

In order to evaluate the impact of the feeding regimen on the susceptibility of corals to bleaching under MP pollution, the coral fragments were subjected to a short-term heat stress assay following a six-week exposure to MPs. For this, the temperature in all experimental tanks was increased from ambient (26 °C) to 35 °C in 3 h, held at 35 °C for 3 h, and then returned to ambient within 2 h, following the CBASS design (Voolstra et al., 2020). We took standardised pictures of the fragments at the end of the heat phase to measure tissue brightness as a bleaching proxy. To achieve this, we photographed each fragment 18 hours after heat stress using a digital SLR camera (Nikon D7000, Nikon, Germany) in an evenly illuminated macrophoto studio (80 x 80 x 80 cm, Life of Photo, Germany). The images were edited in Adobe Photoshop CC 2019 software, where the coral was cropped and the background of each fragment removed. Pictures of the fragments were then analyzed in Python (Reichert et al., 2021), generating color histograms of tissue brightness (red, blue, green, and gray channels). Coral tissue brightness, i.e., bleaching severity was calculated as means from the histograms for the gray channel on a scale of 0-255, in which 0 corresponds to black and 255 corresponds to white.

2.3.7 Statistical analyses

Statistical analyses were conducted in R (R version 4.2.2, R Core Team, 2022) using the graphical user interface ‘RStudio’ (Version 2022.12.0+353, RStudio Inc., USA). For coral growth, we converted the values from buoyant weight to actual weight using the seacarb package (Gattuso et al., 2021), and the values were standardized to the surface area of the coral. To test the effects of different MPs and feeding regimes on coral physiology, we used linear mixed-effects models with treatment (three levels: Control, MP, and MP+HF) as fixed factor and coral colony as random factor. Individual models were constructed for each response variable and species. The models were fitted using the lme4 package (Bates et al., 2015) and residual distributions were tested for normality and heteroscedasticity. If necessary, data were log-transformed to ensure that test assumptions were met. Models were analyzed using a post hoc test from the ‘multcomp’ package (Hothorn et al. 2020) with Tukey comparison with ‘holm’ adjustment for multiple testing using. All results were visualized using ‘ggplot’ in R with the packages ‘ggplot2’ (Wickham, 2016).

3 Results

3.1 Evaluating the effect of different feeding trials on coral physiology

The following sections (3.1.1–3.1.3) are based on a preprint publication López et al., (2025). For the purposes of this dissertation, the text and figures have been revised and adapted; however, some similarities with the original version may remain.

3.1.1 Effects of food types on the physiology of symbiotic corals

The growth of symbiotic corals was unaffected by the different food types in *G. fascicularis* and *P. lobata* (Fig. 10, Tab. S2, S4). *S. pistillata* showed a marked increase in both volume and surface growth with increasing food complexity. The highest growth rates were achieved through the use of high-complexity feed (Fig. 10F, I, Tab. S6). Respiration rates of all species were comparable (range 10-30 µg O_2 cm^{-2} h^{-1}) and unaffected by food types (Fig. 10J-L, Tab. S3, S5, S7). Similarly to coral growth, the photosynthetic rate of S. pistillata was approximately double that of *G. fascicularis* and *P. lobata*.

3.1.2 Effects of food types on the physiology of bleached corals

The calcification and tissue growth rates, as well as the volume, were all approximately two-fold higher in bleached *S. pistillata* as in *G. fascicularis* and *P. lobata* (Fig. 11; Tab. S8-10). In *S. pistillata*, growth variables in the high complexity feeding trial were two- to three-fold increased compared to the other food types, and all bleached fragments in the thawed plankton treatment died (Fig. 11C, F, I, Tab. S10). Although no mortality was recorded in *P. lobata*, its growth patterns were largely similar to those of *S. pistillata* in terms of both volume and surface area. The medium-complexity feed performed better than the simpler feeds (Fig. 11E, H). A similar trend, although not significant, was observed for *G. fascicularis*. Respiration rates of all bleached species were comparable (range 5-20 µg O_2 cm^{-2} h^{-1}) and unaffected by food types (Fig. 11, Tab. S11).

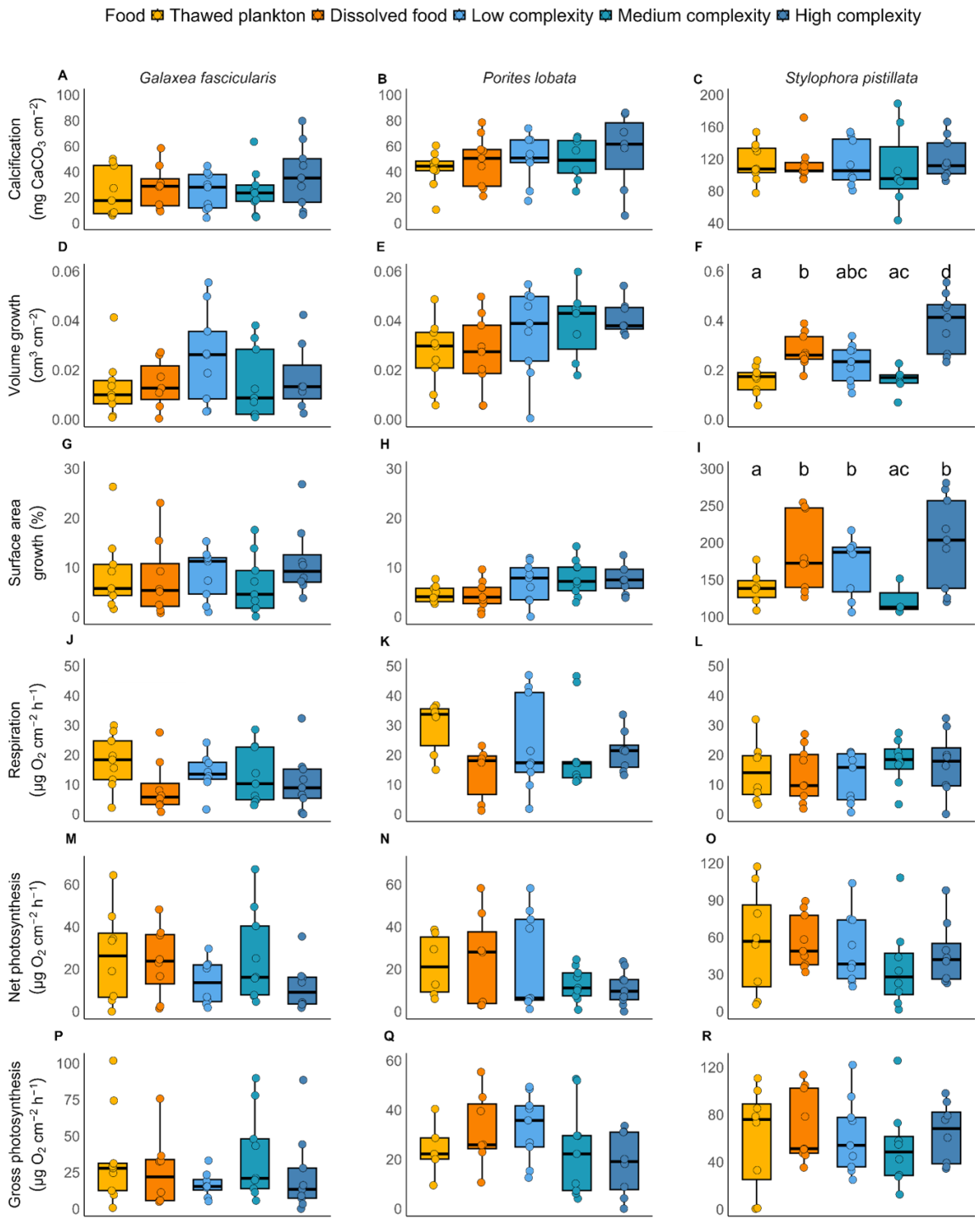

Fig. 10. Growth and photosynthesis rates of the symbiotic stony corals *Galaxea fascicularis*, *Porites lobata,* and *Stylophora pistillata* fed with different food treatments over 18 weeks. The differences between food options in calcification growth (A-C), volume growth (D-F), surface area growth (G-I), respiration (J-L), net photosynthesis (M-O), and gross photosynthesis (P-R) are shown as boxplots. Groups with different letters are significantly different based on linear mixed-effects models ($p < 0.05$). Figure taken from: López et al., (2025).

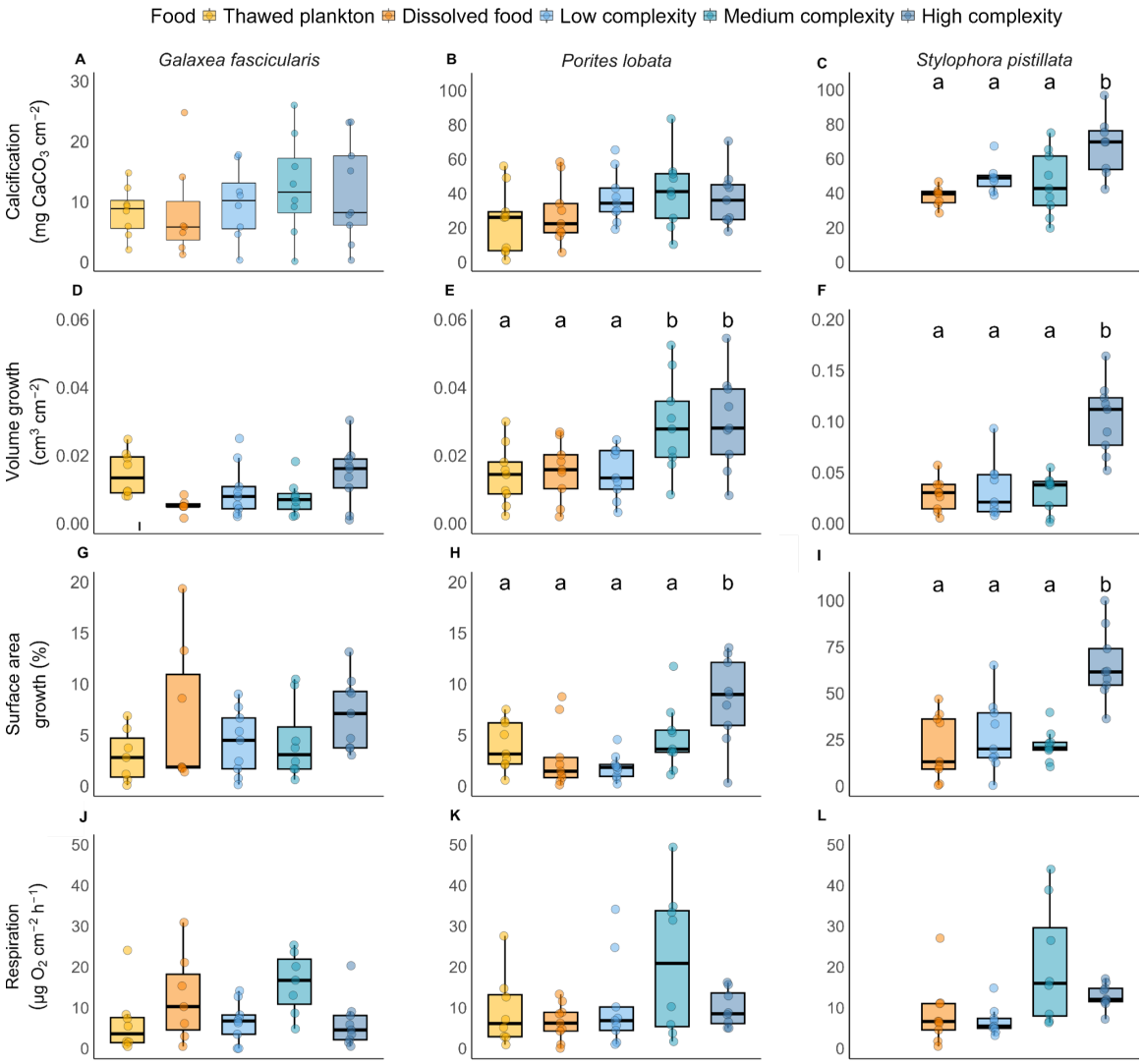

Fig. 11. Growth and respiration of the menthol-bleached stony corals *Galaxea fascicularis*, *Porites lobata,* and *Stylophora pistillata* fed with different food treatments over 18 weeks. The differences between food treatments in calcification (A-C), volume growth (D-F), surface area growth (G-I), and respiration rates (J-L) are shown as boxplots. Groups with different letters are significantly different based on linear mixed-effects models ($p < 0.05$). Figure taken from: López et al., (2025).

3.1.3 Effect of food types on heterotrophic compensation

Across all species, the metabolic rates of symbiotic fragments were consistently higher than those of their bleached clones (Fig. 12, Tab. S12-S17). The food treatments had no discernible impact on the differences between the bleached and symbiotic fragments of any species. The differences were smallest in *G. fascicularis*, where the growth and respiration of bleached fragments resembled those of symbiotic fragments across all food treatments, except in a few cases (Fig. 12A, G, M, S). In *P. lobata*, the growth and respiration rates of symbiotic corals were significantly higher than those of bleached corals for most food treatments (Fig. 12H, T). Significant differences were also observed in calcification and surface growth rates for some food treatments, despite their smaller size (Fig. 9B, N). In *S. pistillata*, the difference in growth between symbiotic and bleached fragments was approximately twice as large as in the other species. Symbiotic corals grew significantly more than bleached fragments in all food treatments (Fig. 12C, I, O). There was a trend showing that the differences between symbiotic and bleached *S. pistillata* were most apparent in the dissolved food treatment, and that these differences decreased with increasing food complexity. Although not significant, this trend is noteworthy (Tab. S18-S20). The respiration rates were similar across species, and also between symbiotic and bleached S. pistillata, regardless of the food treatment (Fig. 12U).

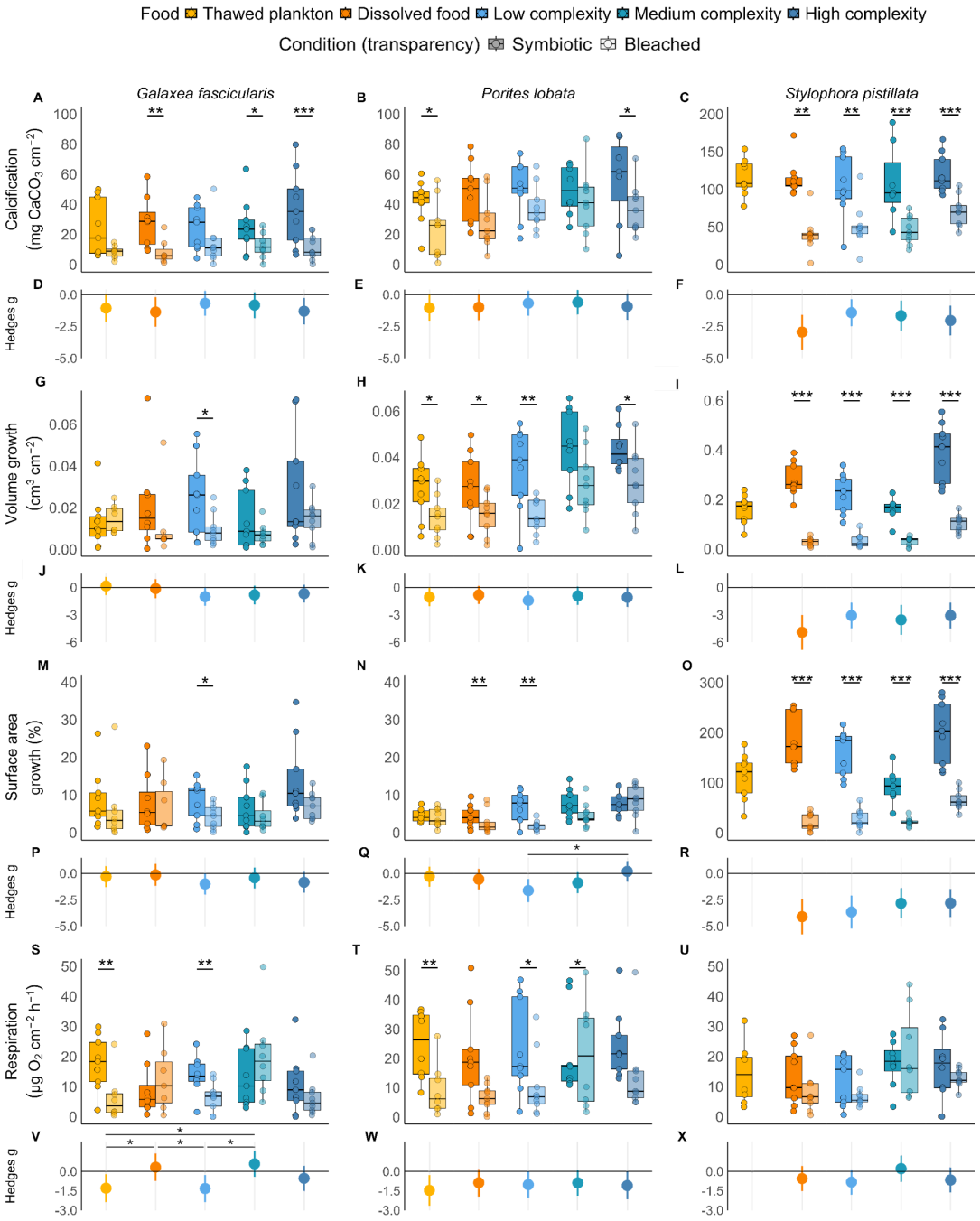

Fig. 12. Growth rates and respiration of the symbiotic and bleached stony corals *Galaxea fascicularis*, *Porites lobata,* and *Stylophora pistillata* fed with five food treatments over 18 weeks. The differences between symbiotic and bleached corals in calcification (A-C), volume growth (G-I), surface area growth (M-O), and respiration rates (S-U) are shown as boxplots, and the magnitude of these differences between symbiotic and bleached fragments in calcification (D-F), volume growth (J-L), surface area growth (P-R), and respiration rates (V-X) are shown as Hedges' g effect sizes. Bleached *S. pistillata* fragments fed with thawed plankton died during the experiment. Significance codes used are defined as: $p < 0.001$ (***), $p < 0.01$ (**), $p < 0.05$ (*). Figure taken from: López et al., (2025).

3.2 Assessment of heterotrophic feeding of bleached coral *in situ*

3.2.1 $\delta^{13}C$ and $\delta^{15}N$ isotopic signature of source amino acids

The $\delta^{13}C$ and $\delta^{15}N$ isotope signature of source amino acids in *C. echinata* and *P. verrucosa* were modulated by bleaching, though the extent of this effect depended on the coral species (Fig. 13, Tab. S21). Additionally, isotope signatures were significantly different between host fractions, however, these differences were primarily driven by the type of amino acid (Fig. 13, linear mixed-effects models, Tab. S22-23). Overall, Asparagyne (ASP), Glycine (GLY), and lysine (LYS) were enriched in all host fractions compared to Methionine (MET) and Phenylananine (PHE) in both species.

$\delta^{13}C_{ASP}$ isotope signature ranged from approx. −6.1 to −7.5‰ in *C. echinata* and from −6.7 to −12.3‰ in *P. verrucosa*. An Enriched signature was observed in symbionts compared to bleached and symbiotic tissue (both $p < 0.001$), though this trend was only significant in *P. verrucosa*. $\delta^{15}N$ isotope signature ranged from approx. 5.0 to 8.0‰ in *C. echinata* and from 1.0 to 4.2‰ in *P. verrucosa*. An enrichment signature was observed in bleached corals, followed by symbiotic tissue and symbionts in both species ($p < 0.001$).

$\delta^{13}C_{GLY}$ isotope signature ranged from approx. −8.3 to −9.4‰ in *C. echinata* and from −0.8 to −10.0‰ in *P. verrucosa*. No significant differences were observed between host fractions in *C. echinata*. However, in *P. verrucosa*, an enriched signature was observed in bleached corals compared to symbiotic tissue and symbionts (both $p < 0.001$). $\delta^{15}N$ isotope signature ranged from approx. 1.5 to 1.6‰ in *C. echinata* and from −2.6 to 0.4‰ in *P. verrucosa*. While no significant differences were observed between host fractions in *C. echinata*, in *P. verrucosa*, an enriched signature was observed in symbiotic corals, followed by symbionts and bleached corals ($p < 0.01$, $p < 0.001$).

$\delta^{13}C_{LYS}$ isotope signature ranged from approx. −8.3 to −8.6‰ in *C. echinata* and from −10.5 to −11.5‰ in *P. verrucosa*, with no significant differences between host fractions. $\delta^{15}N$ isotope signature ranged from approx. 1.5 to 2.7‰ in *C. echinata* and from 1.0 to 2.8‰ in *P. verrucosa*. An enriched signature was observed in bleached corals compared to symbionts ($p < 0.001$). However, this trend was only significant in *P. verrucosa*.

$\delta^{13}C_{MET}$ isotope signature ranged from approx. −15.1 to −18.7‰ in *C. echinata* and from −13.2 to −24.1‰ in *P. verrucosa*. An enriched signature was observed in symbionts, followed by symbiotic tissue and bleached corals in both species (*C. echinata*: $p < 0.001$ and $p < 0.01$, *P. verrucosa*: both $p < 0.001$). $\delta^{15}N$ isotope signature ranged from approx. 1.0 to 2.2‰ in *C. echinata* and from 2.2 to 6.1‰ in *P. verrucosa*. No significant differences were observed between

host fractions in *C. echinata*. However, in *P. verrucosa*, enriched signature was observed in bleached corals compared to symbiotic tissue and symbionts (both $p < 0.001$).

$\delta^{13}C_{PHE}$ isotope signature ranged from approx. −18.8 to −20.0‰ in *C. echinata* and had a more marine signature in *P. verrucosa* with values ranging from −19.4 to −22.3‰. An enriched signature was observed in symbionts compared to both symbiotic and bleached tissues in both species (*C. echinata*: both $p < 0.01$, *P. verrucosa* both $p < 0.001$), which were not significantly different from each other (*C. echinata*: $p < 0.98$, *P. verrucosa*: $p < 0.5$). $\delta^{15}N$ isotope signatures were stable between tissue and symbiont compartments in *C. echinata* ranging between approx. -0.3 and 0.5‰. In *P. verrucosa* the signature was enriched (2.2- 4.2‰) and bleached tissues had an enriched signature than symbiotic tissues and the symbionts (both $p < 0.001$), but no differences were observed between symbiotic tissues corals and symbionts.

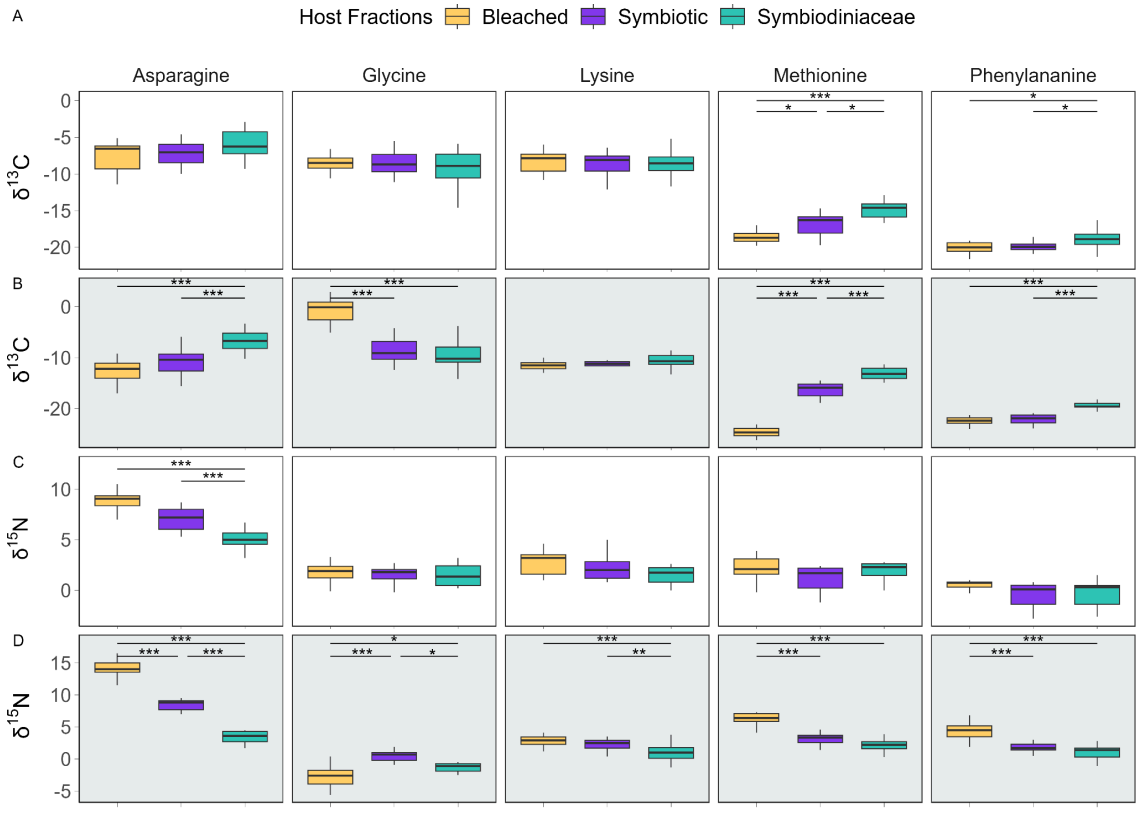

Fig. 13. $\delta^{13}C$ and $\delta^{15}N$ isotope values of five source amino acids of host tissue and symbionts of the bleached and symbiotic corals *Ctenactis echinata* (white) and *Pocillopora verrucosa* (grey): Asparagine, Glycine, Lysine, Methionine and Phenylananine. (AB) $\delta^{13}C$ isotope values (CD) $\delta^{15}N$ isotope values. Significance codes used are defined as $p < 0.001$ (***), $p < 0.01$ (**), $p < 0.05$ (*), $p > 0.05$ (ns = not significant).

3.2.2 $\delta^{13}C$ and $\delta^{15}N$ isotopic signature of trophic amino acids

Similar to the source amino acids, $\delta^{13}C$ and $\delta^{15}N$ isotopic signature of trophic amino acids in *C. echinata* and *P. verrucosa* were also modulated by bleaching (Fig. 14, Tab. S24-25). However here, the effect was more evident in the enrichment of $\delta^{15}N$ across all amino acids; alanine (ALA), glutamic acid (GLU), isoleucine (ISO), proline (PRO) and valine (VAL). More $\delta^{15}N$ enrichment signatures were observed in bleached corals, followed by symbiotic tissue, and symbionts in both species ($p < 0.001$).

$\delta^{13}C_{ALA}$ isotope signature ranged from approx. −12.9 to −14.3‰ in *C. echinata* and from −12.4 to −12.7‰ in *P. verrucosa*. An enrichment signature was observed in symbionts compared to bleached and symbiotic tissue in *C. echinata* ($p < 0.02$ and $p < 0.01$). No significant differences were observed between host fractions in *P. verrucosa*. $\delta^{15}N$ isotope values ranged from approx. 3.4 to 7.8‰ in *C. echinata* and from 2.6 to 12.6‰ in *P. verrucosa*.

$\delta^{13}C_{GLU}$ isotope signature ranged from approx. −9.7 to −11.2‰ in *C. echinata* and from −12.3 to −13.6‰ in *P. verrucosa*. An enrichment signature was observed in symbionts compared to bleached corals in *C. echinata* ($p < 0.02$). A similar pattern was observed in *P. verrucosa* ($p < 0.004$). $\delta^{15}N$ isotope values ranged from approx. 3.4 to 7.8‰ in *C. echinata* and from 2.6 to 12.6‰ in *P. verrucosa*.

$\delta^{13}C_{ISO}$ isotope signature ranged from approx. −9.9 to −10.2‰ in *C. echinata* and from −13.2 to −14.5‰ in *P. verrucosa*. No significant differences were observed between the groups in *C. echinata* while in *P. verrucosa*, an enrichment signature was observed in both bleached tissue and symbionts compared to the symbiotic tissue ($p < 0.002$ and $p < 0.0001$). $\delta^{15}N$ isotope values ranged from approx. 4.9 to 8.9‰ in *C. echinata* and from 2.9 to 14.4‰ in *P. verrucosa*.

$\delta^{13}C_{PRO}$ isotope signature ranged from approx. −5.7 to −6.0‰ in *C. echinata* and from −7.0 to −8.3‰ in *P. verrucosa*. No significant differences were observed between the groups in *C. echinata* while in *P. verrucosa*, an enrichment signature was observed in symbionts rather than symbiotic and bleached tissue (both $p < 0.001$). $\delta^{15}N$ isotope values ranged from approx. 4.3 to 7.9‰ in *C. echinata* and from 3.5 to 11.9‰ in *P. verrucosa*.

$\delta^{13}C_{VAL}$ isotope signature ranged from approx. −20.4 to −20.7‰ in *C. echinata* and from −21.6 to −22.4‰ in *P. verrucosa*. No significant differences between host fractions were observed in the species. $\delta^{15}N$ isotope values ranged from approx. 7.4 to 10.1‰ in *C. echinata* and from 4.6 to 15.3‰ in *P. verrucosa.*

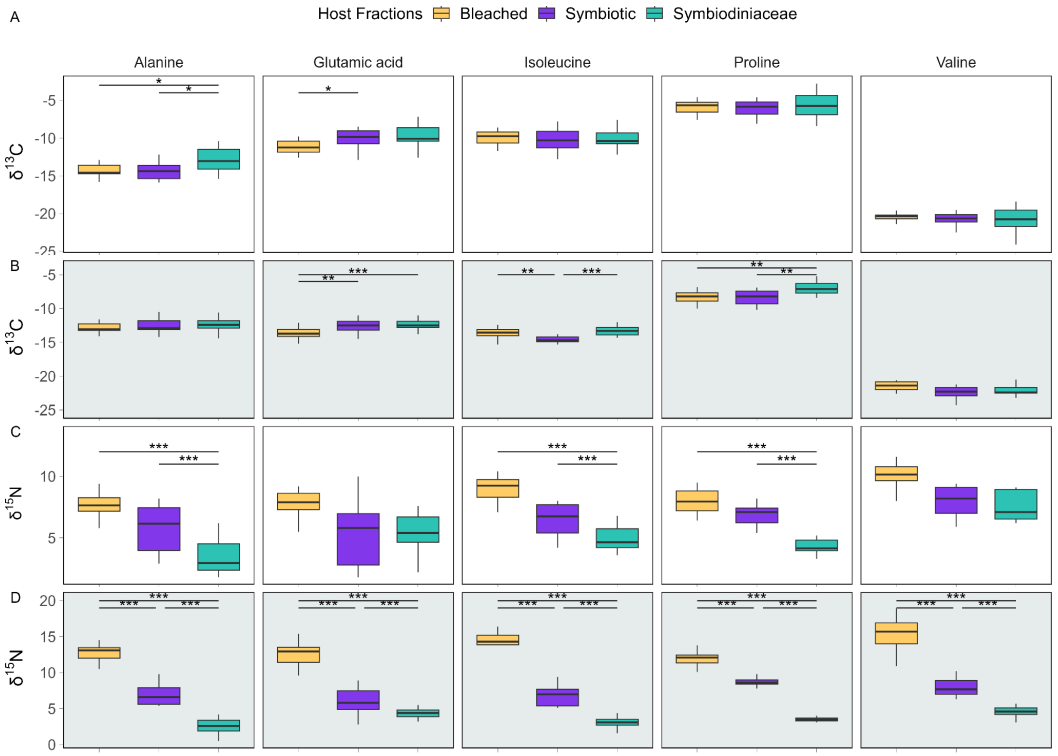

Fig.14. $\delta^{13}C$ and $\delta^{15}N$ isotope values of five trophic amino acids of host tissue and symbionts of symbiotic and bleached corals of *Ctenactis echinata* (white) and *Pocillopora verrucosa* (grey). Alanine, glutamic acid, Isoleucine, Proline and Valine. (AB) $\delta^{13}C$ isotope values (CD) $\delta^{15}N$ isotope values. Significance codes used are defined as $p < 0.001$ (***), $p < 0.01$ (**), $p < 0.05$ (*), $p > 0.05$ (ns = not significant).

3.2.3 Trophic position based on the host tissue and symbionts of bleached and symbiotic corals

The calculated trophic position ($TP_{Glu\text{-}Phe}$) was not significantly different between host fractions in both species, although the highest values were observed in bleached corals of *P. verrucosa* (Fig. 15, linear mixed-effects, Tab. S26-27). *C. echinata* showed ($TP_{Glu\text{-}Phe}$) values ranged from approx. 1.3 to 1.4, while *P. verrucosa* showed values ranged from approx. 1.0 to 1.5.

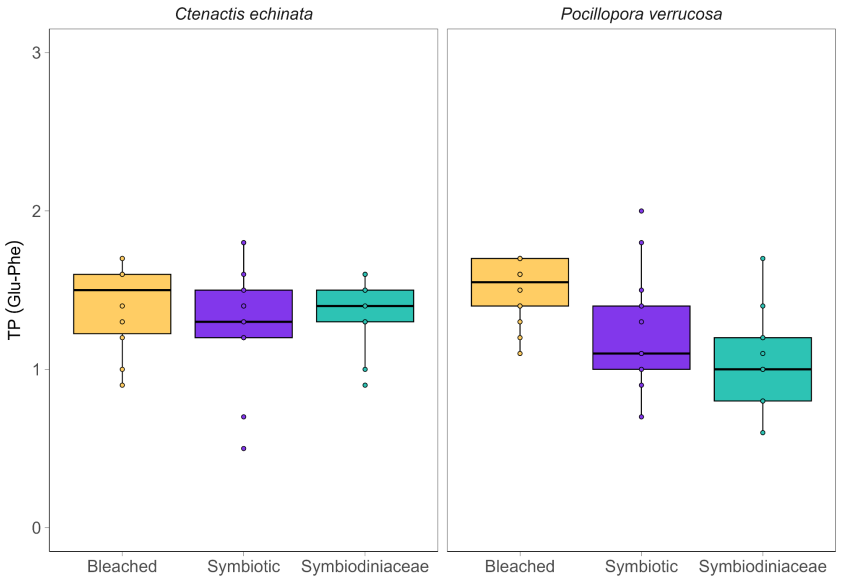

Fig. 15. Calculated trophic position ($TP_{Glu\text{-}Phe}$) from two amino acids (glutamic acid and phenylalanine) of the host tissue and symbionts of bleached and symbiotic *Ctenactis echinata* and *Pocillopora verrucosa*.

3.3 Evaluating interactive effect of heterotrophic feeding, microplastics and heat

The following sections (3.3.1–3.3.4) are based on the publication López et al., (2025). For the purposes of this dissertation, the text and figures have been revised and adapted; however, some similarities with the original version may remain.

3.3.1 Effects of MPs and feeding on coral growth

Exposure to MPs did not affect coral growth when measured as changes in surface area, volume or calcification (Fig. 16a-c, linear mixed-effects models, $p > 0.05$, Tab. S28). Additionally, the feeding regime had no effect on coral growth when exposed to MPs. During the six-week experiment, all corals grew, no regard to the assigned treatment.

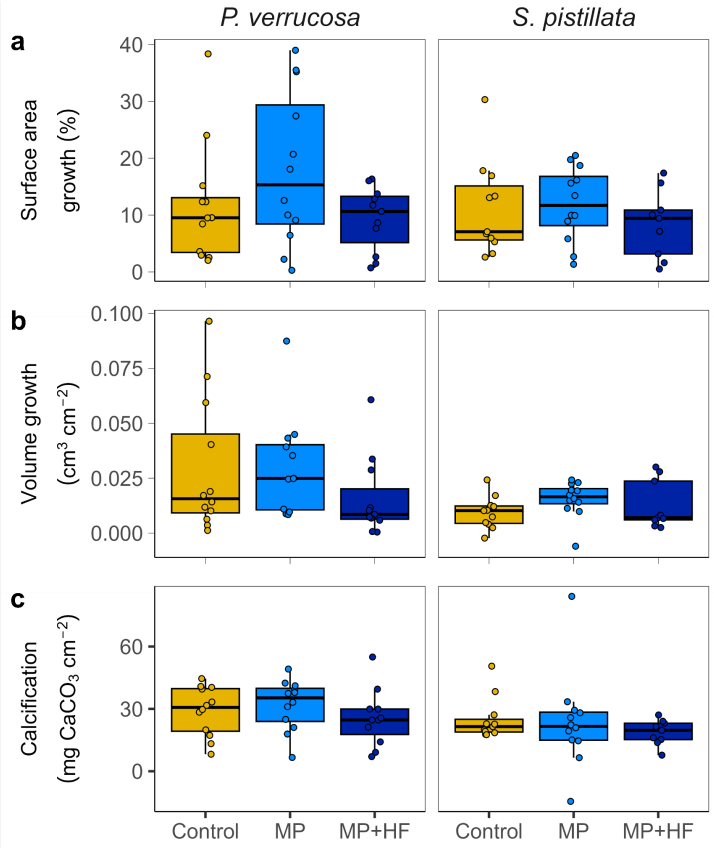

Fig. 16. Growth rates (surface area growth, volume growth, and calcification) of *P. verrucosa* and *S. pistillata* exposed to MPs and two different feeding regimens over six weeks. Control, MP = microplastic, MP+HF = microplastic and high feeding. Figure taken from: López et al., (2025).

3.3.2 Effects of MPs and feeding on photophysiology

The feeding regime and exposure to MPs had different effects on photosynthetic performance (Fig. 17a-c, linear mixed-effects models, Tab. S29). Compared to the control and the MP+HF treatment, the MP treatment increased photosynthetic and respiration rates in *P. verrucosa*. Specifically, net photosynthesis was significantly higher in the MP treatment than in the control and MP+HF treatment ($p < 0.001$), which did not differ significantly from each other (Fig. 17a). Respiration was significantly higher in the MP treatment than in the MP+HF treatment ($p < 0.01$), which were both similar to the control. Gross photosynthesis was also significantly higher in the MP treatment than in the control and MP+HF treatment (both $p < 0.001$), and significantly lower in the MP+HF treatment than in the control treatment ($p < 0.003$). The effective quantum yield was similar between treatments (Fig. 17d). Maximum quantum yield was significantly lower (Fig. 17e) in the MP treatment than in the control treatment ($p < 0.01$), which were both similar to the MP+HF treatment.

The impact of MP and feeding on *S. pistillata* was not the same as the impact on *P. verrucosa* (Fig. 17a-c). Net photosynthesis was significantly lower in the MP+HF treatment than in the MP treatment (linear mixed-effects model, $p = 0.01$), which did not differ significantly from the control treatment. Respiration was significantly lower in the MP+HF treatment than in the control and MP treatment ($p < 0.001$ and $p = 0.001$). Gross photosynthesis was also significantly lower in the MP+HF treatment than in the control and MP treatment ($p = 0.01$ and $p < 0.001$). Photosynthetic efficiency was affected less strongly by the feeding regime and the microplastic exposure than photosynthesis and respiration (Fig. 17d-e, linear mixed-effects models, Tab. S29). Effective quantum yield was similar in all treatments. Maximum quantum yield was significantly higher in the MP+HF treatment than in the control treatment ($p = 0.03$), which did not differ significantly from MP treatment.

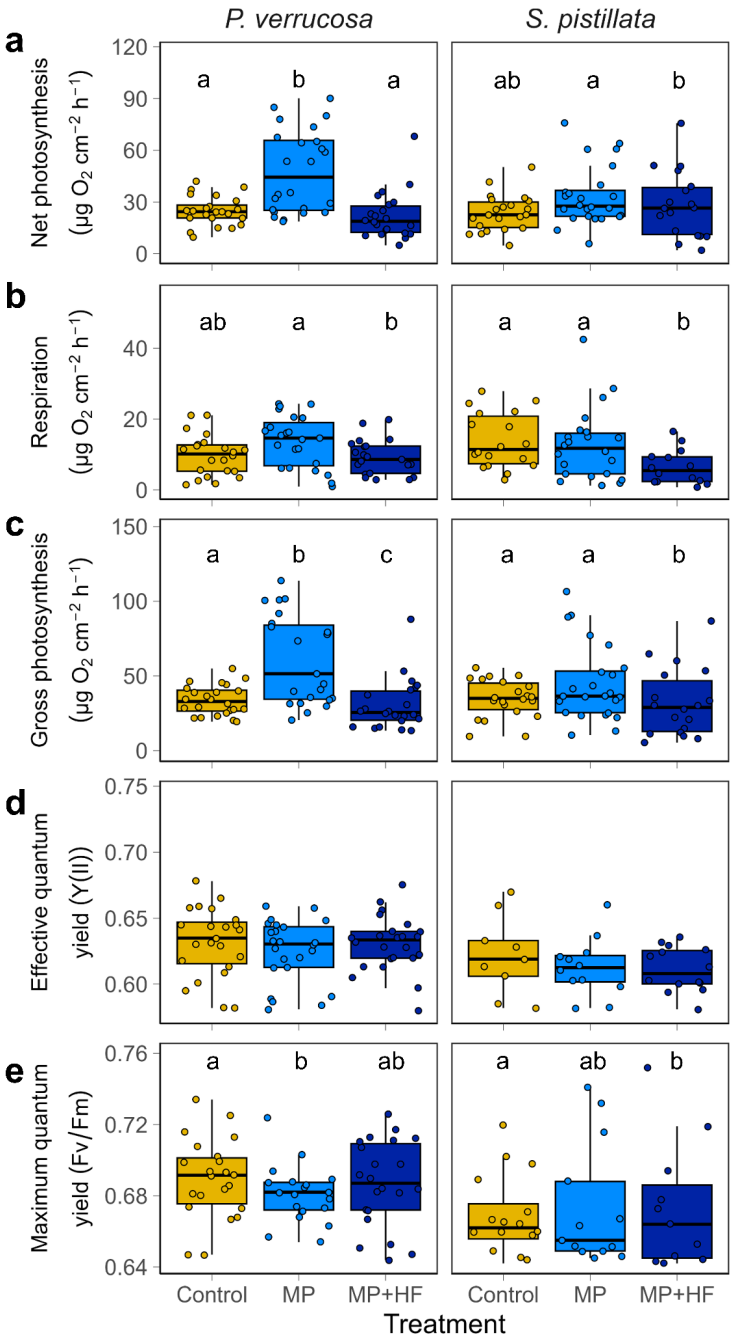

Fig. 17. Photophysiology (net photosynthesis, respiration, gross photosynthesis, effective and maximum quantum yield) of *P. verrucosa* and *S. pistillata* exposed to MPs and two different feeding regimens over six weeks. Control, MP = microplastic, MP+HF = microplastic and high feeding. Groups with different letters are significantly different based on linear mixed-effects models ($p < 0.05$). Figure taken from: López et al., (2025).

3.3.3 Effects of MPs and feeding on tissue composition

MPs and feeding had significant effects on the tissue composition of *P. verrucosa* (Fig. 18a-c, Tab. S30). The carbohydrate content of the holobiont tissue was significantly higher in the control treatment than in either of the MP treatments (linear mixed-effects model, $p < 0.001$ and p <

0.01, Tab. S23), which were not significantly different from each other. Lipid and protein content was significantly higher in the control treatment compared to the MP treatment (both $p < 0.05$), but not the MP+HF treatment, which had intermediate values (Fig. 18b-d). Overall, corals in the control treatment maintained higher tissue energy content than those exposed to the MP treatment for six weeks ($p < 0.05$), while tissue energy content in the MP+HF treatment was intermediate and not significantly different from the other treatments.

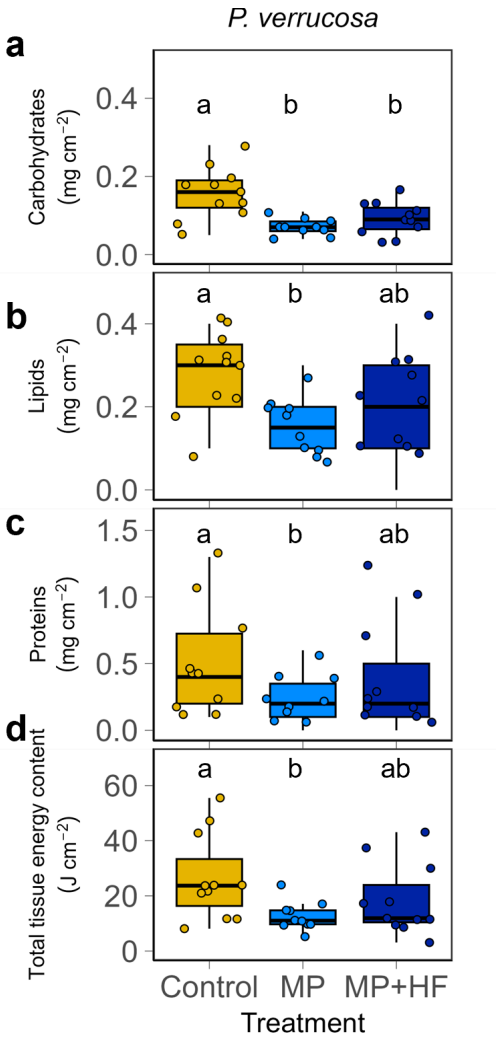

Fig. 18. Tissue composition (carbohydrates, lipids, proteins, and total tissue energy content) of *P. verrucosa* exposed to MPs and two different feeding regimens for six weeks. Control, MP = microplastic, MP+HF = microplastic and high feeding. Groups with different letters are significantly different based on linear mixed-effects models ($p < 0.05$). Figure taken from: López et al., (2025).

3.3.4 Effects of MPs and feeding on coral bleaching susceptibility

The three treatments all resulted in severe bleaching of all corals after the heat stress (Fig. 19). *P. verrucosa* in the MP treatment bleached significantly less than in the control treatment and in the

MP+HF treatment (linear mixed-effects model, $p < 0.05$, $p < 0.01$, Tab. S31). The trend in *S. pistillata* was similar, but no significant differences were detected between treatments.

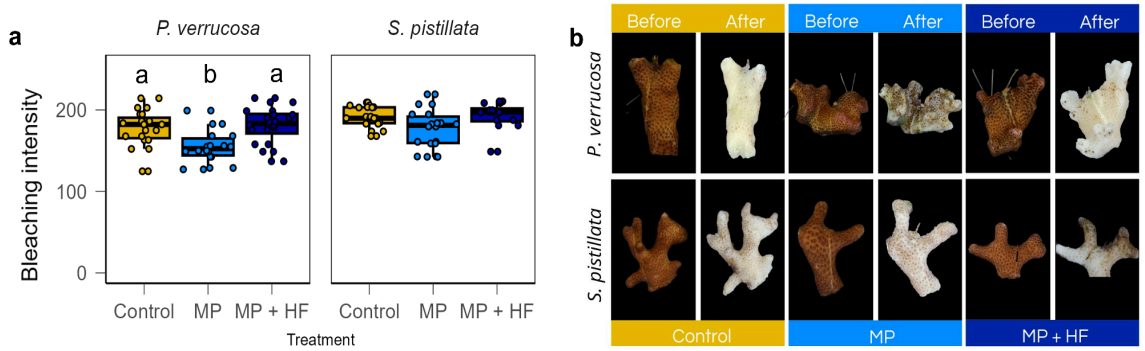

Fig. 19. a) Bleaching intensity of *P. verrucosa* and *S. pistillata* exposed to MPs and two different feeding regimes over six weeks followed by a short-term heat stress. A value of 0 corresponds to black and 255 corresponds to white. Control, MP = microplastic, MP+HF = microplastic and high feeding. Groups with different letters are significantly different based on linear mixed-effects models ($p < 0.05$). b) Example of bleaching severity of *P. verrucosa* (colony B) and *S. pistillata* (colony C) compared at the start of the six-week experiment and after short-term heat stress. Figure taken from: López et al., (2025).

4 Discussion

4.1 Summary of findings

Heterotrophic feeding is widely recognized as a critical mechanism that supports coral survival under environmental stress, particularly in the face of ocean warming (Grottoli et al., 2006; Houlbrèque & Ferrier-Pagès, 2009; Hughes & Grottoli, 2013). This doctoral thesis investigates the role of heterotrophy in enhancing coral tolerance to heat stress and to an emerging local stressor, MPs pollution. Through two controlled laboratory experiments, and a complementary field data analysis, this study provides new insights into how heterotrophic feeding shapes coral performance when exposed to heat stress and MPs pollution, assessed both as isolated stressors and in combination. These findings, published in two peer-reviewed articles with a third manuscript in preparation, advance our understanding of coral trophic plasticity in a multi-stressor context. By integrating controlled experiments with field-based observations, this work offers a holistic perspective on the ecological significance of heterotrophy in corals in a rapidly changing ocean.

In the first study, I examined the physiological responses of both symbiotic and bleached corals to different food types and evaluated the extent to which these diets could offset the loss of photosynthetically derived energy during bleaching. The results indicate that complex diets can bolster the growth of *Galaxea fascicularis, Porites lobata* and *Stylophora pistillata*, although this effect varies by species under non-stressful conditions. The lower metabolic rates observed in bleached fragments compared to their healthy counterparts are consistent with expectations, as the absence of symbionts reduces their contribution to host metabolism. However, the magnitude of the differences between bleached and symbiotic fragments varied among species, with differences being smallest in *G. fascicularis*, followed by *P. lobata* and *S. pistillata*. This pattern likely reflects intrinsic traits such as baseline productivity, heterotrophic capacity, and plasticity in feeding strategies. Together, these results provide new evidence that dietary complexity can enhance the benefits of heterotrophic feeding in bleached corals, highlighting the pivotal role of nutrition in promoting coral resilience.

To provide a broader ecological perspective, the second study examined coral nutritional strategies during a natural bleaching event using *in situ* observations. This represents the first *in situ* evaluation of heterotrophic strategies in bleached corals through compound-specific stable isotope analysis of amino acids (CSIA-AAs). Results showed that, $\delta^{15}N$ values of both source and trophic amino acids were modulated by bleaching, with clear species-specific patterns. Consistent $\delta^{15}N$ enrichment in trophic amino acids among bleached corals indicated metabolic stress and changes in nitrogen processing pathways. Trophic position estimates confirmed the mixotrophic nature of *Ctenactis echinata*, while *Pocillophora verrucosa*, assumed to be primarily autotrophic

(Ziegler et al., 2014), exhibited higher-than-expected heterotrophic plasticity. As the frequency and severity of mass bleaching events continue to rise, understanding the nutritional mechanisms that underpin species-specific resilience in natural environments, is critical for forecasting coral survival.

Building on the finding that food complexity supports the physiology of bleached corals, and considering that contemporary coral reef ecosystems face the threat of multiple stressors, the third study was designed to investigate how food availability interacts with MPs pollution and heat stress. Specifically, I investigated the physiological responses of corals exposed to MPs under two feeding regimes; twice-weekly and daily. After a short-term heat stress event, I further assessed how MPs and food availability influenced coral susceptibility to bleaching. Results revealed that in *Pocillopora verrucosa*, MPs exposure significantly reduced tissue energy reserves, despite increasing photosynthesis and respiration rates. However, high food availability partially mitigated the energy loss induced by MPs while maintaining photosynthesis and respiration levels comparable to controls. In *Stylophora pistillata*, MPs exposure alone did not cause measurable effects; however, in combination with high feeding, photosynthetic rates dropped below those of the control. Both results demonstrate that coral responses to MPs exposure are differentially modulated by food availability. Both results are consistent with recent findings by (Reichert et al., 2024), who identified *P. verrucosa* as a species highly susceptible to MPs, while *S. pistillata* occupies a more intermediate position. Under short-term heat stress, all corals bleached severely, but bleaching was consistently lower in the treatment exposed to MPs and only twice week feeding in both species, supporting the previouss finding that MPs pollution disrupt heterotrophy-mediated thermal resilience in corals (Reichert et al., 2021)**.** These findings underscore the complex nature of coral responses to interacting stressors, with food availability and MPs exposure jointly shaping the outcome of subsequent heat stress. As MPs continue to accumulate in a rapidly warming ocean, further investigation into the interplay between feeding and multi-stressor dynamics is essential for predicting coral resilience.

Together, these three studies converge on the shared goal of elucidating the role of heterotrophic feeding in coral tolerance to ocean warming and MPs pollution. The findings show that complex diets can enhance the benefits of heterotrophy in bleached corals. Additionally, *in situ* bleaching was associated with $\delta^{15}N$ enrichment in both source and trophic amino acids, suggesting shifts in nitrogen acquisition and processing under stress. Finally, food availability was found to mitigate the physiological costs of MPs exposure; however, MPs may also disrupt the relationship between energy balance and thermal resilience.

4.2 Complex diets provide consistent support during coral bleaching

Regardless of symbiotic state and food treatment, photosynthesis and respiration rates remained stable in all species. While earlier studies reported that heterotrophic feeding and food availability enhance photosynthetic and respiration rates (Borell et al., 2008; Dobson et al., 2021; Ferrier-Pagès et al., 2010; Hoogenboom et al., 2010a; Houlbrèque & Ferrier-Pagès, 2009), our analysis provide evidence that diets with different complexity and nutritional value, do not directly affect these variables. This might be explained by the comparably low light levels used during the experiment, which may have limited the capacity to extend autotrophic pathways.

Growth rates observed in both symbiotic and bleached corals provide compelling evidence that the benefits of nutritionally enriched diets are tangible across coral species, even when such benefits are not apparent under non-stressful conditions. *Galaxea fascicularis*, a species known for its high heterotrophic capacity due to its large polyps (Wijgerde et al., 2011), and *Porites lobata*, which also maintains a high basal feeding rate (Palardy et al., 2008), did not exhibit differential growth under symbiotic conditions when exposed to different diets. However, under bleaching conditions, both species increased growth in response to more complex feeds, with the trend reaching statistical significance only in *P. lobata*. This pattern was also observed in *Stylophora pistillata*, a species characterized by a mixotrophic tendency (Martinez et al., 2024), but unlike with the two previous species, *S. pistillata* exhibited increased growth with more complex feeds under both symbiotic and bleached conditions. This finding aligns with previous work showing higher growth in symbiotic *Goniopora columna* fed with a complex mixture of ingredients compared to corals fed only with yeast and microalgae (Ding et al., 2021). The analysis suggests that the synergistic effect of combining diverse dietary components provides the necessary nutrient input to support accelerated growth. These complex diets have in fact been used in laboratory experiments to induce spawning, a period during which the nutritional demands of corals are particularly high (Craggs et al., 2017). While in our results, this effect of complex diets appears species-specific under non-stressful conditions, it is consistently observed across species during bleaching.

Heterotrophic feeding is well known to support the survival and growth of bleached corals (Grottoli et al., 2006; Hughes & Grottoli, 2013; Rodrigues & Grottoli, 2007). The analysis presented here builds on this understanding by providing new evidence that, when provided with a more complex mixture diet, corals can further enhance the benefits of heterotrophy by boosting growth beyond the levels observed with less complex food sources. Due to its high energetic demands, growth is one of the physiological processes most impacted by stress (Cohen & Holcomb, 2009; Dobson et al., 2021; Grottoli et al., 2017; Schoepf et al., 2015). These findings suggest that nutrient-rich, multi-ingredient diets can play a key role in supporting this process.

While all food components used in our feeding trials are generally recognized as beneficial for the growth of aquarium-reared marine organisms, including corals, the specific mixture used in the high-complexity feeding trial was tested here for the first time. This results opens new avenues for research into the use of tailored nutrient blends in coral restoration, aquaculture, and field supplementation protocols aimed at enhancing the resilience of bleached corals.

4.3 Connection between heterotrophic compensation and baseline productivity of corals

As Chapter 4.2 showed that the physiology of all bleached corals benefited from diet complexity, I proposed that diverse food mixtures could help offset the loss of autotrophic input. However, the coral species differed in response magnitude to the food treatments, which points to underlying biological factors such as the inherent productivity levels, heterotrophic capacity (i.e., the ability to acquire and assimilate nutrients heterotrophically), and heterotrophic plasticity (i.e., the ability to modulate trophic strategies in response to environmental change). *G. fascicularis*, the species with the lowest baseline productivity, exhibited the smallest physiological differences between bleached and symbiotic states, with comparable growth and respiration rates. This may be due to its relatively high nutrient assimilation rates even under bleaching stress, indicating that all food treatments may have been sufficient to meet its reduced energy demands and partially offset the loss of autotrophic input. *Galaxea fascicularis* is a fast-feeding coral that requires large quantities of Artemia to reach satiation (Osinga et al., 2012; Tagliafico et al., 2018). More recently, Saper et al., (2023) reported a capture rate of 75 ind. polyp^{-1} h^{-1}, without observing any signs of satiation. In contrast, *P. lobata*, a species with intermediate baseline productivity, showed more pronounced differences between symbiotic and bleached states. This species exhibits a high basal feeding rate and is capable of meeting 40–50% of its metabolic demand through heterotrophy, regardless of its symbiotic condition (Palardy et al., 2008). Previous studies have demonstrated that between 5 and 11 months after experimentally induced bleaching, *Porites lobata* can recover key physiological parameters, such as chlorophyll content and calcification rates, to levels comparable to non-bleached controls (Levas et al., 2013). It is possible that the 18-week (4.5 months) duration of our study may not have been sufficient to allow full physiological recovery to control levels in *P. lobata*. Yet, overall the pattern we observed is in agreement with previous findings. *S. pistillata*, the most productive species, displayed the greatest differences between symbiotic and bleached corals. This could be attributed to its reduced capacity to assimilate heterotrophic nutrients under thermal stress (Ferrier-Pagès et al., 2010; Grottoli et al., 2017; Martinez et al., 2024; Tremblay et al., 2012), limited heterotrophic plasticity (Alamaru et al., 2009), and/or the use of a conservative strategy involving growth suppression to maintain energy reserves and tissue biomass (Grottoli et al., 2017). New strategies of heterotrophic supplementation are being explored to enhance coral stress tolerance, including the Underwater Zooplankton Enhancement Light Array (UZELA), a device designed to increase local zooplankton concentrations *in situ*

(Grottoli et al., 2025). The results presented here, indicate that not all species will benefit from such interventions.

4.4 Distinct heterotrophic strategies in corals during a bleaching event

In this study, Compound-specific stable isotope analysis of amino acids (CSIA-AAs) was applied to investigate the heterotrophic strategies of *Ctenactis echinata* and *Pocillopora verrucosa* during an *in situ* bleaching event occurring across three localities in the Red Sea. The results showed that the $\delta^{13}C$ and $\delta^{15}N$ isotope signature of both source and trophic amino acids were modulated by bleaching, though the extent of this effect depended on the coral species. The most pronounced response was the enrichment of $\delta^{15}N$ in all trophic amino acids, alanine (ALA), glutamic acid (GLU), isoleucine (ISO), proline (PRO) and valine (VAL). This pattern is consistent with a recent report by Martinez et al., (2024), which showed that the coral host of *S. pistillata* exposed to thermal stress, exhibited nitrogen enrichment in ten amino acids, including ALA, VAL and GLU, compared to the symbionts. This response suggests that the bleached host switched to relying on a different nitrogen source compared to the symbiotic tissue and symbionts, likely transitioning from an autotrophic to a heterotrophic source. Additionally, source amino acids such as Asparagyne (ASP), Glycine (GLY), and lysine (LYS) were enriched in all host fractions compared to Methionine (MET) and Phenylananine (PHE) in both species. The trophic position (TP) was 1.3 for the symbiotic host and symbionts, indicating a mixotrophic diet for *C. echinata.* In contrast, the symbiotic host and symbionts of *P. verrucosa* showed TP values of 1.2 and 1.0, respectively, indicating a trend towards autotrophy. Bleached corals from *C. echinata* showed a TP value of 1.4, indicating a mixotrophic diet, whereas *P. verrucosa* showed a TP value of 1.5, suggesting a possible shift towards heterotrophy. This result suggests a higher heterotrophic plasticity of *P. verrucosa* compared to *C. echinata*.

Since $\delta^{13}C$ and $\delta^{15}N$ profiles act as isotopic "fingerprints" that trace nutrient sources (Martinez et al., 2022), comparison with previously published environmental data from the Red Sea (Kürten et al., 2014, 2016), allows us to approximate the potential origins of carbon and nitrogen acquired during bleaching. For example, the essential amino acid PHE, showed $\delta^{13}C$ isotopic signature ranging in both species from –18 to –20 ‰ suggest a predominantly marine origin, likely derived from planktonic sources (values around –18 ‰ in the Read Sea, Kürten et al., 2014), for heterotrophic carbon acquisition. In contrast, the essential amino acids LYS, exhibited a higher $\delta^{13}C$ isotopic signal, ranging from –8.3 to –11.5 ‰ in both species. This pattern indicates that symbiont-derived photosynthates are the primary carbon source for lysine synthesis across all coral compartments, regardless of symbiotic status. Similar to LYS, ASP and GLY also suggest a potential autotrophic source of carbon, regardless of compartment or symbiotic status, although this pattern was only observed in *C. echinata*. Methionine (MET), on the other hand, revealed that

bleached corals acquire carbon for its synthesis from more pelagic sources, showed $\delta^{13}C$ isotopic signature around –20 ‰, whereas symbiotic compartments displayed a benthic-associated carbon signature, with $\delta^{13}C$ isotopic signature around –16 ‰. The consistent enrichment of $\delta^{15}N$ isotopic signature in all trophic amino acids of bleached corals compared with symbiotic tissue and symbionts, suggesting a shift in nitrogen assimilation, potentially from POM (values around 4 ‰ in the Read Sea, Kürten et al., 2014) toward planktonic prey (values around 8 ‰ in the Read Sea, Kürten et al., 2014).

Coral bleaching disrupts the tightly coupled nutrient exchange between coral hosts and their Symbiodiniaceae symbionts, leading to measurable isotopic shifts (Martinez et al., 2024). During bleaching, the collapse of symbiosis reduces autotrophic nitrogen assimilation and photosynthetically fixed carbon supply, forcing corals to increase their reliance on heterotrophic feeding and catabolism of internal nitrogen reserves. Together, our findings suggest that *Ctenactis echinata* exhibits stable mixotrophy with moderate adjustments under stress, despite being considered a highly heterotrophic species (Pogoreutz et al., 2017), whereas *Pocillophora verrucosa*, although typically more autotrophic (Ziegler et al., 2014); shows higher heterotrophic plasticity when bleached. In conclusion, compound-specific isotope analysis of amino acids provides a sensitive framework to detect nutritional plasticity and resilience in corals facing thermal stress. Trophic amino acids serve as reliable indicators of metabolic stress, while source amino acids trace carbon origin, making CSIA-AAs a powerful tool to reconstruct bleaching trajectories and post-bleaching recovery strategies.

4.5 High food availability modulates the effects of MPs exposure

Considering that feeding significantly influences coral physiology, even under stressful conditions, and the fact that reef ecosystems are increasingly exposed to multiple co-occurring stressors alongside ocean warming, an analysis was conducted to examine the physiological effects of MPs pollution and food availability on corals. In both coral species studied, photosynthesis was modulated by MPs exposure. *P. verrucosa* exhibited an upregulation of photosynthesis and respiration under MPs exposure and twice-weekly feeding, consistent with previous studies suggesting a compensatory stress response (Lanctôt et al., 2020; Mendrik et al., 2021; Reichert et al., 2019, 2021; Reichert et al., 2024). However, this response to MPs was mitigated under conditions of daily food availability, which might have buffered the stress response sufficiently to maintain stable photosynthetic rates. In contrast, *S. pistillata* did not show changes in photosynthetic performance due to MPs alone, but a down-regulation was observed when MPs exposure was combined with daily feeding. This contradicts the established assumption that heterotrophic feeding enhances photosynthesis (Houlbrèque & Ferrier-Pagès, 2009) and suggests that MPs may interfere with the response of the symbionts to feeding in this

species. Additionally, *P. verrucosa* exhibited a marked reduction in tissue content of carbohydrates, lipids, and proteins as well as in total energy reserves under MPs exposure, indicating a depletion of energy reserves. This physiological response mirrors that observed under other environmental stressors such as thermal stress and ocean acidification (Rodrigues & Grottoli, 2007; Schoepf et al., 2013), and represents the first documented evidence linking MPs exposure to compromised tissue composition in *P. verrucosa*.

Heterotrophic feeding plays a key role in coral resilience under stressful conditions. Under limited food availability, an increase in autotrophic energy acquisition proved insufficient to prevent tissue energy depletion. In contrast, daily feeding mitigated the negative effects of MPs exposure on tissue energy stores, highlighting the potential of consistent food supply in modulating MPs impacts on coral physiology. It has been suggested that MPs pollution interferes with the heterotrophic feeding of corals, as they are initially unable to distinguish MPs from natural food particles (Reichert, Tirpitz, Oponczewski, et al., 2024). In this study, daily food availability during MPs exposure seemed to be sufficient to cover the metabolic demands. While we did not investigate the processes of uptake of MPs or handling times of particles during our experiment, our results indicate that on an ecological basis, MPs do not seem to affect heterotrophic energy uptake, when enough food is available. These findings emphasise the importance of natural food sources (e.g., plankton and particulate organic matter) for the survival of coral reef ecosystems, and suggest that conservation strategies should aim to preserve and enhance the systems that support the food chain. In this study, *Pocillopora verrucosa* demonstrated greater susceptibility to MPs pollution compared to *Stylophora pistillata*, consistent with previous studies (Reichert et al., 2019, 2021) and with the predictive framework proposed by Reichert et al., (2024). This model identified *P. verrucosa* as the most vulnerable of six coral species, primarily due to its high MPs encounter rate and densely packed polyp morphology, whereas *S. pistillata* was classified as having intermediate susceptibility.

4.6 Microplastics disrupt heterotrophy-mediated thermal resilience in corals

Building on the observation that corals with higher food availability maintained enhanced energy reserves even during MPs exposure, an analysis was conducted to evaluate the connection between the physiological responses to MPs exposure and food availability with the coral's susceptibility to bleaching. The results revealed that corals with a higher tissue energy content were most susceptible to heat stress and bleached more; this pattern was consistent across both the control (MPs-free) and the MPs-treated fragments. These findings challenge the well-established paradigm that enhanced heterotrophic nutrition, resulting in increased tissue stores of carbohydrates, lipids, and proteins, bolsters coral resilience to thermal stress and reduces bleaching susceptibility (Grottoli et al., 2006). Instead, the analysis is more closely aligned with

the report by Reichert et al., (2021), who observed reduced bleaching severity in *Stylophora pistillata* exposed to MPs compared to MPs-free controls under similar feeding regimes. Together, these observations suggest that MPs pollution may disrupt the connection between tissue energy reserves and thermal tolerance.

Heterotrophic feeding is generally accepted to mitigate the effects of thermal stress on corals by reducing their reliance on autotrophic energy pathways (Grottoli et al., 2006; Hoogenboom et al., 2010b). However, the present findings suggest that these buffering mechanisms may be compromised in the presence of MPs. Recently, Isa et al., (2024) demonstrated that under control temperature conditions, MPs addition led to a general down-regulation of stress related genes such as *caspase-3 (cas3)* and *heat shock protein 70 (hsp70)*. In contrast, at elevated temperatures, MPs enrichment strongly up-regulated the expression of these same genes. This cellular response indicates that under heat stress, coral homeostasis is affected by MPs exposure. This effect may be directly linked to the observed disruption between high tissue energy reserves and thermal tolerance, whereby MPs interfere with the effective use of stored carbohydrates, lipids, and proteins. To clarify the underlying processes, future studies should include a daily-fed control group without MPs exposure to determine whether MPs directly affect cellular pathways involved in energy storage, metabolic regulation, or stress signaling. While MPs pollution represents a growing and complex threat to coral health, it is essential to interpret these findings within the broader context of climate change. Ultimately, ocean warming remains the most pervasive driver of coral reef decline, and understanding how emerging stressors like MPs interact with thermal stress is critical to predicting, and potentially mitigating future scenarios.

4.7 Future perspectives: Expanding the understanding of heterotrophic feeding in coral resilience to ocean warming and microplastic pollution

Heterotrophic feeding is a well-established key survival mechanism for corals undergoing bleaching (Grottoli et al., 2006; Hughes & Grottoli, 2013). However, the new insight that enriching coral diets with both particulate and dissolved food sources can further enhance the physiology of bleached corals, opens up an important and largely unexplored area of research. Incorporating a broader range of dietary components into restoration, aquaculture, or field-based supplementation protocols could significantly strengthen coral resilience to the increasing frequency and severity of mass bleaching events. Furthermore, the evidence that MPs pollution disrupts the link between tissue energy reserves and bleaching susceptibility highlights the urgent need to investigate how ocean warming interacts with local stressors (Solomon et al., 2025). Similar to MPs, other local stressors (e.g., nutrient input) may diminish the physiological benefits typically conferred by heterotrophic feeding, further reducing coral survival prospects under current and future climate scenarios (Harris, 2020). Understanding these complex interactions is

essential to refine conservation strategies and maximize the effectiveness of the applied interventions.

Our discovery that the degree to which corals rely on heterotrophy for amino acid synthesis varies between species, underscores the importance of species-specific traits in mediating resilience. This interspecific variability not only highlights the complexity of coral nutritional ecology, but also emphasizes the need to integrate species-specific feeding strategies into management and restoration approaches. Coral trophic strategies are also variable across spatial and temporal gradients (Price et al., 2021; Sturaro et al., 2021; Wall et al., 2019). Trophic behavior can shift with depth (Carmignani et al., 2023; Maier et al., 2010), in response to changes in light availability and turbidity (Anthony & Connolly, 2004; Lesser et al., 2010), or along gradients of inorganic nutrient concentrations (Fox et al., 2018; Thibault et al., 2022). Crucially, not all corals rely on heterotrophy as a compensatory mechanism under environmental stress. For example, Solomon et al., (2025) demonstrated that *Porites* spp. maintained a primarily autotrophic diet even during the wet season, when environmental conditions were more extreme. In contrast, Siderastrea *siderea* and *Siderastrea radians* exhibited a pronounced shift towards heterotrophy under the same conditions. Similarly, Martinez et al., (2024) reported that *Stylophora pistillata*, despite reducing in food assimilation rates under thermal stress, the acquisition of amino acids by the coral host and symbionts still relies on heterotrophy. These findings suggest that coral tolerance to extreme environments is not exclusively dependent on increased heterotrophy, but rather on dynamic, species-specific adjustments in both diet and metabolic pathways. Together, these studies highlight the complexity and nuance of coral nutritional strategies under stress, challenging the notion of a simple binary shift from autotrophy to heterotrophy.

Future investigations must evaluate species-specific dietary dynamics under interacting stressors, both global (e.g., ocean warming, acidification) and local (e.g., MPs pollution, eutrophication, turbidity), rather than assuming that a shift from autotrophy to heterotrophy is a universally beneficial response. A more refined understanding of trophic plasticity together with other mechanisms of resilience such as shifting symbiont community dynamics and energy reserve management, will be critical to predicting coral responses to multifactorial environmental change.

4.8 Conclusions and outlook

This thesis demonstrates the central role of heterotrophic feeding in modulating coral tolerance to the dual pressures of ocean warming and MPs pollution. While the nutritional benefits of heterotrophy vary across species, our findings show that access to diverse heterotrophic food sources can broadly support the physiological performance of bleached corals, regardless of their baseline productivity, heterotrophic capacity or plasticity. Importantly, we reveal that coral

responses to MPs exposure are strongly influenced by food availability. Although heterotrophic feeding modulated the impacts of MPs on photosymbiont performance and host-tissue composition, this buffering did not translate into reduced bleaching susceptibility. Furthermore, this thesis presents the first application of CSIA-AAs during an in situ bleaching event, uncovering species-specific heterotrophic strategies in bleached corals. Together, this novel insights highlights the complexity of coral nutritional ecology and underscores the importance of interspecific differences in determining resilience to environmental stress.

As ocean warming and local stressors intensify, advancing our understanding of coral stress responses under complex, multifactorial conditions will be critical for the design of more effective conservation and management strategies. Addressing these dimensions of heterotrophic plasticity will also be essential for predicting future shifts in reef community composition and identifying the coral species most likely to persist in the near-future predicted global warming scenarios.

5 References

Alamaru, A., Loya, Y., Brokovich, E., Yam, R., & Shemesh, A. (2009). Carbon and nitrogen utilization in two species of Red Sea corals along a depth gradient: Insights from stable isotope analysis of total organic material and lipids. *Geochimica et Cosmochimica Acta*, *73*(18), 5333–5342. https://doi.org/10.1016/j.gca.2009.06.018

Al-Moghrabi, S., Allemand, D., Couret, J., & Jaubert, J. (1995). Fatty acids of the scleractinian coral Galaxea fascicularis: Effect of light and feeding. *Journal of Comparative Physiology B*, *165*, 183–192.

Andrady, A. L. (2011). Microplastics in the marine environment. *Marine Pollution Bulletin*, *62*(8), 1596–1605. https://doi.org/10.1016/j.marpolbul.2011.05.030

Anthony, K. R. N., & Fabricius, K. E. (2000). Shifting roles of heterotrophy and autotrophy in coral energetics under varying turbidity. *Journal of Experimental Marine Biology and Ecology*, *252*(2), 221–253. https://doi.org/10.1016/S0022-0981(00)00237-9

Anthony, K. R., & Connolly, S. R. (2004). Environmental limits to growth: Physiological niche boundaries of corals along turbidity–light gradients. *Oecologia*, *141*(3), 373–384.

Arvedlund, M., Craggs, J., Pecorelli, J., Cato, J., & Brown, C. (2003). Coral culture-possible future trends and directions. *Marine Ornamental Species: Collection, Culture and Conservation*, 233–248.

Axworthy, J. B., & Padilla-Gamiño, J. L. (2019). Microplastics ingestion and heterotrophy in thermally stressed corals. *Scientific Reports*, *9*(1), 18193. https://doi.org/10.1038/s41598-019-54698-7

Barnes, H., & Blackstock, J. (1973). Estimation of lipids in marine animals and tissues: Detailed investigation of the sulphophosphovanilun method for 'total'lipids. *Journal of Experimental Marine Biology and Ecology*, *12*(1), 103–118.

Bates, D., Mächler, M., Bolker, B., & Walker, S. (2015). Fitting Linear Mixed-Effects Models Using lme4. *Journal of Statistical Software*, *67*(1), 1–48. https://doi.org/10.18637/jss.v067.i01

Bauer, L., Ferrara, E., Puntin, G., Paulus, A.-L., Reiser, M., Schmidt, F., Zeh, M., & Ziegler, M. (2025). Establishment of menthol bleaching protocols for six stony coral species. *bioRxiv*, 2025–07.

Badylak, S., Phlips, E., Batich, C., Jackson, M., & Wachnicka, A. (2021). Polystyrene microplastic contamination versus microplankton abundances in two lagoons of the Florida Keys. *Scientific Reports*, *11*(1), 6029. https://doi.org/10.1038/s41598-021-85388-y

Baker, A. C., Glynn, P. W., & Riegl, B. (2008). Climate change and coral reef bleaching: An ecological assessment of long-term impacts, recovery trends and future outlook. *Estuarine, Coastal and Shelf Science*, *80*(4), 435–471. https://doi.org/10.1016/j.ecss.2008.09.003

Bellworthy, J., Spangenberg, J. E., & Fine, M. (2019). Feeding increases the number of offspring but decreases parental investment of Red Sea coral Stylophora pistillata. *Ecology and Evolution*, *9*(21), 12245–12258.

Borell, E. M., Yuliantri, A. R., Bischof, K., & Richter, C. (2008). The effect of heterotrophy on photosynthesis and tissue composition of two scleractinian corals under elevated temperature. *Journal of Experimental Marine Biology and Ecology*, *364*(2), 116–123. https://doi.org/10.1016/j.jembe.2008.07.033

Bove, C. B., Greene, K., Sugierski, S., Kriefall, N. G., Huzar, A. K., Hughes, A. M., Sharp, K., Fogarty, N. D., & Davies, S. W. (2023). Exposure to global change and microplastics elicits an immune response in an endangered coral. *Frontiers in Marine Science*, *9*, 1037130.

Bower, A. S., & Farrar, J. T. (2015). Air–Sea Interaction and Horizontal Circulation in the Red Sea. In N. M. A. Rasul & I. C. F. Stewart (Eds.), *The Red Sea: The Formation, Morphology, Oceanography and Environment of a Young Ocean Basin* (pp. 329–342). Springer Berlin Heidelberg. https://doi.org/10.1007/978-3-662-45201-1_19

Brainard, R. E., Weijerman, M., Eakin, C. M., Mcelhany, P., Miller, M. W., Patterson, M., Piniak, G. A., Dunlap, M. J., & Birkeland, C. (2013). Incorporating Climate and Ocean Change into Extinction Risk Assessments for 82 Coral Species. *Conservation Biology*, *27*(6), 1169–1178. https://doi.org/10.1111/cobi.12171

Brown, B. E. (1997). Coral bleaching: Causes and consequences. *Coral Reefs*, *16*(0), S129–S138. https://doi.org/10.1007/s003380050249

Burge, C. A., Mark Eakin, C., Friedman, C. S., Froelich, B., Hershberger, P. K., Hofmann, E. E., Petes, L. E., Prager, K. C., Weil, E., Willis, B. L., & others. (2014). Climate change influences on marine infectious diseases: Implications for management and society. *Annual Review of Marine Science*, *6*(1), 249–277.

Cantin, N. E., & Lough, J. M. (2014). Surviving Coral Bleaching Events: Porites Growth Anomalies on the Great Barrier Reef. *PLoS ONE*, *9*(2), e88720. https://doi.org/10.1371/journal.pone.0088720

Carmignani, A., Radice, V. Z., McMahon, K. M., Holman, A. I., Miller, K., Grice, K., & Richards, Z. (2023). Levels of autotrophy and heterotrophy in mesophotic corals near the end photic zone. *Frontiers in Marine Science*, *10*, 1089746.

Chaidez, V., Dreano, D., Agusti, S., Duarte, C. M., & Hoteit, I. (2017). Decadal trends in Red Sea maximum surface temperature. *Scientific Reports*, *7*(1), 8144. https://doi.org/10.1038/s41598-017-08146-z

Chikaraishi, Y., Ogawa, N. O., Kashiyama, Y., Takano, Y., Suga, H., Tomitani, A., Miyashita, H., Kitazato, H., & Ohkouchi, N. (2009). Determination of aquatic food-web structure based on compound-specific nitrogen isotopic composition of amino acids. *Limnology and Oceanography: Methods*, *7*(11), 740–750.

Chikaraishi, Y., Steffan, S. A., Ogawa, N. O., Ishikawa, N. F., Sasaki, Y., Tsuchiya, M., & Ohkouchi, N. (2014). High-resolution food webs based on nitrogen isotopic composition of amino acids. *Ecology and Evolution*, *4*(12), 2423–2449.

Cohen, A. L., & Holcomb, M. (2009). Why corals care about ocean acidification: Uncovering the mechanism. *Oceanography*, *22*(4), 118–127.

Conlan, J. A., Bay, L. K., Severati, A., Humphrey, C., & Francis, D. S. (2018). Comparing the capacity of five different dietary treatments to optimise growth and nutritional composition in two scleractinian corals. *PLOS ONE*, *13*(11), e0207956. https://doi.org/10.1371/journal.pone.0207956

Conti-Jerpe, I. E., Thompson, P. D., Wong, C. W. M., Oliveira, N. L., Duprey, N. N., Moynihan, M. A., & Baker, D. M. (2020). Trophic strategy and bleaching resistance in reef-building corals. *Science Advances*, *6*(15), eaaz5443. https://doi.org/10.1126/sciadv.aaz5443

Corinaldesi, C., Canensi, S., Dell'Anno, A., Tangherlini, M., Di Capua, I., Varrella, S., Willis, T. J., Cerrano, C., & Danovaro, R. (2021). Multiple impacts of microplastics can threaten marine habitat-forming species. *Communications Biology*, *4*(1), 431.

Corr, L. T., Berstan, R., & Evershed, R. P. (2007). Optimisation of derivatisation procedures for the determination of δ13C values of amino acids by gas chromatography/combustion/isotope ratio mass spectrometry. *Rapid Communications in Mass Spectrometry: An International Journal Devoted to the Rapid Dissemination of Up-to-the-Minute Research in Mass Spectrometry*, *21*(23), 3759–3771.

Craggs, J., Guest, J. R., Davis, M., Simmons, J., Dashti, E., & Sweet, M. (2017). Inducing broadcast coral spawning ex situ: Closed system mesocosm design and husbandry protocol. *Ecology and Evolution*, *7*(24), 11066–11078.

De La Peña, M. R., Franco, A. V., Igcasan, H. P., Arnaldo, M. D. G. N., Piloton, R. M., Garibay, S. S., & Balinas, V. T. (2018). Microalgal paste production of the diatom Chaetoceros calcitrans using electrolytic flocculation method at optimum culture conditions. *Aquaculture International*, *26*(4), 1119–1134. https://doi.org/10.1007/s10499-018-0272-0

DeCarlo, T. M. (2020). The past century of coral bleaching in the Saudi Arabian central Red Sea. *PeerJ*, *8*, e10200.

De Groot, R., Brander, L., Van Der Ploeg, S., Costanza, R., Bernard, F., Braat, L., Christie, M., Crossman, N., Ghermandi, A., Hein, L., Hussain, S., Kumar, P., McVittie, A., Portela, R., Rodriguez, L. C., Ten Brink, P., & Van Beukering, P. (2012). Global estimates of the value of ecosystems and their services in monetary units. *Ecosystem Services*, *1*(1), 50–61. https://doi.org/10.1016/j.ecoser.2012.07.005

Denis, V., Ferrier-Pagès, C., Schubert, N., Coppari, M., Baker, D. M., Camp, E. F., Gori, A., Grottoli, A. G., Houlbrèque, F., Maier, S. R., & others. (2024). Heterotrophy in marine animal forests in an era of climate change. *Biological Reviews*, *99*(3), 965–978.

DiBattista, J. D., Roberts, M. B., Bouwmeester, J., Bowen, B. W., Coker, D. J., Lozano‐Cortés, D. F., Howard Choat, J., Gaither, M. R., Hobbs, J. A., Khalil, M. T., Kochzius, M., Myers, R. F., Paulay, G., Robitzch, V. S. N., Saenz‐Agudelo, P., Salas, E., Sinclair‐Taylor, T. H., Toonen, R. J., Westneat, M. W., … Berumen, M. L. (2016). A review of contemporary patterns of endemism for shallow water reef fauna in the Red Sea. *Journal of Biogeography*, *43*(3), 423–439. https://doi.org/10.1111/jbi.12649

Ding, D.-S., Sun, W.-T., & Pan, C.-H. (2021). Feeding of a Scleractinian Coral, Goniopora columna, on Microalgae, Yeast, and Artificial Feed in Captivity. *Animals*, *11*(11), 3009. https://doi.org/10.3390/ani11113009

Dobson, K. L., Ferrier-Pagès, C., Saup, C. M., & Grottoli, A. G. (2021). The Effects of Temperature, Light, and Feeding on the Physiology of Pocillopora damicornis, Stylophora pistillata, and Turbinaria reniformis Corals. *Water*, *13*(15), 2048. https://doi.org/10.3390/w13152048

Docherty, G., Jones, V., & Evershed, R. P. (2001). Practical and theoretical considerations in the gas chromatography/combustion/isotope ratio mass spectrometry δ^{13} C analysis of small polyfunctional compounds. *Rapid Communications in Mass Spectrometry*, *15*(9), 730–738. https://doi.org/10.1002/rcm.270

Eakin, C. M., Devotta, D., Heron, S., Connolly, S., Liu, G., Geiger, E., Cour, J. D. L., Gomez, A., Skirving, W., Baird, A., Cantin, N., Couch, C., Donner, S., Gilmour, J., Gonzalez-Rivero, M., Gudka, M., Harrison, H., Hodgson, G., Hoegh-Guldberg, O., … Manzello, D. (2022). *The 2014-17 Global Coral Bleaching Event: The Most Severe and Widespread Coral Reef Destruction* [Preprint]. In Review. https://doi.org/10.21203/rs.3.rs-1555992/v1

Edwards, F. J. (1987). Chapter 3—Climate and Oceanography. In A. J. Edwards & S. M. Head (Eds.), *Red Sea* (pp. 45–69). Pergamon. https://doi.org/10.1016/B978-0-08-028873-4.50008-6

Ferrier-Pagès, C., Hoogenboom, M., & Houlbrèque, F. (2011). The Role of Plankton in Coral Trophodynamics. In Z. Dubinsky & N. Stambler (Eds.), *Coral Reefs: An Ecosystem in Transition* (pp. 215–229). Springer Netherlands. https://doi.org/10.1007/978-94-007-0114-4_15

Ferrier-Pagès, C., Martinez, S., Grover, R., Cybulski, J., Shemesh, E., & Tchernov, D. (2021). Tracing the Trophic Plasticity of the Coral–Dinoflagellate Symbiosis Using Amino Acid Compound-Specific Stable Isotope Analysis. *Microorganisms*, *9*(1), 182. https://doi.org/10.3390/microorganisms9010182

Ferrier-Pagès, C., Rottier, C., Beraud, E., & Levy, O. (2010). Experimental assessment of the feeding effort of three scleractinian coral species during a thermal stress: Effect on the rates of photosynthesis. *Journal of Experimental Marine Biology and Ecology*, *390*(2), 118–124. https://doi.org/10.1016/j.jembe.2010.05.007

Ferrier-Pagès, C., Sauzéat, L., & Balter, V. (2018). Coral bleaching is linked to the capacity of the animal host to supply essential metals to the symbionts. *Global Change Biology*, *24*(7), 3145–3157.

Fine, M., Cinar, M., Voolstra, C. R., Safa, A., Rinkevich, B., Laffoley, D., Hilmi, N., & Allemand, D. (2019). Coral reefs of the Red Sea—Challenges and potential solutions. *Regional Studies in Marine Science*, *25*, 100498. https://doi.org/10.1016/j.rsma.2018.100498

Fisher, R., O'Leary, R. A., Low-Choy, S., Mengersen, K., Knowlton, N., Brainard, R. E., & Caley, M. J. (2015). Species Richness on Coral Reefs and the Pursuit of Convergent Global Estimates. *Current Biology*, *25*(4), 500–505. https://doi.org/10.1016/j.cub.2014.12.022

Fox, M. D., Elliott Smith, E. A., Smith, J. E., & Newsome, S. D. (2019). Trophic plasticity in a common reef-building coral: Insights from δ13C analysis of essential amino acids. *Functional Ecology*, *33*(11), 2203–2214.

Frölicher, T. L., Fischer, E. M., & Gruber, N. (2018). Marine heatwaves under global warming. *Nature*, *560*(7718), 360–364.

Furby, K. A., Bouwmeester, J., & Berumen, M. L. (2013). Susceptibility of central Red Sea corals during a major bleaching event. *Coral Reefs*, *32*(2), 505–513. https://doi.org/10.1007/s00338-012-0998-5

Gattuso, J.-P., Epitalon, J.-M., Lavigne, H., & James Orr. (2021). *seacarb: Seawater Carbonate Chemistry*. https://CRAN.R-project.org/package=seacarb

Gnaiger, E., & Bitterlich, G. (1984). Proximate biochemical composition and caloric content calculated from elemental CHN analysis: A stoichiometric concept. *Oecologia*, *62*(3), 289–298. https://doi.org/10.1007/BF00384259

Gori, A., Tolosa, I., Orejas, C., Rueda, L., Viladrich, N., Grinyó, J., Flögel, S., Grover, R., & Ferrier-Pagès, C. (2018). Biochemical composition of the cold-water coral Dendrophyllia cornigera under contrasting productivity regimes: Insights from lipid biomarkers and compound-specific isotopes. *Deep Sea Research Part I: Oceanographic Research Papers*, *141*, 106–117. https://doi.org/10.1016/j.dsr.2018.08.010

Grottoli, A. G., Rodrigues, L. J., & Palardy, J. E. (2006). Heterotrophic plasticity and resilience in bleached corals. *Nature*, *440*(7088), 1186–1189. https://doi.org/10.1038/nature04565

Grottoli, A., & Wellington, G. (1999). Effect of light and zooplankton on skeletal δ13C values in the eastern Pacific corals Pavona clavus and Pavona gigantea. *Coral Reefs*, *18*, 29–41.

Grottoli, A. G., Tchernov, D., & Winters, G. (2017). Physiological and Biogeochemical Responses of Super-Corals to Thermal Stress from the Northern Gulf of Aqaba, Red Sea. *Frontiers in Marine Science*, *4*, 215. https://doi.org/10.3389/fmars.2017.00215

Grottoli, A. G., Dixon, S. L., Hulver, A. M., Bardin, C. E., Lewis, C. J., Suchocki, C. R., Consortium, R., Toonen, R. J., Jones, B., Levy, J., & others. (2025). Underwater Zooplankton Enhancement Light Array (UZELA): A technology solution to enhance zooplankton abundance and coral feeding in bleached and non-bleached corals. *Limnology and Oceanography: Methods*, *23*(3), 201–211.

Harris, P. T. (2020). Anthropogenic threats to benthic habitats. In *Seafloor geomorphology as benthic habitat* (pp. 35–61). Elsevier.

Hammerman, N. M., Rodriguez-Ramirez, A., Staples, T. L., DeCarlo, T. M., Saderne, V., Roff, G., Leonard, N., Zhao, J., Rossbach, S., Havlik, M. N., Duarte, C. M., & Pandolfi, J. M. (2021). Variable response of Red Sea coral communities to recent disturbance events along a latitudinal gradient. *Marine Biology*, *168*(12), 177. https://doi.org/10.1007/s00227-021-03984-y

Heimann, K., & Huerlimann, R. (2015). Chapter 3—Microalgal Classification: Major Classes and Genera of Commercial Microalgal Species. In S.-K. Kim (Ed.), *Handbook of Marine Microalgae* (pp. 25–41). Academic Press. https://doi.org/10.1016/B978-0-12-800776-1.00003-0

Hoogenboom, M., Rodolfo-Metalpa, R., & Ferrier-Pagès, C. (2010a). Co-variation between autotrophy and heterotrophy in the Mediterranean coral *Cladocora caespitosa*. *Journal of Experimental Biology*, *213*(14), 2399–2409. https://doi.org/10.1242/jeb.040147

Hoogenboom, M., Rodolfo-Metalpa, R., & Ferrier-Pagès, C. (2010b). Co-variation between autotrophy and heterotrophy in the Mediterranean coral Cladocora caespitosa. *Journal of Experimental Biology*, *213*(14), 2399–2409.

Houlbrèque, F., & Ferrier-Pagès, C. (2009). Heterotrophy in Tropical Scleractinian Corals. *Biological Reviews*, *84*(1), 1–17. https://doi.org/10.1111/j.1469-185X.2008.00058.x

Houlbrèque, F., Tambutté, E., & Ferrier-Pagès, C. (2003). Effect of zooplankton availability on the rates of photosynthesis, and tissue and skeletal growth in the scleractinian coral Stylophora pistillata. *Journal of Experimental Marine Biology and Ecology*, *296*(2), 145–166. https://doi.org/10.1016/S0022-0981(03)00259-4

Houlbrèque, F., Tambutté, E., Richard, C., & Ferrier-Pagès, C. (2004). Importance of a micro-diet for scleractinian corals. *Marine Ecology Progress Series*, *282*, 151–160.

Huang, W., Chen, M., Song, B., Deng, J., Shen, M., Chen, Q., Zeng, G., & Liang, J. (2021). Microplastics in the coral reefs and their potential impacts on corals: A mini-review. *Science of The Total Environment*, *762*, 143112. https://doi.org/10.1016/j.scitotenv.2020.143112

Huang, Y.-L., Mayfield, A. B., & Fan, T.-Y. (2020). Effects of feeding on the physiological performance of the stony coral Pocillopora acuta. *Scientific Reports*, *10*(1), 19988. https://doi.org/10.1038/s41598-020-76451-1

Hughes, A. D., & Grottoli, A. G. (2013). Heterotrophic Compensation: A Possible Mechanism for Resilience of Coral Reefs to Global Warming or a Sign of Prolonged Stress? *PLoS ONE*, *8*(11), e81172. https://doi.org/10.1371/journal.pone.0081172

Hughes, T. P., Anderson, K. D., Connolly, S. R., Heron, S. F., Kerry, J. T., Lough, J. M., Baird, A. H., Baum, J. K., Berumen, M. L., Bridge, T. C., Claar, D. C., Eakin, C. M., Gilmour, J. P., Graham, N. A. J., Harrison, H., Hobbs, J.-P. A., Hoey, A. S., Hoogenboom, M., Lowe, R. J., … Wilson, S. K. (2018). Spatial and temporal patterns of mass bleaching of corals in the Anthropocene. *Science*, *359*(6371), 80–83. https://doi.org/10.1126/science.aan8048

Iglesias-Prieto, R., Matta, J. L., Robins, W. A., & Trench, R. K. (1992). Photosynthetic response to elevated temperature in the symbiotic dinoflagellate Symbiodinium microadriaticum in culture. *Proceedings of the National Academy of Sciences*, *89*(21), 10302–10305.

Isa, V., Seveso, D., Diamante, L., Montalbetti, E., Montano, S., Gobbato, J., Lavorano, S., Galli, P., & Louis, Y. D. (2024). Physical and cellular impact of environmentally relevant microplastic exposure on thermally challenged Pocillopora damicornis (Cnidaria, Scleractinia). *Science of The Total Environment*, *918*, 170651. https://doi.org/10.1016/j.scitotenv.2024.170651

Jensen, L. H., Motti, C. A., Garm, A. L., Tonin, H., & Kroon, F. J. (2019). Sources, distribution and fate of microfibres on the Great Barrier Reef, Australia. *Scientific Reports*, *9*(1), 9021. https://doi.org/10.1038/s41598-019-45340-7

Jungblut, S., Liebich, V., & Bode-Dalby, M. (Eds.). (2020). *YOUMARES 9 - The Oceans: Our Research, Our Future: Proceedings of the 2018 conference for Young Marine Researcher in Oldenburg, Germany*. Springer International Publishing. https://doi.org/10.1007/978-3-030-20389-4

LaJeunesse, T. C., Parkinson, J. E., Gabrielson, P. W., Jeong, H. J., Reimer, J. D., Voolstra, C. R., & Santos, S. R. (2018). Systematic Revision of Symbiodiniaceae Highlights the Antiquity and Diversity of Coral Endosymbionts. *Current Biology*, *28*(16), 2570-2580.e6. https://doi.org/10.1016/j.cub.2018.07.008

Kürten, B., Al-Aidaroos, A. M., Kürten, S., El-Sherbiny, M. M., Devassy, R. P., Struck, U., Zarokanellos, N., Jones, B. H., Hansen, T., Bruss, G., & others. (2016). Carbon and nitrogen stable isotope ratios of pelagic zooplankton elucidate ecohydrographic features in the oligotrophic Red Sea. *Progress in Oceanography*, *140*, 69–90.

Kürten, B., Al-Aidaroos, A. M., Struck, U., Khomayis, H. S., Gharbawi, W. Y., & Sommer, U. (2014). Influence of environmental gradients on C and N stable isotope ratios in coral reef biota of the

Red Sea, Saudi Arabia. *Journal of Sea Research*, *85*, 379–394. https://doi.org/10.1016/j.seares.2013.07.008

Lanctôt, C. M., Bednarz, V. N., Melvin, S., Jacob, H., Oberhaensli, F., Swarzenski, P. W., Ferrier-Pagès, C., Carroll, A. R., & Metian, M. (2020). Physiological stress response of the scleractinian coral Stylophora pistillata exposed to polyethylene microplastics. *Environmental Pollution*, *263*, 114559. https://doi.org/10.1016/j.envpol.2020.114559

Leal, M. C., Ferrier‐Pagès, C., Calado, R., Thompson, M. E., Frischer, M. E., & Nejstgaard, J. C. (2014). Coral feeding on microalgae assessed with molecular trophic markers. *Molecular Ecology*, *23*(15), 3870–3876. https://doi.org/10.1111/mec.12486

Lesser, M. P., Slattery, M., Stat, M., Ojimi, M., Gates, R. D., & Grottoli, A. (2010). Photoacclimatization by the coral Montastraea cavernosa in the mesophotic zone: Light, food, and genetics. *Ecology*, *91*(4), 990–1003.

Levas, S. J., Grottoli, A. G., Hughes, A., Osburn, C. L., & Matsui, Y. (2013). Physiological and Biogeochemical Traits of Bleaching and Recovery in the Mounding Species of Coral Porites lobata: Implications for Resilience in Mounding Corals. *PLoS ONE*, *8*(5), e63267. https://doi.org/10.1371/journal.pone.0063267

Lewis, J. B., & Price, W. S. (1975). Feeding mechanisms and feeding strategies of Atlantic reef corals. *Journal of Zoology*, *176*(4), 527–544. https://doi.org/10.1111/j.1469-7998.1975.tb03219.x

López, M. A., Hiemer, L., Engel, M., & Ziegler, M. (2025). *Complex food sources aid physiological compensation of bleached corals*.

López, M. A., Tirpitz, V., Do, M.-S., Czermak, M., Ferrier-Pagés, C., Reichert, J., & Ziegler, M. (2025). Heterotrophic feeding modulates the effects of microplastic on corals, but not when combined with heat stress. *Science of The Total Environment*, *972*, 179026. https://doi.org/10.1016/j.scitotenv.2025.179026

Maier, C., Weinbauer, M. G., & Pätzold, J. (2010). Stable isotopes reveal limitations in C and N assimilation in the Caribbean reef corals Madracis auretenra, M. carmabi and M. formosa. *Marine Ecology Progress Series*, *412*, 103–112.

Martinez, S., Grover, R., Baker, D. M., & Ferrier-Pagès, C. (2022). Symbiodiniaceae Are the First Site of Heterotrophic Nitrogen Assimilation in Reef-Building Corals. *mBio*, *13*(5), e01601-22. https://doi.org/10.1128/mbio.01601-22

Martinez, S., Lalzar, M., Shemesh, E., Einbinder, S., Goodman Tchernov, B., & Tchernov, D. (2020). Effect of Different Derivatization Protocols on the Calculation of Trophic Position Using Amino Acids Compound-Specific Stable Isotopes. *Frontiers in Marine Science*, *7*, 561568. https://doi.org/10.3389/fmars.2020.561568

McMahon, K. W., Hamady, L. L., & Thorrold, S. R. (2013). A review of ecogeochemistry approaches to estimating movements of marine animals. *Limnology and Oceanography*, *58*(2), 697–714.

McMahon, K. W., Thorrold, S. R., Houghton, L. A., & Berumen, M. L. (2016). Tracing carbon flow through coral reef food webs using a compound-specific stable isotope approach. *Oecologia*, *180*, 809–821.

Mendrik, F. M., Henry, T. B., Burdett, H., Hackney, C. R., Waller, C., Parsons, D. R., & Hennige, S. J. (2021). Species-specific impact of microplastics on coral physiology. *Environmental Pollution*, *269*, 116238. https://doi.org/10.1016/j.envpol.2020.116238

Mellin, C., Brown, S., Cantin, N., Klein-Salas, E., Mouillot, D., Heron, S. F., & Fordham, D. A. (2024). Cumulative risk of future bleaching for the world's coral reefs. *Science Advances*, *10*(26), eadn9660. https://doi.org/10.1126/sciadv.adn9660

Miller, M. E., Motti, C. A., Hamann, M., & Kroon, F. J. (2023). Assessment of microplastic bioconcentration, bioaccumulation and biomagnification in a simple coral reef food web. *Science of The Total Environment*, *858*, 159615. https://doi.org/10.1016/j.scitotenv.2022.159615

Monroe, A. A., Ziegler, M., Roik, A., Röthig, T., Hardenstine, R. S., Emms, M. A., Jensen, T., Voolstra, C. R., & Berumen, M. L. (2018). In situ observations of coral bleaching in the central Saudi Arabian Red Sea during the 2015/2016 global coral bleaching event. *PLOS ONE*, *13*(4), e0195814. https://doi.org/10.1371/journal.pone.0195814

Montoya Montoya, L. M., Pérez, A. A. A., Giraldo Calderón, N. D., & Garcés, L. A. (2024). Analysis of cell growth, photosynthetic behavior and the fatty acid profile in Tetraselmis subcordiformis under different lighting scenarios. *Journal of Applied Phycology*, 1–17.

Muscatine, L. (1980). Productivity of zooxanthellae. In *Primary productivity in the sea* (pp. 381–402). Springer.

Muscatine, L., & Cernichiari, E. (1969). Assimilation of photosynthetic products of zooxanthellae by a reef coral. *The Biological Bulletin*, *137*(3), 506–523. https://doi.org/10.2307/1540172

Muscatine, L., Falkowski, P., Dubinsky, Z., Cook, P., & McCloskey, L. (1989). The effect of external nutrient resources on the population dynamics of zooxanthellae in a reef coral. *Proceedings of the Royal Society of London. B. Biological Sciences*, *236*(1284), 311–324.

Osinga, R., Schutter, M., Griffioen, B., Wijffels, R. H., Verreth, J. A. J., Shafir, S., Henard, S., Taruffi, M., Gili, C., & Lavorano, S. (2011). The Biology and Economics of Coral Growth. *Marine Biotechnology*, *13*(4), 658–671. https://doi.org/10.1007/s10126-011-9382-7

Osinga, R., Van Delft, S., Lewaru, M. W., Janse, M., & Verreth, J. A. (2012). Determination of prey capture rates in the stony coral Galaxea fascicularis: A critical reconsideration of the clearance rate concept. *Journal of the Marine Biological Association of the United Kingdom*, *92*(4), 713–719.

Osman, E. O., Smith, D. J., Ziegler, M., Kürten, B., Conrad, C., El-Haddad, K. M., Voolstra, C. R., & Suggett, D. J. (2018). Thermal refugia against coral bleaching throughout the northern Red Sea. *Global Change Biology*, *24*(2), e474–e484.

Palardy, J. E., Rodrigues, L. J., & Grottoli, A. G. (2008). The importance of zooplankton to the daily metabolic carbon requirements of healthy and bleached corals at two depths. *Journal of Experimental Marine Biology and Ecology*, *367*(2), 180–188.

Patterson, J., Jeyasanta, K. I., Sathish, N., Edward, J. P., & Booth, A. M. (2020). Microplastic and heavy metal distributions in an Indian coral reef ecosystem. *Science of the Total Environment*, *744*, 140706.

Pineda, J., Starczak, V., Tarrant, A., Blythe, J., Davis, K., Farrar, T., Berumen, M., & Da Silva, J. C. B. (2013). Two spatial scales in a bleaching event: Corals from the mildest and the most extreme thermal environments escape mortality. *Limnology and Oceanography*, *58*(5), 1531–1545. https://doi.org/10.4319/lo.2013.58.5.1531

Popp, B. N., Graham, B. S., Olson, R. J., Hannides, C. C., Lott, M. J., López-Ibarra, G. A., Galván-Magaña, F., & Fry, B. (2007). Insight into the trophic ecology of yellowfin tuna, Thunnus albacares, from compound-specific nitrogen isotope analysis of proteinaceous amino acids. *Terrestrial Ecology*, *1*, 173–190.

Pogoreutz, C., Rädecker, N., Cárdenas, A., Gärdes, A., Wild, C., & Voolstra, C. R. (2017). Nitrogen fixation aligns with nifH abundance and expression in two coral trophic functional groups. *Frontiers in Microbiology*, *8*, 1187.

Prézelin, B. (1987). Photosynthetic physiology of dinoflagellates. *The Biology of Dinoflagellates*.

Price, J. T., McLachlan, R. H., Jury, C. P., Toonen, R. J., & Grottoli, A. G. (2021). Isotopic approaches to estimating the contribution of heterotrophic sources to Hawaiian corals. *Limnology and Oceanography*, *66*(6), 2393–2407.

Price, W. S., & Patterson, M. R. (2023). Microscale flow dynamics and particle capture in scleractinian corals: I. Role of the tentacles. *Coral Reefs*, *42*(3), 761–783.

Puntin, G., Wong, J. C., Roethig, T., Baker, D. M., Sweet, M., & Ziegler, M. (2023). The bacterial microbiome of symbiotic and menthol-bleached polyps of Galaxea fascicularis in captivity. *bioRxiv*, 2023–08.

R Core Team. (2022). *R: A Language and Environment for Statistical Computing*. R Foundation for Statistical Computing. https://www.R-project.org/

Raitsos, D. E., Hoteit, I., Prihartato, P. K., Chronis, T., Triantafyllou, G., & Abualnaja, Y. (2011). Abrupt warming of the Red Sea: Red Sea climate driven warming. *Geophysical Research Letters*, *38*(14), n/a-n/a. https://doi.org/10.1029/2011GL047984

Ramsperger, A. F., Stellwag, A. C., Caspari, A., Fery, A., Lueders, T., Kress, H., Löder, M. G., & Laforsch, C. (2020). Structural diversity in early-stage biofilm formation on microplastics depends on environmental medium and polymer properties. *Water*, *12*(11), 3216.

Reichert, J., Tirpitz, V., Anand, R., Bach, K., Knopp, J., Schubert, P., Wilke, T., & Ziegler, M. (2021). Interactive effects of microplastic pollution and heat stress on reef-building corals. *Environmental Pollution*, *290*, 118010. https://doi.org/10.1016/j.envpol.2021.118010

Reichert, J., Tirpitz, V., Oponczewski, M., Lin, C., Franke, N., Ziegler, M., & Wilke, T. (2024a). Feeding responses of reef-building corals provide species-and concentration-dependent risk assessment of microplastic. *Science of the Total Environment*, *913*, 169485.

Reichert, J., Tirpitz, V., Oponczewski, M., Lin, C., Franke, N., Ziegler, M., & Wilke, T. (2024b). Feeding responses of reef-building corals provide species-and concentration-dependent risk assessment of microplastic. *Science of The Total Environment*, *913*, 169485.

Reichert, J., Tirpitz, V., Plaza, K., Wörner, E., Bösser, L., Kühn, S., Primpke, S., Schubert, P., Ziegler, M., & Wilke, T. (2024). Common types of microdebris affect the physiology of reef-building corals. *Science of The Total Environment*, *912*, 169276. https://doi.org/10.1016/j.scitotenv.2023.169276

Ripple, W. J., Wolf, C., Gregg, J. W., Rockström, J., Mann, M. E., Oreskes, N., Lenton, T. M., Rahmstorf, S., Newsome, T. M., Xu, C., Svenning, J.-C., Pereira, C. C., Law, B. E., & Crowther, T. W. (2024). The 2024 state of the climate report: Perilous times on planet Earth. *BioScience*, *74*(12), 812–824. https://doi.org/10.1093/biosci/biae087

Rodrigues, L. J., & Grottoli, A. G. (2007). Energy reserves and metabolism as indicators of coral recovery from bleaching. *Limnology and Oceanography*, *52*(5), 1874–1882. https://doi.org/10.4319/lo.2007.52.5.1874

Rotjan, R. D., Sharp, K. H., Gauthier, A. E., Yelton, R., Lopez, E. M. B., Carilli, J., Kagan, J. C., & Urban-Rich, J. (2019). Patterns, dynamics and consequences of microplastic ingestion by the temperate coral, *Astrangia poculata*. *Proceedings of the Royal Society B: Biological Sciences*, *286*(1905), 20190726. https://doi.org/10.1098/rspb.2019.0726

Saper, J., Høj, L., Humphrey, C., & Bourne, D. G. (2023). Quantifying capture and ingestion of live feeds across three coral species. *Coral Reefs*, *42*(4), 931–943.

Savinelli, B., Fernández, T. V., Galasso, N. M., D'Anna, G., Pipitone, C., Prada, F., Zenone, A., Badalamenti, F., & Musco, L. (2020). Microplastics impair the feeding performance of a Mediterranean habitat-forming coral. *Marine Environmental Research*, *155*, 104887.

Sebens, K., Grace, S., Helmuth, B., Maney Jr, E., & Miles, J. (1998). Water flow and prey capture by three scleractinian corals, Madracis mirabilis, Montastrea cavernosa and Porites porites, in a field enclosure. *Marine Biology*, *131*, 347–360.

Selosse, M., Charpin, M., & Not, F. (2017). Mixotrophy everywhere on land and in water: The *grand écart* hypothesis. *Ecology Letters*, *20*(2), 246–263. https://doi.org/10.1111/ele.12714

Sheridan, C., Grosjean, P., Leblud, J., Palmer, C. V., Kushmaro, A., & Eeckhaut, I. (2014). Sedimentation rapidly induces an immune response and depletes energy stores in a hard coral. *Coral Reefs*, *33*, 1067–1076.

Schoepf, V., Grottoli, A. G., Levas, S. J., Aschaffenburg, M. D., Baumann, J. H., Matsui, Y., & Warner, M. E. (2015). Annual coral bleaching and the long-term recovery capacity of coral. *Proceedings of the Royal Society B: Biological Sciences*, *282*(1819), 20151887.

Schoepf, V., Grottoli, A. G., Warner, M. E., Cai, W.-J., Melman, T. F., Hoadley, K. D., Pettay, D. T., Hu, X., Li, Q., Xu, H., Wang, Y., Matsui, Y., & Baumann, J. H. (2013). Coral Energy Reserves and Calcification in a High-CO2 World at Two Temperatures. *PLoS ONE*, *8*(10), e75049. https://doi.org/10.1371/journal.pone.0075049

Sofianos, S. S., & Johns, W. E. (2003). An Oceanic General Circulation Model (OGCM) investigation of the Red Sea circulation: 2. Three‐dimensional circulation in the Red Sea. *Journal of Geophysical Research: Oceans*, *108*(C3), 2001JC001185. https://doi.org/10.1029/2001JC001185

Solomon, S. L., de Goeij, J. M., Croasdale, E. M., & Schoepf, V. (2025). *Limnology and Oceanography*.

Spencer Davies, P. (1989). Short-term growth measurements of corals using an accurate buoyant weighing technique. *Marine Biology*, *101*(3), 389–395. https://doi.org/10.1007/BF00428135

Sturaro, N., Hsieh, Y. E., Chen, Q., Wang, P., & Denis, V. (2021). Trophic plasticity of mixotrophic corals under contrasting environments. *Functional Ecology*, *35*(12), 2841–2855. https://doi.org/10.1111/1365-2435.13924

Swain, T. D., Vega‐Perkins, J. B., Oestreich, W. K., Triebold, C., DuBois, E., Henss, J., Baird, A., Siple, M., Backman, V., & Marcelino, L. (2016). Coral bleaching response index: A new tool to standardize and compare susceptibility to thermal bleaching. *Global Change Biology*, *22*(7), 2475–2488. https://doi.org/10.1111/gcb.13276

Swanson, R., & Hoegh-Guldberg, O. (1998). Amino acid synthesis in the symbiotic sea anemone Aiptasia pulchella. *Marine Biology*, *131*, 83–93.

Tagliafico, A., Rangel, S., Kelaher, B., & Christidis, L. (2018). Optimizing heterotrophic feeding rates of three commercially important scleractinian corals. *Aquaculture*, *483*, 96–101. https://doi.org/10.1016/j.aquaculture.2017.10.013

Thibault, M., Houlbreque, F., Duprey, N. N., Choisnard, N., Gillikin, D. P., Meunier, V., Benzoni, F., Ravache, A., & Lorrain, A. (2022). Seabird-derived nutrients supply modulates the trophic strategies of mixotrophic corals. *Frontiers in Marine Science*, *8*, 790408.

Tignat-Perrier, R., Van De Water, J. A. J. M., Guillemain, D., Aurelle, D., Allemand, D., & Ferrier-Pagès, C. (2022). The Effect of Thermal Stress on the Physiology and Bacterial Communities of Two Key Mediterranean Gorgonians. *Applied and Environmental Microbiology*, *88*(6), e02340-21. https://doi.org/10.1128/aem.02340-21

Toh, T. C., Ng, C. S. L., Peh, J. W. K., Toh, K. B., & Chou, L. M. (2014). Augmenting the post-transplantation growth and survivorship of juvenile scleractinian corals via nutritional enhancement. *PLoS One*, *9*(6), e98529.

Tolosa, I., Treignier, C., Grover, R., & Ferrier-Pagès, C. (2011). Impact of feeding and short-term temperature stress on the content and isotopic signature of fatty acids, sterols, and alcohols in the scleractinian coral Turbinaria reniformis. *Coral Reefs*, *30*, 763–774.

Treignier, C., Grover, R., Ferrier-Pages, C., & Tolosa, I. (2008). Effect of light and feeding on the fatty acid and sterol composition of zooxanthellae and host tissue isolated from the scleractinian coral Turbinaria reniformis. *Limnology and Oceanography*, *53*(6), 2702–2710.

Tremblay, P., Gori, A., Maguer, J. F., Hoogenboom, M., & Ferrier-Pagès, C. (2016). Heterotrophy promotes the re-establishment of photosynthate translocation in a symbiotic coral after heat stress. *Scientific Reports*, *6*(1), 38112. https://doi.org/10.1038/srep38112

Tremblay, P., Maguer, J. F., Grover, R., & Ferrier-Pages, C. (2015). Trophic dynamics of scleractinian corals: Stable isotope evidence. *The Journal of Experimental Biology*, *218*(8), 1223–1234.

Tremblay, P., Naumann, M., Sikorski, S., Grover, R., & Ferrier-Pagès, C. (2012). Experimental assessment of organic carbon fluxes in the scleractinian coral Stylophora pistillata during a thermal and photo stress event. *Marine Ecology Progress Series*, *453*, 63–77. https://doi.org/10.3354/meps09640

Voolstra, C. R., Buitrago-López, C., Perna, G., Cárdenas, A., Hume, B. C., Rädecker, N., & Barshis, D. J. (2020). Standardized short-term acute heat stress assays resolve historical differences in coral thermotolerance across microhabitat reef sites. *Global Change Biology*, *26*(8), 4328–4343.

Wall, C. B., Ritson-Williams, R., Popp, B. N., & Gates, R. D. (2019). Spatial variation in the biochemical and isotopic composition of corals during bleaching and recovery. *Limnology and Oceanography*, *64*(5), 2011–2028.

Wang, J., & Douglas, A. (1999). Essential amino acid synthesis and nitrogen recycling in an alga–invertebrate symbiosis. *Marine Biology*, *135*, 219–222.

Wang, J.-T., Chen, Y.-Y., Tew, K. S., Meng, P.-J., & Chen, C. A. (2012). *Physiological and biochemical performances of menthol-induced aposymbiotic corals*.

Wickham, H. (2016). *ggplot2: Elegant Graphics for Data Analysis*. Springer-Verlag New York. https://ggplot2.tidyverse.org

Wijgerde, T., Diantari, R., Lewaru, M. W., Verreth, J. A., & Osinga, R. (2011). Extracoelenteric zooplankton feeding is a key mechanism of nutrient acquisition for the scleractinian coral Galaxea fascicularis. *Journal of Experimental Biology*, *214*(20), 3351–3357.

Wilkinson, C. (2008). Status of coral reefs of the world: 2008 global coral reef monitoring network and reef and rainforest research centre. *Townsville, Australia*, *296*.

Yarnes, C. T., & Herszage, J. (2017). The relative influence of derivatization and normalization procedures on the compound-specific stable isotope analysis of nitrogen in amino acids. *Rapid Communications in Mass Spectrometry*, *31*(8), 693–704.

Yonge, C. (1931). Studies on the physiology of corals. IV. The structure, distribution and physiology of the zooxanthellae. *Great Barrier Reef Exped 1928-29 Sci Rep*, *1*, 135–176.

Zaidi, P. N., Mustaffa, F. A. A., & Chun, T. (2023). Influence of different feeding regimes on the survival and growth of Acropora digitifera in husbandry. *Journal of Sustainability Science and Management*, *18*(1), 118–132.

Ziegler, M., Roder, C. M., Büchel, C., & Voolstra, C. R. (2014). Limits to physiological plasticity of the coral Pocillopora verrucosa from the central Red Sea. *Coral Reefs*, *33*(4), 1115–1129.

6 Appendix

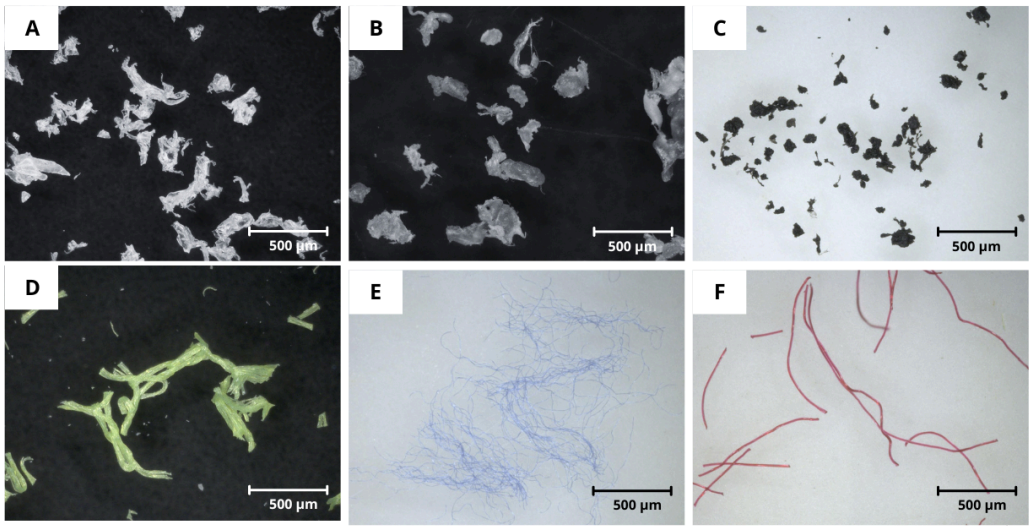

Fig. S1. Types of microplastics used during the experiment. A: polystyrene (PS), B: polyvinyl chloride (PVC), C: polyethylene (PE), D: polyamide (PA), E: polyethylene terephthalate (PET), and F: polypropylene (PP). A, B, and C are fragments; D, E, and F are fibers.

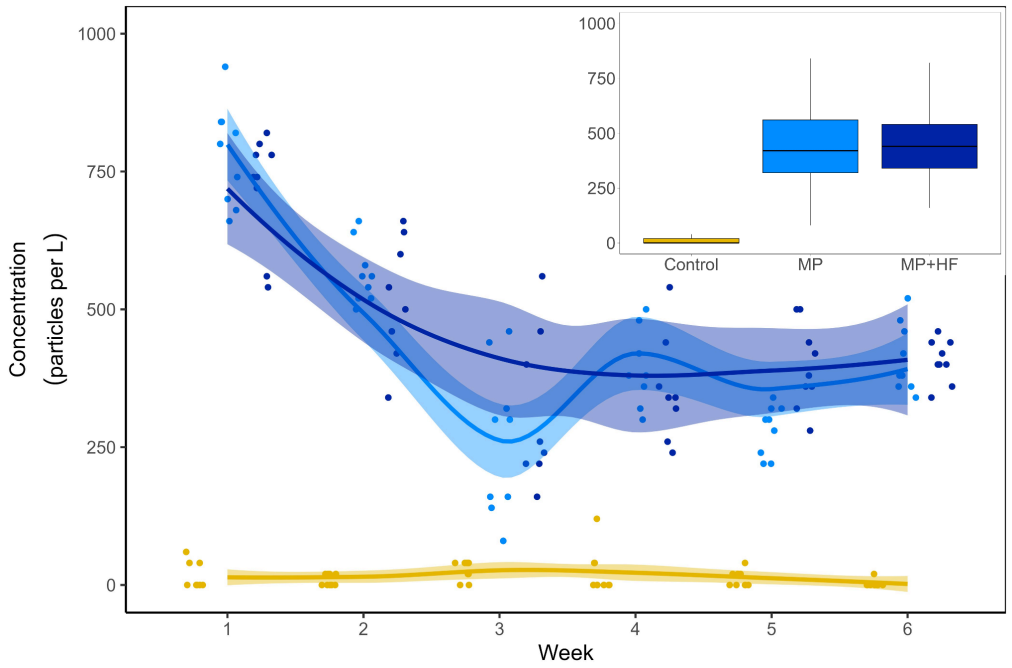

Fig. S2. Total microplastic concentration during six weeks of exposure shown as smooth line plots. Average concentrations over the whole experimental period are displayed as boxplots. Control (yellow), MP = microplastic (light blue), MP+HF = microplastic and high feeding (dark blue).

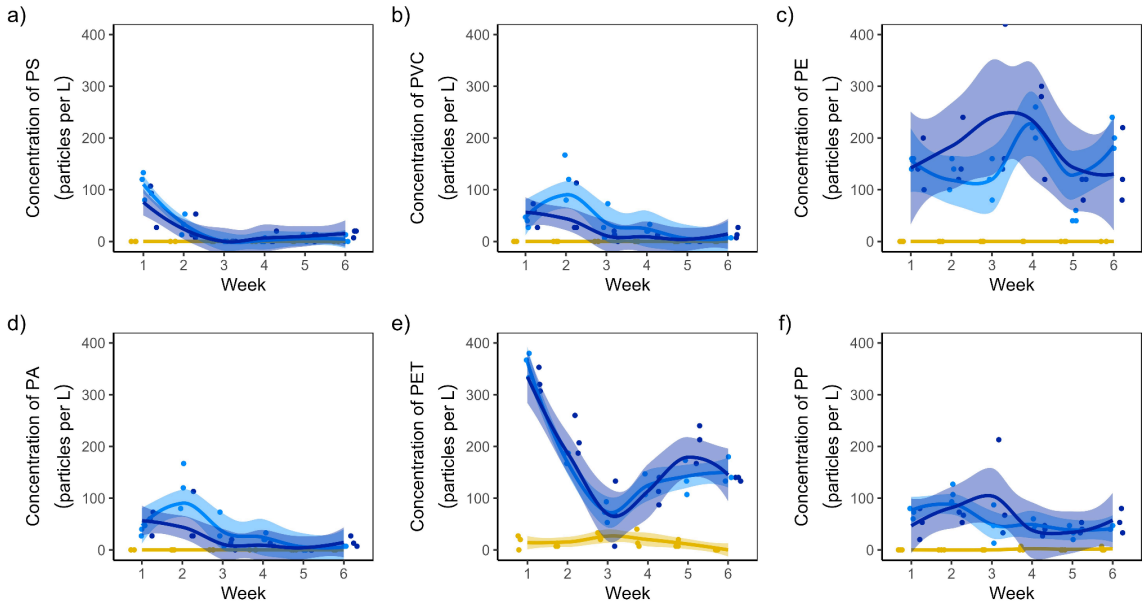

Fig. S3. Microplastic concentrations of the different polymers used during the six-week experiment. a) polystyrene (PS), b) polyvinyl chloride (PVC), c) polyethylene (PE), d) polyamide (PA), e) polyethylene terephthalate (PET), and f) polypropylene (PP). Control (yellow), MP = microplastic (light blue), MP+HF = microplastic and high feeding (dark blue).

Tab. S1. Literature reviewed (2006 – July 2025). Heterotrophic feeding (HF) in bleaching corals and MPs pollution.

N°	Year	HF+Heat	HF+Heat+MPs	Citation
1	2006	✔		Grottoli et al., 2006
2	2008	✔		Borell et al., 2008
3	2008	✔		Rodolfo-Metalpa et al., 2008
4	2008	✔		Palardy et al., 2008
5	2008	✔		Borell & Bischof, 2008
6	2010	✔		Ferrier-Pagès et al., 2010
7	2010	✔		Hughes et al., 2010
8	2011	✔		Tolosa et al., 2011
9	2012	✔		Connolly et al., 2012
10	2012	✔		Seemann et al., 2012
11	2012	✔		Tremblay et al., 2012
12	2012	✔		Hoogenboom et al., 2012
13	2013	✔		Hughes & Grottoli, 2013
14	2013	✔		Levas et al., 2013
15	2016	✔		Tremblay et al., 2016
16	2016	✔		Levy et al., 2016
17	2016	✔		Levas et al., 2016
18	2016	✔		Aichelman et al., 2016
19	2017	✔		Tagliafico et al., 2017
20	2018	✔		Krueger et al., 2018
21	2018	✔		Ferrier-Pagès et al., 2018
22	2019		✔	Axworthy & Padilla-Gamiño, 2019
23	2019	✔		Ezzat et al., 2019
24	2020	✔		Sangmanee et al., 2020
25	2021	✔		Huffmyer et al., 2021
26	2024	✔		Martinez et al., 2024
27	2024	✔		Hendrickson et al., 2024
28	2025		✔	López et al., 2025

Tab. S2. Linear mixed effects model results of calcification, volume growth and surface area growth of symbiotic *Galaxea fascicularis* fed with different food treatments over 18 weeks. Standard error (st.error), statistics (stats.), and significance (sig.). Model specifications: model <- lmer(scale(variable) ~food + (1|genotype), data=data. Significance codes used are defined for p values: p < 0.001 (***), p < 0.01 (**), p < 0.05 (*), ns = not significant.

Variable/Food options	std. error	statistic	p-value	sig.
Calcification				
Dissolved food - Thawed plankton	0.41	0.35	1.00	ns
Low complexity - Thawed plankton	0.40	0.07	1.00	ns
Medium complexity - Thawed plankton	0.40	0.12	1.00	ns
High complexity - Thawed plankton	0.42	1.20	0.75	ns
Low complexity - Dissolved food	0.41	-0.29	1.00	ns
Medium complexity - Dissolved food	0.41	-0.24	1.00	ns
High complexity - Dissolved food	0.43	0.84	0.92	ns
Medium complexity - Low complexity	0.40	0.05	1.00	ns
High complexity - Low complexity	0.42	1.14	0.79	ns
High complexity - Medium complexity	0.42	1.09	0.81	ns
Volume growth				
Dissolved food - Thawed plankton	0.50	0.17	1.00	ns
Low complexity - Thawed plankton	0.47	1.79	0.38	ns
Medium complexity - Thawed plankton	0.47	0.25	1.00	ns
High complexity - Thawed plankton	0.50	0.54	0.98	ns
Low complexity - Dissolved food	0.50	1.50	0.56	ns
Medium complexity - Dissolved food	0.50	0.06	1.00	ns
High complexity - Dissolved food	0.53	0.35	1.00	ns
Medium complexity - Low complexity	0.47	-1.54	0.54	ns
High complexity - Low complexity	0.50	-1.13	0.79	ns
High complexity - Medium complexity	0.50	0.31	1.00	ns
Surface area growth				
Dissolved food - Thawed plankton	0.50	-0.61	0.97	ns
Low complexity - Thawed plankton	0.47	-0.04	1.00	ns
Medium complexity - Thawed plankton	0.47	-0.68	0.96	ns
High complexity - Thawed plankton	0.51	0.94	0.88	ns
Low complexity - Dissolved food	0.50	0.58	0.98	ns
Medium complexity - Dissolved food	0.50	-0.03	1.00	ns
High complexity - Dissolved food	0.54	1.46	0.59	ns
Medium complexity - Low complexity	0.47	-0.65	0.97	ns
High complexity - Low complexity	0.51	0.97	0.87	ns
High complexity - Medium complexity	0.51	1.57	0.51	ns

Tab. S3. Linear mixed effects model results of net photosynthesis, respiration, and gross photosynthesis of symbiotic *Galaxea fascicularis* fed with different food treatments over 18 weeks. Standard error (st.error), statistics (stats.), significance (sig.). Model specifications: model <- lmer(scale(variable) ~food + (1|genotype), data=data. Significance codes used are defined as: $p < 0.001$ (***), $p < 0.01$ (**), $p < 0.05$ (*), ns = not significant.

Variable/Food options	std. error	statistic	p-value	sig.
Net photosynthesis				
Dissolved food - Thawed plankton	0.51	-0.24	1.00	ns
Low complexity - Thawed plankton	0.51	-1.24	0.73	ns
Medium complexity - Thawed plankton	0.50	-0.01	1.00	ns
High complexity - Thawed plankton	0.50	-0.77	0.94	ns
Low complexity - Dissolved food	0.51	-0.99	0.86	ns
Medium complexity - Dissolved food	0.50	0.24	1.00	ns
High complexity - Dissolved food	0.50	-0.52	0.99	ns
Medium complexity - Low complexity	0.50	1.26	0.72	ns
High complexity - Low complexity	0.50	0.50	0.99	ns
High complexity - Medium complexity	0.48	-0.78	0.94	ns
Respiration				
Dissolved food - Thawed plankton	0.48	-2.04	0.25	ns
Low complexity - Thawed plankton	0.48	-0.89	0.90	ns
Medium complexity - Thawed plankton	0.46	-1.16	0.78	ns
High complexity - Thawed plankton	0.47	-1.67	0.45	ns
Low complexity - Dissolved food	0.49	1.12	0.80	ns
Medium complexity - Dissolved food	0.48	0.92	0.89	ns
High complexity - Dissolved food	0.48	0.42	0.99	ns
Medium complexity - Low complexity	0.48	-0.24	1.00	ns
High complexity - Low complexity	0.48	-0.73	0.95	ns
High complexity - Medium complexity	0.47	-0.51	0.99	ns
Gross photosynthesis				
Dissolved food - Thawed plankton	0.53	-0.95	0.88	ns
Low complexity - Thawed plankton	0.51	-1.20	0.75	ns
Medium complexity - Thawed plankton	0.53	-0.37	1.00	ns
High complexity - Thawed plankton	0.51	-1.40	0.63	ns
Low complexity - Dissolved food	0.53	-0.21	1.00	ns
Medium complexity - Dissolved food	0.54	0.56	0.98	ns
High complexity - Dissolved food	0.53	-0.40	0.99	ns
Medium complexity - Low complexity	0.53	0.79	0.93	ns
High complexity - Low complexity	0.51	-0.20	1.00	ns
High complexity - Medium complexity	0.53	-0.98	0.86	ns

Tab. S4. Linear mixed effects model results of calcification, volume growth and surface area growth of symbiotic *Porites lobata* fed with different food treatments over 18 weeks. Standard error (st.error), statistics (stats.), significance (sig.). Model specifications: model <- lmer(scale(variable) ~food + (1|genotype), data=data. Significance codes used are defined as: p < 0.001 (***), p < 0.01 (**), p < 0.05 (*), ns = not significant.

Variable/Food options	std. error	statistic	p-value	sig.
Calcification				
Dissolved food - Thawed plankton	0.47	0.60	0.98	ns
Low complexity - Thawed plankton	0.47	0.73	0.95	ns
Medium complexity - Thawed plankton	0.47	1.28	0.71	ns
High complexity - Thawed plankton	0.49	1.83	0.35	ns
Low complexity - Dissolved food	0.47	0.13	1.00	ns
Medium complexity - Dissolved food	0.47	0.68	0.96	ns
High complexity - Dissolved food	0.49	1.26	0.72	ns
Medium complexity - Low complexity	0.47	0.55	0.98	ns
High complexity - Low complexity	0.49	1.13	0.79	ns
High complexity - Medium complexity	0.49	0.59	0.98	ns
Volume growth				
Dissolved food - Thawed plankton	0.43	-0.06	1.00	ns
Low complexity - Thawed plankton	0.43	1.22	0.74	ns
Medium complexity - Thawed plankton	0.43	2.47	0.10	ns
High complexity - Thawed plankton	0.44	2.34	0.13	ns
Low complexity - Dissolved food	0.43	1.28	0.71	ns
Medium complexity - Dissolved food	0.43	2.53	0.08	ns
High complexity - Dissolved food	0.44	2.40	0.12	ns
Medium complexity - Low complexity	0.43	1.25	0.72	ns
High complexity - Low complexity	0.44	1.16	0.77	ns
High complexity - Medium complexity	0.44	-0.05	1.00	ns
Surface area growth				
Dissolved food - Thawed plankton	0.41	-0.06	1.00	ns
Low complexity - Thawed plankton	0.41	1.72	0.42	ns
Medium complexity - Thawed plankton	0.41	2.46	0.10	ns
High complexity - Thawed plankton	0.42	2.03	0.25	ns
Low complexity - Dissolved food	0.41	1.79	0.38	ns
Medium complexity - Dissolved food	0.41	2.52	0.09	ns
High complexity - Dissolved food	0.42	2.09	0.22	ns
Medium complexity - Low complexity	0.41	0.74	0.95	ns
High complexity - Low complexity	0.42	0.36	1.00	ns
High complexity - Medium complexity	0.42	-0.35	1.00	ns

Tab. S5. Linear mixed effects model results of net photosynthesis, respiration, and gross photosynthesis of symbiotic *Porites lobata* fed with different food treatments over 18 weeks. Standard error (st.error), statistics (stats.), significance (sig.). Model specifications: model <- lmer(scale(variable) ~food + (1|genotype), data=data. Significance codes used are defined as: p < 0.001 (***), p < 0.01 (**), p < 0.05 (*), ns = not significant.

Variable/Food options	std. error	statistic	p-value	sig.
Net photosynthesis				
Dissolved food - Thawed plankton	0.52	0.23	1.00	ns
Low complexity - Thawed plankton	0.49	0.19	1.00	ns
Medium complexity - Thawed plankton	0.49	-1.11	0.80	ns
High complexity - Thawed plankton	0.49	-1.33	0.67	ns
Low complexity - Dissolved food	0.47	-0.05	1.00	ns
Medium complexity - Dissolved food	0.47	-1.42	0.61	ns
High complexity - Dissolved food	0.47	-1.64	0.47	ns
Medium complexity - Low complexity	0.44	-1.46	0.59	ns
High complexity - Low complexity	0.44	-1.70	0.43	ns
High complexity - Medium complexity	0.44	-0.24	1.00	ns
Respiration				
Dissolved food - Thawed plankton	0.51	-1.37	0.65	ns
Low complexity - Thawed plankton	0.48	-0.86	0.91	ns
Medium complexity - Thawed plankton	0.48	-1.21	0.74	ns
High complexity - Thawed plankton	0.48	-0.72	0.95	ns
Low complexity - Dissolved food	0.46	0.62	0.97	ns
Medium complexity - Dissolved food	0.46	0.25	1.00	ns
High complexity - Dissolved food	0.46	0.76	0.94	ns
Medium complexity - Low complexity	0.43	-0.39	0.99	ns
High complexity - Low complexity	0.43	0.16	1.00	ns
High complexity - Medium complexity	0.43	0.55	0.98	ns
Gross photosynthesis				
Dissolved food - Thawed plankton	0.55	-0.06	1.00	ns
Low complexity - Thawed plankton	0.52	0.03	1.00	ns
Medium complexity - Thawed plankton	0.52	-0.95	0.88	ns
High complexity - Thawed plankton	0.52	-0.97	0.87	ns
Low complexity - Dissolved food	0.50	0.09	1.00	ns
Medium complexity - Dissolved food	0.50	-0.93	0.89	ns
High complexity - Dissolved food	0.50	-0.94	0.88	ns
Medium complexity - Low complexity	0.47	-1.09	0.81	ns
High complexity - Low complexity	0.47	-1.11	0.80	ns
High complexity - Medium complexity	0.47	-0.02	1.00	ns

Tab. S6. Linear mixed effects model results of calcification, volume growth, and surface area growth of symbiotic *Stylophora pistillata* fed with different food treatments over 18 weeks. Standard error (st.error), statistics (stats.), significance (sig.). Model specifications: model <- lmer(scale(variable)~food + (1|genotype), data=data. Significance codes used are defined as: p < 0.001 (***), p < 0.01 (**), p < 0.05 (*), ns = not significant.

Variable/Food options	std. error	statistic	p-value	sig.
Calcification				
Dissolved food - Thawed plankton	0.40	-0.19	1.00	ns
Low complexity - Thawed plankton	0.42	0.13	1.00	ns
Medium complexity - Thawed plankton	0.45	-1.55	0.53	ns
High complexity - Thawed plankton	0.40	0.43	0.99	ns
Low complexity - Dissolved food	0.42	0.32	1.00	ns
Medium complexity - Dissolved food	0.45	-1.37	0.64	ns
High complexity - Dissolved food	0.40	0.63	0.97	ns
Medium complexity - Low complexity	0.47	-1.62	0.48	ns
High complexity - Low complexity	0.42	0.29	1.00	ns
High complexity - Medium complexity	0.45	1.93	0.30	ns
Volume growth				
Dissolved food - Thawed plankton	0.25	4.40	<0.001	***
Low complexity - Thawed plankton	0.26	2.13	0.21	ns
Medium complexity - Thawed plankton	0.28	0.34	1.00	ns
High complexity - Thawed plankton	0.26	7.66	<0.001	***
Low complexity - Dissolved food	0.26	-2.12	0.21	ns
Medium complexity - Dissolved food	0.28	-3.57	0.01	**
High complexity - Dissolved food	0.26	3.41	0.01	**
Medium complexity - Low complexity	0.29	-1.58	0.51	ns
High complexity - Low complexity	0.27	5.36	<0.001	***
High complexity - Medium complexity	0.29	6.56	<0.001	***
Surface area growth				
Dissolved food - Thawed plankton	0.24	5.05	<0.001	***
Low complexity - Thawed plankton	0.25	2.95	0.03	*
Medium complexity - Thawed plankton	0.27	-0.58	0.98	ns
High complexity - Thawed plankton	0.25	5.60	<0.001	***
Low complexity - Dissolved food	0.25	-1.94	0.30	ns
Medium complexity - Dissolved food	0.27	-5.06	<0.001	***
High complexity - Dissolved food	0.25	0.71	0.95	ns
Medium complexity - Low complexity	0.28	-3.21	0.01	*
High complexity - Low complexity	0.26	2.56	0.08	ns
High complexity - Medium complexity	0.28	5.60	<0.001	***

Tab. S7. Linear mixed effects model results of net photosynthesis, respiration and gross photosynthesis of symbiotic *Stylophora pistillata* fed with different food options over 18 weeks. Standard error (st.error), statistics (stats.), significance (sig.). Model specifications: model <- lmer(scale(variable)~food + (1|genotype), data=data. Significance codes used are defined as: p < 0.001 (***), p < 0.01 (**), p < 0.05 (*), ns = not significant.

Variable/Food options	std. error	statistic	p-value	sig.
Net photosynthesis				
Dissolved food - Thawed plankton	0.50	-0.02	1.00	ns
Low complexity - Thawed plankton	0.50	-0.45	0.99	ns
Medium complexity - Thawed plankton	0.51	-1.33	0.67	ns
High complexity - Thawed plankton	0.51	-0.62	0.97	ns
Low complexity - Dissolved food	0.48	-0.44	0.99	ns
Medium complexity - Dissolved food	0.50	-1.35	0.66	ns
High complexity - Dissolved food	0.50	-0.62	0.97	ns
Medium complexity - Low complexity	0.50	-0.92	0.89	ns
High complexity - Low complexity	0.50	-0.19	1.00	ns
High complexity - Medium complexity	0.51	0.71	0.95	ns
Respiration				
Dissolved food - Thawed plankton	0.46	-0.36	1.00	ns
Low complexity - Thawed plankton	0.46	-0.60	0.97	ns
Medium complexity - Thawed plankton	0.48	0.63	0.97	ns
High complexity - Thawed plankton	0.48	0.61	0.97	ns
Low complexity - Dissolved food	0.45	-0.25	1.00	ns
Medium complexity - Dissolved food	0.46	1.00	0.85	ns
High complexity - Dissolved food	0.46	0.99	0.86	ns
Medium complexity - Low complexity	0.46	1.25	0.72	ns
High complexity - Low complexity	0.46	1.23	0.73	ns
High complexity - Medium complexity	0.48	-0.01	1.00	ns
Gross photosynthesis				
Dissolved food - Thawed plankton	0.50	0.59	0.98	ns
Low complexity - Thawed plankton	0.50	0.13	1.00	ns
Medium complexity - Thawed plankton	0.52	-0.45	0.99	ns
High complexity - Thawed plankton	0.52	0.23	1.00	ns
Low complexity - Dissolved food	0.49	-0.47	0.99	ns
Medium complexity - Dissolved food	0.50	-1.05	0.83	ns
High complexity - Dissolved food	0.50	-0.35	1.00	ns
Medium complexity - Low complexity	0.50	-0.59	0.98	ns
High complexity - Low complexity	0.50	0.11	1.00	ns
High complexity - Medium complexity	0.52	0.68	0.96	ns

Tab. S8. Linear mixed effects model results of calcification, volume growth and surface area growth of bleached *Galaxea fascicularis* fed with different food options over 18 weeks. Standard error (st.error), statistics (stats.), significance (sig.). Model specifications: model <- lmer(scale(variable)~food + (1|genotype), data=data. Significance codes used are defined as: p < 0.001 (***), p < 0.01 (**), p < 0.05 (*), ns = not significant.

Variable/Food options	std. error	statistic	p-value	sig.
Calcification				
Dissolved food - Thawed plankton	0.53	0.03	1.00	ns
Low complexity - Thawed plankton	0.51	0.38	1.00	ns
Medium complexity - Thawed plankton	0.51	1.16	0.77	ns
High complexity - Thawed plankton	0.50	0.91	0.89	ns
Low complexity - Dissolved food	0.53	0.34	1.00	ns
Medium complexity - Dissolved food	0.53	1.09	0.81	ns
High complexity - Dissolved food	0.52	0.85	0.91	ns
Medium complexity - Low complexity	0.51	0.78	0.94	ns
High complexity - Low complexity	0.50	0.52	0.99	ns
High complexity - Medium complexity	0.50	-0.28	1.00	ns
Volume growth				
Dissolved food - Thawed plankton	0.50	-2.54	0.08	ns
Low complexity - Thawed plankton	0.46	-1.19	0.76	ns
Medium complexity - Thawed plankton	0.46	-2.06	0.24	ns
High complexity - Thawed plankton	0.45	-0.06	1.00	ns
Low complexity - Dissolved food	0.50	1.43	0.60	ns
Medium complexity - Dissolved food	0.50	0.63	0.97	ns
High complexity - Dissolved food	0.49	2.54	0.08	ns
Medium complexity - Low complexity	0.46	-0.87	0.91	ns
High complexity - Low complexity	0.45	1.17	0.77	ns
High complexity - Medium complexity	0.45	2.06	0.24	ns
Surface area growth				
Dissolved food - Thawed plankton	0.57	0.48	0.99	ns
Low complexity - Thawed plankton	0.51	0.79	0.93	ns
Medium complexity - Thawed plankton	0.51	0.73	0.95	ns
High complexity - Thawed plankton	0.49	2.25	0.16	ns
Low complexity - Dissolved food	0.56	0.23	1.00	ns
Medium complexity - Dissolved food	0.56	0.17	1.00	ns
High complexity - Dissolved food	0.54	1.53	0.54	ns
Medium complexity - Low complexity	0.49	-0.06	1.00	ns
High complexity - Low complexity	0.47	1.49	0.57	ns
High complexity - Medium complexity	0.47	1.55	0.53	ns

Tab. S9. Linear mixed effects model results of calcification, volume growth, and surface area growth of bleached *Porites lobata* fed with different food options over 18-weeks. Standard error (st.error), statistics (stats.), significance (sig.). Model specifications: model <- lmer(scale(variable)~food + (1|genotype), data=data. Significance codes used are defined for p values: $p < 0.001$ (***), $p < 0.01$ (**), $p < 0.05$ (*), ns = not significant.

Variable/Food options	std. error	statistic	p-value	sig.
Calcification				
Dissolved food - Thawed plankton	0.41	0.68	0.96	ns
Low complexity - Thawed plankton	0.41	1.88	0.33	ns
Medium complexity - Thawed plankton	0.41	2.36	0.13	ns
High complexity - Thawed plankton	0.41	1.83	0.36	ns
Low complexity - Dissolved food	0.41	1.20	0.75	ns
Medium complexity - Dissolved food	0.41	1.67	0.45	ns
High complexity - Dissolved food	0.41	1.15	0.78	ns
Medium complexity - Low complexity	0.41	0.48	0.99	ns
High complexity - Low complexity	0.41	-0.05	1.00	ns
High complexity - Medium complexity	0.41	-0.53	0.98	ns
Volume growth				
Dissolved food - Thawed plankton	0.33	0.28	0.99	ns
Low complexity - Thawed plankton	0.33	0.13	1.00	ns
Medium complexity - Thawed plankton	0.33	3.47	0.005	**
High complexity - Thawed plankton	0.33	3.67	0.002	**
Low complexity - Dissolved food	0.33	-0.14	1.00	ns
Medium complexity - Dissolved food	0.33	3.19	0.012	*
High complexity - Dissolved food	0.33	3.39	0.006	**
Medium complexity - Low complexity	0.33	3.33	0.007	**
High complexity - Low complexity	0.33	3.54	0.004	**
High complexity - Medium complexity	0.33	0.20	1.00	ns
Surface area growth				
Dissolved food - Thawed plankton	0.35	-0.92	0.89	ns
Low complexity - Thawed plankton	0.35	-1.64	0.47	ns
Medium complexity - Thawed plankton	0.35	0.60	0.98	ns
High complexity - Thawed plankton	0.35	3.47	0.005	**
Low complexity - Dissolved food	0.35	-0.72	0.95	ns
Medium complexity - Dissolved food	0.35	1.51	0.55	ns
High complexity - Dissolved food	0.35	4.38	<0.001	***
Medium complexity - Low complexity	0.35	2.24	0.17	ns
High complexity - Low complexity	0.35	5.11	<0.001	***
High complexity - Medium complexity	0.35	2.87	0.03	*

Tab. S10. Linear mixed effects model results of calcification, volume growth, and surface area growth of bleached *Stylophora pistillata* fed with different food options over 18weeks. All bleached corals fed with the thawed plankton died during the experiment and were not included in the analysis. Standard error (st.error), statistics (stats.), significance (sig.). Model specifications: model <- lmer(scale(variable)~food + (1|genotype), data=data. Significance codes used are defined for p values: p < 0.001 (***), p < 0.01 (**), p < 0.05 (*), ns = not significant.

Variable/Food options	std. error	statistic	p-value	sig.
Calcification				
Low complexity - Dissolved food	0.43	0.35	0.99	ns
Medium complexity - Dissolved food	0.41	0.55	0.95	ns
High complexity - Dissolved food	0.41	3.24	0.01	**
Medium complexity - Low complexity	0.43	0.19	1.00	ns
High complexity - Low complexity	0.43	2.79	0.03	*
High complexity - Medium complexity	0.41	2.68	0.04	*
Volume growth				
Low complexity - Dissolved food	0.32	0.73	0.88	ns
Medium complexity - Dissolved food	0.31	0.24	0.99	ns
High complexity - Dissolved food	0.32	6.04	<0.001	***
Medium complexity - Low complexity	0.32	-0.50	0.96	ns
High complexity - Low complexity	0.32	5.16	<0.001	***
High complexity - Medium complexity	0.32	5.80	<0.001	***
Surface area growth				
Low complexity - Dissolved food	0.31	1.04	0.73	ns
Medium complexity - Dissolved food	0.30	0.12	1.00	ns
High complexity - Dissolved food	0.31	5.68	<0.001	***
Medium complexity - Low complexity	0.31	-0.92	0.80	ns
High complexity - Low complexity	0.32	4.52	<0.001	***
High complexity - Medium complexity	0.31	5.56	<0.001	***

Tab. S11. Linear mixed effects model results of respiration rates of bleached *Galaxea fascicularis, Porites lobata,* and *Stylophora pistillata* fed with different food options over 18 **weeks.** Standard error (st.error), statistics (stats.), significance (sig.). All bleached corals of *S. pistillata* fed with thawed plankton died during the experiment and were not included in the analysis. Model specifications: model <- lmer(scale(variable)~food + (1|genotype), data=data. Significance codes used are defined for p values: $p < 0.001$ (***), $p < 0.01$ (**), $p < 0.05$ (*), ns = not significant.

Species/Food options	std. error	statistic	p-value	sig.
Galaxea fascicularis				
Dissolved food - Thawed plankton	0.48	1.60	0.50	ns
Low complexity - Thawed plankton	0.45	0.09	1.00	ns
Medium complexity - Thawed plankton	0.48	2.53	0.08	ns
High complexity - Thawed plankton	0.45	-0.02	1.00	ns
Low complexity - Dissolved food	0.46	-1.56	0.52	ns
Medium complexity - Dissolved food	0.49	0.90	0.90	ns
High complexity - Dissolved food	0.46	-1.67	0.45	ns
Medium complexity - Low complexity	0.46	2.51	0.09	ns
High complexity - Low complexity	0.43	-0.11	1.00	ns
High complexity - Medium complexity	0.46	-2.62	0.07	ns
Porites lobata				
Dissolved food - Thawed plankton	0.50	-0.88	0.90	ns
Low complexity - Thawed plankton	0.51	-0.47	0.99	ns
Medium complexity - Thawed plankton	0.63	-0.98	0.86	ns
High complexity - Thawed plankton	0.51	0.18	1.00	ns
Low complexity - Dissolved food	0.50	0.40	0.99	ns
Medium complexity - Dissolved food	0.62	-0.29	1.00	ns
High complexity - Dissolved food	0.50	1.06	0.82	ns
Medium complexity - Low complexity	0.63	-0.60	0.97	ns
High complexity - Low complexity	0.51	0.65	0.97	ns
High complexity - Medium complexity	0.63	1.13	0.79	ns
Stylophora pistillata				
Low complexity - Dissolved food	0.42	-0.63	0.92	ns
Medium complexity - Dissolved food	0.47	1.81	0.27	ns
High complexity - Dissolved food	0.42	1.73	0.31	ns
Medium complexity - Low complexity	0.47	2.37	0.08	ns
High complexity - Low complexity	0.42	2.35	0.09	ns
High complexity - Medium complexity	0.47	-0.27	0.99	ns

Tab. S12. Linear mixed effects model results of calcification, volume growth, surface area growth and respiration of symbiotic and bleached *Galaxea fascicularis* fed with different food options over 18 weeks. Standard error (st.error), statistics (stats.), significance (sig.). Model specifications: model <- lmer(scale(variable)~condition + (1|genotype), data=data. Significance codes used are defined as: $p < 0.001$ (***), $p < 0.01$ (**), $p < 0.05$ (*), ns = not significant.

Variable/Food options	std. error	statistic	p-value	sig.
Calcification				
Thawed plankton	0.38	2.96	0.96	ns
Dissolved food	0.42	2.82	0.004	**
Low complexity	0.32	3.83	0.12	ns
Medium complexity	0.28	2.43	0.01	*
High complexity	0.30	3.73	<0.001	***
Volume growth				
Thawed plankton	0.49	-0.33	0.73	ns
Dissolved food	0.51	0.95	0.33	ns
Low complexity	0.41	2.31	0.02	*
Medium complexity	0.47	1.33	0.18	ns
High complexity	0.70	0.45	0.12	ns
Surface area growth				
Thawed plankton	0.49	0.63	0.52	ns
Dissolved food	0.53	0.25	0.79	ns
Low complexity	0.30	2.42	0.01	*
Medium complexity	0.48	0.89	0.37	ns
High complexity	0.44	1.85	0.63	ns
Respiration				
Thawed plankton	0.40	2.80	0.005	**
Dissolved food	0.47	-1.28	0.19	ns
Low complexity	0.39	2.94	0.003	**
Medium complexity	0.49	-0.77	0.43	ns
High complexity	0.46	1.17	0.23	ns

Tab. S13. Hedges' g effect sizes of calcification, volume growth, surface area growth, and respiration of symbiotic and bleached *Galaxea fascicularis* fed with different food treatments over 18 weeks. Lower confidence interval (lower C.I.), upper confidence interval (upper C.I.) and effect sizes are given.

Variable/Food options	estimate	lower C.I.	upper C.I.	effect size
Calcification				
Thawed plankton	-1.06	-2.11	-0.01	large
Dissolved food	-1.36	-2.52	-0.19	large
Low complexity	-0.68	-1.66	0.30	medium
Medium complexity	-0.82	-1.85	0.20	large
High complexity	-1.30	-2.35	-0.26	large
Volume growth				
Thawed plankton	0.15	-0.84	1.13	negligible
Dissolved food	-0.14	-1.19	0.91	negligible
Low complexity	-1.02	-2.03	-0.01	large
Medium complexity	-0.82	-1.85	0.20	large
High complexity	-0.69	-1.67	0.29	medium
Surface area growth				
Thawed plankton	-0.29	-1.28	0.69	small
Dissolved food	-0.13	-1.18	0.93	negligible
Low complexity	-0.99	-1.99	0.02	large
Medium complexity	-0.41	-1.41	0.58	small
High complexity	-0.83	-1.83	0.16	large
Respiration				
Thawed plankton	-1.29	-2.37	-0.21	large
Dissolved food	0.33	-0.73	1.39	small
Low complexity	-1.32	-2.37	-0.27	large
Medium complexity	0.59	-0.41	1.60	medium
High complexity	-0.53	-1.50	0.44	medium

Tab. S14. Linear mixed effects model results of calcification, volume growth, surface area growth and respiration of symbiotic and bleached *Porites lobata* fed with different food options over 18 weeks. Standard error (st.error), statistics (stats.), significance (sig.). Model specifications: model <- lmer(scale(variable)~condition + (1|genotype), data=data. Significance codes used are defined as: p < 0.001 (***), p < 0.01 (**), p < 0.05 (*), ns = not significant.

Variable/Food options	std. error	statistic	p-value	sig.
Calcification				
Thawed plankton	0.38	2.54	0.01	*
Dissolved food	0.40	1.49	0.13	ns
Low complexity	0.45	1.50	1.13	ns
Medium complexity	0.45	1.88	0.06	ns
High complexity	0.44	2.54	0.01	*
Volume growth				
Thawed plankton	0.40	2.45	0.01	*
Dissolved food	0.36	2.47	0.01	*
Low complexity	0.37	2.23	0.001	**
Medium complexity	0.43	1.95	0.05	ns
High complexity	0.38	2.50	0.01	*
Surface area growth				
Thawed plankton	0.46	1.70	0.08	ns
Dissolved food	0.33	2.69	0.007	**
Low complexity	0.39	2.77	0.005	**
Medium complexity	0.43	1.32	0.18	ns
High complexity	0.39	-1.21	0.22	ns
Respiration				
Thawed plankton	0.40	2.97	0.002	**
Dissolved food	0.50	-0.01	0.98	ns
Low complexity	0.43	1.96	0.04	*
Medium complexity	0.41	2.46	0.01	*
High complexity	0.40	1.87	0.06	ns

Tab. S15. Hedges' g effect sizes of calcification, volume growth, surface area growth and respiration of symbiotic and bleached *Porites lobata* fed with different food options over 18 weeks. Lower confidence interval (lower C.I.), upper confidence interval (upper C.I.) and effect sizes are given.

Variable/Food options	estimate	lower C.I.	upper C.I.	effect size
Calcification				
Thawed plankton	-1.03	-2.05	-0.02	large
Dissolved food	-0.99	-2.00	0.01	large
Low complexity	-0.67	-1.65	0.30	medium
Medium complexity	-0.58	-1.56	0.38	medium
High complexity	-0.93	-1.96	0.10	large
Volume growth				
Thawed plankton	-1.06	-2.07	-0.04	large
Dissolved food	-0.83	-1.83	0.16	large
Low complexity	-1.43	-2.5	-0.37	large
Medium complexity	-0.93	-1.93	0.08	large
High complexity	-1.09	-2.14	-0.04	large
Surface area growth				
Thawed plankton	-0.28	-1.24	0.67	small
Dissolved food	-0.54	-1.5	0.43	medium
Low complexity	-1.61	-2.71	-0.52	large
Medium complexity	-0.88	-1.88	0.12	large
High complexity	0.2	-0.79	1.19	negligible
Respiration				
Thawed plankton	-1.41	-2.53	-0.27	large
Dissolved food	-1.13	-2.15	-0.10	large
Low complexity	-0.88	-1.87	0.11	large
Medium complexity	0.00	-0.97	0.98	negligible
High complexity	-0.76	-1.74	0.22	medium

Tab. S16. Linear mixed effects model results of calcification, volume growth, surface area growth and respiration of symbiotic and bleached *Stylophora pistillata* fed with different food options over 18 weeks. Standard error (st.error), statistics (stats.), significance (sig.). Model specifications: model <- lmer(scale(variable)~condition + (1|genotype), data=data. All bleached corals fed with thawed plankton died during the experiment and were not included in the analysis (NA). Significance codes used are defined as: $p < 0.001$ (***), $p < 0.01$ (**), $p < 0.05$ (*), ns = not significant.

Variable/Food options	std. error	statistic	p-value	sig.
Calcification				
Thawed plankton	NA	NA	NA	NA
Dissolved food	15.4	3.27	0.001	**
Low complexity	17.4	3.14	0.001	**
Medium complexity	0.25	6.56	<0.001	***
High complexity	8.48	5.83	<0.001	***
Volume growth				
Thawed plankton	NA	NA	NA	NA
Dissolved food	0.01	7.56	<0.001	***
Low complexity	0.29	7.43	<0.001	***
Medium complexity	0.16	11.1	<0.001	***
High complexity	0.13	10.3	<0.001	***
Surface area growth				
Thawed plankton	NA	NA	NA	NA
Dissolved food	0.20	6.52	<0.001	***
Low complexity	0.69	11.05	<0.001	***
Medium complexity	0.16	11.07	<0.001	***
High complexity	0.55	10.90	<0.001	***
Respiration				
Thawed plankton	NA	NA	NA	NA
Dissolved food	0.51	-0.46	0.64	ns
Low complexity	0.44	1.84	0.06	ns
Medium complexity	0.46	1.22	0.21	ns
High complexity	0.45	1.46	0.14	ns

Tab. S17. Hedges' g effect sizes of calcification, volume growth, and surface area growth of symbiotic and bleached *Stylophora pistillata* fed with different food options over 18 weeks. All bleached corals fed with thawed plankton died during the experiment and were not included in the analysis (NA). Lower confidence interval (lower C.I.), upper confidence interval (upper C.I.) and effect size are given.

Variable/Food options	estimate	lower C.I.	upper C.I.	effect size
Calcification				
Thawed plankton	NA	NA	NA	NA
Dissolved food	-2.94	-4.32	-1.57	large
Low complexity	-1.41	-2.48	-0.35	large
Medium complexity	-1.65	-2.83	-0.47	large
High complexity	-2.03	-3.2	-0.86	large
Volume growth				
Thawed plankton	NA	NA	NA	NA
Dissolved food	-4.91	-6.82	-3.01	large
Low complexity	-3.08	-4.48	-1.67	large
Medium complexity	-3.55	-5.19	-1.92	large
High complexity	-3.09	-4.5	-1.68	large
Surface area growth				
Thawed plankton	NA	NA	NA	NA
Dissolved food	-4.09	-5.76	-2.41	large
Low complexity	-3.65	-5.2	-2.09	large
Medium complexity	-2.82	-4.26	-1.38	large
High complexity	-2.8	-4.14	-1.46	large
Respiration				
Thawed plankton	NA	NA	NA	NA
Dissolved food	-0.55	-1.52	0.42	medium
Low complexity	-0.82	-1.81	0.16	large
Medium complexity	0.22	-0.79	1.23	small
High complexity	-0.66	-1.63	0.31	medium

Tab. S18. Comparison of effect sizes between food options of symbiotic and bleached *Galaxea fascicularis* fed over 18 weeks.

Variable/Food 1	Food 2	EZ diff	SE diff	Z-Statistic	p-value	sig.
Calcification						
Thawed plankton	Dissolved food	0.3	0.8	0.4	0.7	ns
Thawed plankton	High complexity	0.24	0.8	0.3	0.8	ns
Thawed plankton	Low complexity	-0.38	0.7	-0.5	0.6	ns
Thawed plankton	Medium complexity	-0.24	0.7	-0.3	0.7	ns
Dissolved food	High complexity	-0.06	0.8	-0.1	0.9	ns
Dissolved food	Low complexity	-0.68	0.8	-0.9	0.4	ns
Dissolved food	Medium complexity	-0.54	0.8	-0.7	0.5	ns
High complexity	Low complexity	-0.62	0.7	-0.8	0.4	ns
High complexity	Medium complexity	-0.48	0.7	-0.6	0.5	ns
Low complexity	Medium complexity	0.14	0.7	0.2	0.8	ns
Volume growth						
Thawed plankton	Dissolved food	0.29	0.73	0.39	0.69	ns
Thawed plankton	High complexity	0.84	0.71	1.18	0.24	ns
Thawed plankton	Low complexity	1.17	0.72	1.63	0.10	ns
Thawed plankton	Medium complexity	0.97	0.73	1.34	0.18	ns
Dissolved food	High complexity	0.55	0.73	0.75	0.45	ns
Dissolved food	Low complexity	0.88	0.74	1.18	0.24	ns
Dissolved food	Medium complexity	0.68	0.75	0.91	0.36	ns
High complexity	Low complexity	0.33	0.72	0.46	0.65	ns
High complexity	Medium complexity	0.13	0.72	0.18	0.86	ns
Low complexity	Medium complexity	-0.2	0.73	-0.27	0.79	ns
Surface area growth						
Thawed plankton	Dissolved food	-0.16	0.74	-0.22	0.83	ns
Thawed plankton	High complexity	0.54	0.71	0.76	0.45	ns
Thawed plankton	Low complexity	0.7	0.72	0.97	0.33	ns
Thawed plankton	Medium complexity	0.12	0.71	0.17	0.87	ns
Dissolved food	High complexity	0.7	0.74	0.95	0.34	ns
Dissolved food	Low complexity	0.86	0.74	1.16	0.25	ns
Dissolved food	Medium complexity	0.28	0.74	0.38	0.71	ns
High complexity	Low complexity	0.16	0.72	0.22	0.82	ns
High complexity	Medium complexity	-0.42	0.72	-0.59	0.56	ns
Low complexity	Medium complexity	-0.58	0.72	-0.80	0.42	ns
Respiration						
Thawed plankton	Dissolved food	-1.62	0.77	-2.10	0.04	*
Thawed plankton	High complexity	-0.76	0.74	-1.03	0.30	ns
Thawed plankton	Low complexity	0.03	0.77	0.04	0.97	ns
Thawed plankton	Medium complexity	-1.88	0.75	-2.50	0.01	*
Dissolved food	High complexity	0.86	0.73	1.17	0.24	ns
Dissolved food	Low complexity	1.65	0.76	2.17	0.03	*
Dissolved food	Medium complexity	-0.26	0.75	-0.35	0.73	ns
High complexity	Low complexity	0.79	0.73	1.08	0.28	ns
High complexity	Medium complexity	-1.12	0.71	-1.57	0.12	ns
Low complexity	Medium complexity	-1.91	0.74	-2.58	0.01	*

Tab. S19. Comparison of effect sizes between symbiotic and bleached *Porites lobata* fed over 18 weeks. Differences between effect sizes (EZ diff), standard error (SE diff), Z-Statistic and *p*-value are given.

Variable/Food 1	Food 2	EZ diff	SE diff	Z-Statistic	p-value	sig.
Calcification						
Thawed plankton	Dissolved food	-0.05	0.73	-0.07	0.95	ns
Thawed plankton	High complexity	-0.11	0.74	-0.15	0.88	ns
Thawed plankton	Low complexity	-0.37	0.72	-0.51	0.61	ns
Thawed plankton	Medium complexity	-0.45	0.72	-0.63	0.53	ns
Dissolved food	High complexity	-0.06	0.74	-0.08	0.94	ns
Dissolved food	Low complexity	-0.32	0.72	-0.45	0.66	ns
Dissolved food	Medium complexity	-0.4	0.71	-0.56	0.58	ns
High complexity	Low complexity	-0.26	0.73	-0.36	0.72	ns
High complexity	Medium complexity	-0.34	0.72	-0.47	0.64	ns
Low complexity	Medium complexity	-0.08	0.70	-0.11	0.91	ns
Volume growth						
Thawed plankton	Dissolved food	-0.23	0.73	-0.32	0.75	ns
Thawed plankton	High complexity	0.03	0.75	0.04	0.97	ns
Thawed plankton	Low complexity	0.37	0.75	0.49	0.62	ns
Thawed plankton	Medium complexity	-0.13	0.73	-0.18	0.86	ns
Dissolved food	High complexity	0.26	0.74	0.35	0.72	ns
Dissolved food	Low complexity	0.6	0.74	0.81	0.42	ns
Dissolved food	Medium complexity	0.1	0.72	0.14	0.89	ns
High complexity	Low complexity	0.34	0.76	0.45	0.66	ns
High complexity	Medium complexity	-0.16	0.74	-0.22	0.83	ns
Low complexity	Medium complexity	-0.5	0.75	-0.67	0.50	ns
Surface area growth						
Thawed plankton	Dissolved food	0.26	0.69	0.38	0.71	ns
Thawed plankton	High complexity	-0.48	0.70	-0.68	0.49	ns
Thawed plankton	Low complexity	1.33	0.74	1.79	0.07	ns
Thawed plankton	Medium complexity	0.6	0.71	0.85	0.40	ns
Dissolved food	High complexity	-0.74	0.71	-1.05	0.29	ns
Dissolved food	Low complexity	1.07	0.74	1.44	0.15	ns
Dissolved food	Medium complexity	0.34	0.71	0.48	0.63	ns
High complexity	Low complexity	1.81	0.75	2.40	0.02	*
High complexity	Medium complexity	1.08	0.72	1.50	0.13	ns
Low complexity	Medium complexity	-0.73	0.76	-0.96	0.33	ns
Respiration						
Thawed plankton	Dissolved food	-0.28	0.78	-0.36	0.72	ns
Thawed plankton	High complexity	-0.65	0.76	-0.85	0.39	ns
Thawed plankton	Low complexity	-0.53	0.77	-0.69	0.49	ns
Thawed plankton	Medium complexity	-1.41	0.76	-1.85	0.06	ns
Dissolved food	High complexity	-0.37	0.72	-0.51	0.61	ns
Dissolved food	Low complexity	-0.25	0.73	-0.34	0.73	ns
Dissolved food	Medium complexity	-1.13	0.72	-1.57	0.12	ns
High complexity	Low complexity	0.12	0.71	0.17	0.87	ns
High complexity	Medium complexity	-0.76	0.71	-1.08	0.28	ns
Low complexity	Medium complexity	-0.88	0.71	-1.24	0.21	ns

Tab. S20. Comparison of effect sizes between food options of symbiotic and bleached *Stylophora pistillata* fed over 18-weeks. All bleached corals fed with thawed plankton died during the experiment and were not included in the analysis. Differences between effect sizes (EZ diff), standard error (SE diff), Z-Statistic and *p*-value are given. Significance codes used are defined as: p < 0.001 (***), p < 0.01 (**), p < 0.05 (*), ns = not significant.

Variable/Food 1	Food 2	EZ diff	SE diff	Z-Statistic	p-value	sig.
Calcification						
Dissolved food	High complexity	-0.91	0.92	-0.99	0.32	ns
Dissolved food	Low complexity	-1.53	0.89	-1.72	0.08	ns
Dissolved food	Medium complexity	-1.29	0.92	-1.40	0.16	ns
High complexity	Low complexity	-0.62	0.81	-0.77	0.44	ns
High complexity	Medium complexity	-0.38	0.85	-0.45	0.65	ns
Low complexity	Medium complexity	0.24	0.81	0.30	0.77	ns
Volume growth						
Dissolved food	High complexity	-1.82	1.21	-1.51	0.13	ns
Dissolved food	Low complexity	-1.83	1.21	-1.52	0.13	ns
Dissolved food	Medium complexity	-1.36	1.28	-1.06	0.29	ns
High complexity	Low complexity	-0.01	1.02	-0.01	0.99	ns
High complexity	Medium complexity	0.46	1.10	0.42	0.68	ns
Low complexity	Medium complexity	0.47	1.10	0.43	0.67	ns
Surface area growth						
Dissolved food	High complexity	-1.29	1.09	-1.18	0.24	ns
Dissolved food	Low complexity	-0.44	1.17	-0.38	0.71	ns
Dissolved food	Medium complexity	-1.27	1.13	-1.13	0.26	ns
High complexity	Low complexity	0.85	1.05	0.81	0.42	ns
High complexity	Medium complexity	0.02	1.00	0.02	0.98	ns
Low complexity	Medium complexity	-0.83	1.08	-0.77	0.44	ns
Respiration						
Dissolved food	High complexity	0.11	0.70	0.16	0.88	ns
Dissolved food	Low complexity	0.27	0.71	0.38	0.70	ns
Dissolved food	Medium complexity	-0.77	0.71	-1.08	0.28	ns
High complexity	Low complexity	0.16	0.71	0.23	0.82	ns
High complexity	Medium complexity	-0.88	0.71	-1.23	0.22	ns
Low complexity	Medium complexity	-1.04	0.72	-1.44	0.15	ns

Tab. S21. $\delta^{13}C$ and $\delta^{15}N$ isotope signature of the source amino acids contained in host tissue and symbionts of bleached and symbiotic *Ctenactis echinata* and *Pocillopora verrucosa*. (mean ± standard deviation).

	$\delta^{13}C$			$\delta^{15}N$		
Amino acid	Bleached	Symbiotic	Symbiodiniaceae	Bleached	Symbiotic	Symbiodiniaceae
C. echinata						
Asparagine	-7.5 ± 2.1	-7.3 ± 1.7	-6.1 ± 2.1	8 ± 1.0	7.4 ± 1.9	5.0 ± 1.2
Glycine	-8.3 ± 1.5	-8.4 ± 1.8	-9.4 ± 2.7	1.6 ± 1.2	1.5 ± 1.0	1.5 ± 1.0
Lysine	-8.3 ± 1.5	-8.6 ± 1.6	-8.6 ± 1.7	2.7 ± 1.1	2.2 ± 1.2	1.5 ± 0.9
Methionine	-18.7 ± 1.8	-16.9 ± 2.0	-15.1 ± 1.5	2.2 ± 1.1	1.0 ± 1.3	1.9 ± 0.9
Phenylananine	-20.0 ± 0.8	-19.9 ± 0.8	-18.8 ± 1.2	0.5 ± 0.4	-0.5 ± 1.2	-0.3 ± 1.2
P. verrucosa						
Asparagine	-12.3 ± 1.9	-10.9 ± 2.7	-6.7 ± 2.0	4.2 ± 1.3	1.6 ± 0.8	1.0 ± 1.0
Glycine	-8.8 ± 2.3	-8.7 ± 2.4	-10.0 ± 3.3	-2.6 ± 1.1	0.4 ± 0.8	-1.0 ± 1.3
Lysine	-11.5 ± 0.8	-11.4 ± 1.8	-10.5 ± 1.4	2.8 ± 0.8	2.3 ± 0.9	1 ± 1.5
Methionine	-24.1 ± 2.1	-16.4 ± 1.5	-13.2 ± 1.1	6.1 ± 1.2	3.0 ± 1.0	2.2 ± 0.9
Phenylananine	-22.3 ± 0.7	-22.0 ± 0.9	-19.4 ± 0.6	4.2 ± 1.3	3.0 ± 1.0	2.2 ± 0.9

Tab. S22. Linear mixed effects models result from $\delta^{13}C$ isotope values of five source amino acids: asparagine, glycine, lysine, methionine and phenilananine of the host tissue and symbionts of bleached and symbiotic corals of *Ctenactis echinata* (white) and *Pocillopora verrucosa* (gray). Standard error (st.error), *p* value, significance (sig.) and model specifications are given. Significance codes used are defined for p values: p < 0.001 (***), p < 0.01 (**), p < 0.05 (*), ns = not significant.

Amino acid	Host fraction	std. error	*p* value	Sig.
Asparagine	Symbiotic tissue - Bleached tissue	0.47	0.92	ns
	Symbiodiniaceae -Bleached tissue	0.47	0.66	ns
	Symbiodiniaceae - Symbiotic tissue	0.35	0.23	ns
	Symbiotic tissue - Bleached tissue	0.29	1.12	ns
	Symbiodiniaceae -Bleached tissue	0.29	< 0.001	***
	Symbiodiniaceae - Symbiotic tissue	0.25	< 0.001	***
Glycine	Symbiotic tissue - Bleached tissue	0.42	0.99	ns
	Symbiodiniaceae -Bleached tissue	0.42	0.48	ns
	Symbiodiniaceae - Symbiotic tissue	0.40	0.52	ns
	Symbiotic tissue - Bleached tissue	0.24	< 0.001	***
	Symbiodiniaceae -Bleached tissue	0.24	< 0.001	***
	Symbiodiniaceae - Symbiotic tissue	0.20	0.42	ns
Lysine	Symbiotic tissue - Bleached tissue	0.46	0.87	ns
	Symbiodiniaceae -Bleached tissue	0.45	0.89	ns
	Symbiodiniaceae - Symbiotic tissue	0.42	0.99	ns
	Symbiotic tissue - Bleached tissue	0.43	0.98	ns
	Symbiodiniaceae -Bleached tissue	0.40	0.13	ns
	Symbiodiniaceae - Symbiotic tissue	0.40	0.20	ns
Methionine	Symbiotic tissue - Bleached tissue	0.30	0.02	*
	Symbiodiniaceae -Bleached tissue	0.30	< 0.001	***
	Symbiodiniaceae - Symbiotic tissue	0.30	0.01	*
	Symbiotic tissue - Bleached tissue	0.14	< 0.001	***
	Symbiodiniaceae -Bleached tissue	0.14	< 0.001	***
	Symbiodiniaceae - Symbiotic tissue	0.11	< 0.001	***
Phenylananine	Symbiotic tissue - Bleached tissue	0.38	0.98	ns
	Symbiodiniaceae -Bleached tissue	0.38	0.01	*
	Symbiodiniaceae - Symbiotic tissue	0.36	0.01	*
	Symbiotic tissue - Bleached tissue	0.19	0.5	ns
	Symbiodiniaceae -Bleached tissue	0.19	< 0.001	***
	Symbiodiniaceae - Symbiotic tissue	0.20	< 0.001	***

Tab. S23. Linear mixed effects models result from $\delta^{15}N$ isotope values of five source amino acids: asparagine, glycine, lysine, methionine and phenilananine of the host tissue and symbionts of bleached and symbiotic corals of *Ctenactis echinata (white)* and *Pocillopora verrucosa (gray)*. Standard error (st.error), *p* value, significance (sig.) and model specifications are given. Significance codes used are defined for p values: p < 0.001 (***), p < 0.01 (**), p < 0.05 (*), ns = not significant.

Amino acid	Host fraction	std. error	p value	Sig.
Asparagine	Symbiotic tissue - Bleached tissue	0.32	*0.65*	*ns*
	Symbiodiniaceae -Bleached tissue	*0.32*	< 0.001	***
	Symbiodiniaceae - Symbiotic tissue	*0.23*	< 0.001	***
	Symbiotic tissue - Bleached tissue	0.12	< 0.001	***
	Symbiodiniaceae -Bleached tissue	*0.12*	< 0.001	***
	Symbiodiniaceae - Symbiotic tissue	*0.9*	< 0.001	***
Glycine	Symbiotic tissue - Bleached tissue	*0.42*	*0.95*	*ns*
	Symbiodiniaceae -Bleached tissue	*0.42*	*0.93*	*ns*
	Symbiodiniaceae - Symbiotic tissue	*0.42*	*0.99*	*ns*
	Symbiotic tissue - Bleached tissue	*0.29*	< 0.001	***
	Symbiodiniaceae -Bleached tissue	*0.29*	*0.02*	*
	Symbiodiniaceae - Symbiotic tissue	*0.28*	*0.01*	*
Lysine	Symbiotic tissue - Bleached tissue	*0.48*	*0.61*	*ns*
	Symbiodiniaceae -Bleached tissue	*0.48*	*0.96*	*ns*
	Symbiodiniaceae - Symbiotic tissue	*0.48*	*0.22*	*ns*
	Symbiotic tissue - Bleached tissue	*0.35*	*0.18*	*ns*
	Symbiodiniaceae -Bleached tissue	*0.35*	< 0.001	***
	Symbiodiniaceae - Symbiotic tissue	*0.35*	*0.005*	**
Methionine	Symbiotic tissue - Bleached tissue	*0.48*	*0.99*	*ns*
	Symbiodiniaceae -Bleached tissue	*0.48*	*0.31*	*ns*
	Symbiodiniaceae - Symbiotic tissue	*0.31*	*0.07*	*ns*
	Symbiotic tissue - Bleached tissue	*0.21*	< 0.001	***
	Symbiodiniaceae -Bleached tissue	*0.21*	< 0.001	***
	Symbiodiniaceae - Symbiotic tissue	*0.22*	*0.1*	*ns*
Phenylananine	Symbiotic tissue - Bleached tissue	*0.36*	*0.80*	*ns*
	Symbiodiniaceae -Bleached tissue	*0.36*	*0.50*	*ns*
	Symbiodiniaceae - Symbiotic tissue	*0.25*	*0.75*	*ns*
	Symbiotic tissue - Bleached tissue	*0.26*	< 0.001	***
	Symbiodiniaceae -Bleached tissue	*0.26*	< 0.001	***
	Symbiodiniaceae - Symbiotic tissue	*0.22*	*ns*	*ns*

Tab. S24. Linear mixed effects models result from $\delta^{13}C$ isotope values of five trophic amino acids: alanine, glutamic acid, isoleucine, proline and valine of the host tissue and symbionts of bleached and symbiotic corals of *Ctenactis echinata* (white) and *Pocillopora verrucosa* (gray). Standard error (st.error), *p* value, significance (sig.) and model specifications are given. Significance codes used are defined for p values: p < 0.001 (***), p < 0.01 (**), p < 0.05 (*), ns = not significant.

Amino acid	Host fraction	std. error	p value	Sig.
Alanine	Symbiotic tissue - Bleached tissue	0.42	0.93	ns
	Symbiodiniaceae -Bleached tissue	0.42	0.02	*
	Symbiodiniaceae - Symbiotic tissue	0.35	0.01	*
	Symbiotic tissue - Bleached tissue	0.41	0.84	ns
	Symbiodiniaceae -Bleached tissue	0.41	0.82	ns
	Symbiodiniaceae - Symbiotic tissue	0.41	0.99	ns
Glutamic acid	Symbiotic tissue - Bleached tissue	0.38	0.15	ns
	Symbiodiniaceae -Bleached tissue	0.38	0.02	*
	Symbiodiniaceae - Symbiotic tissue	0.38	0.72	ns
	Symbiotic tissue - Bleached tissue	0.32	0.006	**
	Symbiodiniaceae -Bleached tissue	0.32	0.0004	***
	Symbiodiniaceae - Symbiotic tissue	0.33	0.75	ns
Isoleucine	Symbiotic tissue - Bleached tissue	0.48	0.84	ns
	Symbiodiniaceae -Bleached tissue	0.48	0.86	ns
	Symbiodiniaceae - Symbiotic tissue	0.38	0.99	ns
	Symbiotic tissue - Bleached tissue	0.35	0.002	**
	Symbiodiniaceae -Bleached tissue	0.35	0.90	ns
	Symbiodiniaceae - Symbiotic tissue	0.35	0.0001	***
Proline	Symbiotic tissue - Bleached tissue	0.47	0.89	ns
	Symbiodiniaceae -Bleached tissue	0.47	0.99	ns
	Symbiodiniaceae - Symbiotic tissue	0.40	0.79	ns
	Symbiotic tissue - Bleached tissue	0.32	1.00	ns
	Symbiodiniaceae -Bleached tissue	0.32	0.001	**
	Symbiodiniaceae - Symbiotic tissue	0.33	0.001	**
Valine	Symbiotic tissue - Bleached tissue	0.42	0.78	ns
	Symbiodiniaceae -Bleached tissue	0.42	0.85	ns
	Symbiodiniaceae - Symbiotic tissue	0.41	0.98	ns
	Symbiotic tissue - Bleached tissue	0.41	0.36	ns
	Symbiodiniaceae -Bleached tissue	0.41	0.86	ns
	Symbiodiniaceae - Symbiotic tissue	0.35	0.57	ns

Tab. S25. Linear mixed effects models result from $\delta^{15}N$ isotope values of five trophic amino acids: alanine, glutamic acid, isoleucine, proline and valine of the host tissue and symbionts of bleached and symbiotic corals of *Ctenactis echinata (white)* and *Pocillopora verrucosa (gray)*. Standard error (st.error), *p* value, significance (sig.) and model specifications are given. Significance codes used are defined for p values: p < 0.001 (***), p < 0.01 (**), p < 0.05 (*), ns = not significant.

Amino acid	Host fraction	std. error	p value	Sig.
Alanine	Symbiotic tissue - Bleached tissue	0.29	0.44	ns
	Symbiodiniaceae -Bleached tissue	0.29	< 0.001	***
	Symbiodiniaceae - Symbiotic tissue	0.20	< 0.001	***
	Symbiotic tissue - Bleached tissue	0.12	< 0.001	***
	Symbiodiniaceae -Bleached tissue	0.12	< 0.001	***
	Symbiodiniaceae - Symbiotic tissue	0.11	< 0.001	***
Glutamic acid	Symbiotic tissue - Bleached tissue	0.37	0.62	ns
	Symbiodiniaceae -Bleached tissue	0.37	0.72	ns
	Symbiodiniaceae - Symbiotic tissue	0.26	0.97	ns
	Symbiotic tissue - Bleached tissue	0.16	< 0.001	***
	Symbiodiniaceae -Bleached tissue	0.16	< 0.001	***
	Symbiodiniaceae - Symbiotic tissue	0.12	< 0.001	***
Isoleucine	Symbiotic tissue - Bleached tissue	0.32	0.13	ns
	Symbiodiniaceae -Bleached tissue	0.32	< 0.001	***
	Symbiodiniaceae - Symbiotic tissue	0.23	0.0005	***
	Symbiotic tissue - Bleached tissue	0.13	< 0.001	***
	Symbiodiniaceae -Bleached tissue	0.13	< 0.001	***
	Symbiodiniaceae - Symbiotic tissue	0.13	< 0.001	***
Proline	Symbiotic tissue - Bleached tissue	0.28	0.6	ns
	Symbiodiniaceae -Bleached tissue	0.28	< 0.001	***
	Symbiodiniaceae - Symbiotic tissue	0.20	< 0.001	***
	Symbiotic tissue - Bleached tissue	0.10	< 0.001	***
	Symbiodiniaceae -Bleached tissue	0.10	< 0.001	***
	Symbiodiniaceae - Symbiotic tissue	0.08	< 0.001	***
Valine	Symbiotic tissue - Bleached tissue	0.38	0.70	ns
	Symbiodiniaceae -Bleached tissue	0.38	0.08	ns
	Symbiodiniaceae - Symbiotic tissue	0.27	0.14	ns
	Symbiotic tissue - Bleached tissue	0.14	< 0.001	***
	Symbiodiniaceae -Bleached tissue	0.14	< 0.001	***
	Symbiodiniaceae - Symbiotic tissue	0.11	< 0.001	***

Tab. 26. Linear mixed effects models result from calculated trophic position ($TP_{Glu-Phe}$) values from two amino acids (glutamic acid and phenylalanine) of the host tissue and symbionts of bleached and symbiotic *Ctenactis echinata* and *Pocillopora verrucosa*. Standard error (st.error), *p* value, significance (sig.) and model specifications are given. Significance codes used are defined for p values: p < 0.001 (***), p < 0.01 (**), p < 0.05 (*), ns = not significant.

Species/Host fractions	std. error	*p* value	Sig.	model specifications
C. echinata				
Symbiotic tissue - Bleached tissue	0.50	0.87	ns	
Symbiodiniaceae -Bleached tissue	0.50	1.00	ns	model <- lmer(scale(TP)
Symbiodiniaceae - Symbiotic tissue	0.38	0.81	ns	~Host fraction + (1|station), data=data
P. verrucosa				
Symbiotic tissue - Bleached tissue	0.32	0.19	ns	
Symbiodiniaceae -Bleached tissue	0.32	0.18	ns	model <- lmer(scale(TP)
Symbiodiniaceae - Symbiotic tissue	0.25	0.08	ns	~Host fraction + (1|station), data=data

Tab. 27. Trophic position ($TP_{Glu\text{-}Phe}$) values from two amino acids (Glutamic acid and Phenylalanine) of the host tissue and symbionts of bleached and symbiotic *Ctenactis echinata* and *Pocillopora verrucosa*. (mean ± standard deviation).

Species	Bleached	Symbiotic	Symbiodiniaceae
Ctenactis echinata	1.4 ± 0.2	1.3 ± 0.3	1.3 ± 0.2
Pocillopora verrucosa	1.5 ± 0.1	1.2 ± 0.3	1.0 ± 0.2

Tab. S28. Linear mixed-effects model results of the growth variables: surface area growth, volume growth, and calcification of *P. verrucosa* and *S. pistillata* exposed to microplastics and two different feeding regimens over six weeks. Treatments Control, MP = microplastic, and MP+HF = microplastic and high feeding were compared. Standard error (st.error), *p*-value, significance (sig.). Model specifications: lmer(scale(variable)~Treatment + (1|genotype), data=data. Significance codes used are defined as: $p < 0.001$ (***), $p < 0.01$ (**), $p < 0.05$ (*), $p > 0.05$ (ns = not significant).

Variable/Species	Treatments	std.error	p-value	sig.
Surface area growth				
P. verrucosa	MP - Control	-0.2	0.8	ns
	MP+HF - Control	0.5	0.2	ns
	MP+HF - MP	0.7	0.1	ns
S. pistillata	MP - Control	-0.3	0.6	ns
	MP+HF - Control	0.1	0.9	ns
	MP+HF - MP	0.5	0.4	ns
Volume growth				
P. verrucosa	MP - Control	-0.5	0.3	ns
	MP+HF - Control	0.1	0.8	ns
	MP+HF - MP	0.7	0.1	ns
S. pistillata	MP - Control	0.3	0.6	ns
	MP+HF - Control	0.7	0.1	ns
	MP+HF - MP	0.3	0.6	ns
Calcification				
P. verrucosa	MP - Control	-0.2	0.6	ns
	MP+HF - Control	0.2	0.6	ns
	MP+HF - MP	0.4	0.1	ns
S. pistillata	MP - Control	-0.4	0.5	ns
	MP+HF - Control	0.1	0.8	ns
	MP+HF - MP	0.5	0.2	ns

Tab. S29. Linear mixed-effects model results of the photophysiology variables: net photosynthesis, respiration, gross photosynthesis, effective quantum yield (Y(II)), and maximum quantum yield (Fv/Fm).

Variable/Species	Treatments	std.error	p-value	sig.
Net photosynthesis				
P. verrucosa	MP - Control	0.13	<0.001	***
	MP+HF - Control	0.13	0.21	ns
	MP+HF - MP	0.14	<0.001	***
S. pistillata	MP - Control	0.29	0.58	ns
	MP+HF - Control	0.32	0.19	ns
	MP+HF - MP	0.31	0.01	**
Respiration				
P. verrucosa	MP - Control	0.21	0.07	ns
	MP+HF - Control	0.21	0.05	ns
	MP+HF - MP	0.22	<0.001	***
S. pistillata	MP - Control	0.34	0.55	ns
	MP+HF - Control	0.41	<0.001	***
	MP+HF - MP	0.38	0.01	**
Gross photosynthesis				
P. verrucosa	MP - Control	0.11	<0.001	***
	MP+HF - Control	0.11	0.003	**
	MP+HF - MP	0.11	<0.001	***
S. pistillata	MP - Control	0.26	0.67	ns
	MP+HF - Control	0.28	0.01	*
	MP+HF - MP	0.27	<0.001	***
Effective quantum yield (Y(II))				
P. verrucosa	MP - Control	0.15	0.54	ns
	MP+HF - Control	0.16	0.93	ns
	MP+HF - MP	0.16	0.78	ns
S. pistillata	MP - Control	0.33	0.97	ns
	MP+HF - Control	0.34	0.92	ns
	MP+HF - MP	0.34	0.83	ns
Maximum quantum yield Fv/Fm				
P. verrucosa	MP - Control	0.37	0.009	**
	MP+HF - Control	0.37	0.31	ns
	MP+HF - MP	0.37	0.29	ns
S. pistillata	MP - Control	0.23	0.68	ns
	MP+HF - Control	0.24	0.03	*
	MP+HF - MP	0.24	0.20	ns

Tab. S30. Linear mixed-effects model results of the tissue composition: total content of carbohydrates (carb), lipids (lip), proteins (prot), and tissue energy content (tot) of P. verrucosa at the end of the six-week MP exposure. Control, MP = microplastic, MP+HF = microplastic + high feeding. Standard error (st.error), *p*-value, significance (sig.). Model specifications: lmer(scale(variable)~Treatment + (1|genotype), data=data. Significance codes used are defined as: $p < 0.001$ (***), $p < 0.01$ (**), $p < 0.05$ (*), $p > 0.05$ (ns = not significant).

Variable	Treatments	std.error	p-value	sig.
Carbohydrates				
	MP - Control	0.35	<0.001	***
	MP+HF - Control	0.34	0.004	**
	MP+HF - MP	0.35	0.5	ns
Lipids				
	MP - Control	0.39	0.009	**
	MP+HF - Control	0.37	0.06	ns
	MP+HF - MP	0.38	0.72	ns
Proteins				
	MP - Control	0.39	0.04	*
	MP+HF - Control	0.38	0.31	ns
	MP+HF - MP	0.39	0.6	ns
Tissue energy content				
	MP - Control	0.40	0.02	*
	MP+HF - Control	0.39	0.25	ns
	MP+HF - MP	0.40	0.51	ns

Tab. S31. Linear mixed-effects model results of the bleaching intensity of *P. verrucosa* and *S. pistillata* exposed to a six-week MP experimental period and a short-term heat stress. Treatments: Control, MP = microplastic, and MP+HF = microplastic and high feeding. Standard error (st.error), *p*-value, significance (sig.). Model specifications: lmer(scale(variable)~Treatment + (1|genotype), data=data. Significance codes used are defined as: $p < 0.001$ (***), $p < 0.01$ (**), $p < 0.05$ (*), $p > 0.05$ (ns = not significant).

Species	Treatments	std.error	*p*-value	sig.
P. verrucosa				
	MP - Control	-0.8	0.04	*
	MP+HF - Control	0.1	0.8	ns
	MP+HF - MP	-1.0	0.008	**
S. pistillata				
	MP - Control	-0.6	0.7	ns
	MP+HF - Control	-0.2	0.1	ns
	MP+HF - MP	-0.3	0.6	ns

7 Abbreviations

AAs	Amino acids
ALA	Alanine
ASP	Asparagyne
B	Boron
Ca	Calcium
C. echinata	*Ctenactis echinata*
Cu	Copper
CSIA-AAs	Compound-specific stable isotope analysis of amino acids
G. fascicularis	*Galaxea fascicularis*
GLU	Glutamic acid
GLY	Glycine
HF	Heterotrophic feeding
ISO	Isoleucine
Mg	Magnesium
MET	Methionine
MPs	Microplastics
N	Nitrogen
Polyamide	PA
P. lobata	*Porites lobata*
P. verrucosa	*Pocillopora verrucosa*
PHE	Phenylananine
Polyethylene	PE
Polyethylene terephthalate	PET
Polypropylene	PP
Polystyrene	PS
Polyvinyl chloride	PVC
PRO	Proline
LYS	Lysine
S. pistillata	*Stylophora pistillata*
TP	Trophic position
VAL	Valine
Zn	Zinc

8 Acknowledgments

From its conception, this project was made possible thanks to the invaluable support of many people. Not only was it an academic challenge, it was also a transformative experience involving moving to a new continent, adapting to a multicultural environment, and developing personally and professionally. None of this would have been possible without the generosity, guidance and encouragement of exceptional people.

Firstly, I would like to express my gratitude to my supervisor, Prof. Dr. Maren Ziegler, for her constant support throughout this project. From the initial stages, she placed her trust in me and provided me with the opportunity to conduct this research in a well-equipped laboratory. Her guidance, patience and constant encouragement since my arrival in Germany have been invaluable and fundamental to completing this thesis. I am also sincerely grateful to Dr. Jessica Reichter for her advice, motivation, and generosity in sharing her knowledge throughout the development of this project. It has been an honor and a privilege to work alongside women of such professional excellence and outstanding human values. Thank you both for inspiring me and supporting me every step of the way.

I extend my heartfelt thanks to the DAAD for funding my doctoral scholarship and giving me the opportunity to pursue this project. I would also like to acknowledge the Marine Holobiomics Lab. team, including all students, Prof. Dr. Patrick Schubert, and Stella Odignal, for their invaluable help, especially during the experimental phases. Likewise, I am very grateful to the professors and staff of Justus Liebig University, such as Prof. Dr. Tom Wilke, Sylvia Nachtigal, Christina Anding and Katrin Meztger, for their constant willingness to provide support.

On a more personal note, I wish to thank my dear friends, Kara Engelhardt, Jana Vetter, José Grillo, Erik Ferrara, Laura del Rio-Hortega, Pablo Sierra, Giullia Putin, Vanessa Tirpitz, Tabea Platz, Zhao Qi, Catarina Martins and Marvin Rades, who became more than friends; they were family during this journey. Their support, companionship, and kindness gave me strength in moments of challenge and made this experience unforgettable. I am also sincerely grateful to my dear friends; Eugenia Martintereso, Jhonathan Vivas, Andrea Prieto, Prof. Dr. Ruth Ramos, Alejandra Verde, Emmy Miyazawa and Andreina Rivera whose support, companionship, and generosity were instrumental in helping me make this dream come true.

Finally, my deepest gratitude goes to my family; my parents and my sister who, despite the distance, were always present with their love, encouragement, and daily motivation. This achievement is not mine alone but ours. **We did it!**